iScience

CellPress

Article

Synthesis of Multisubstituted Benzimidazolones via Copper-Catalyzed Oxidative Tandem C–H Aminations and Alkyl Deconstructive Carbofunctionalization

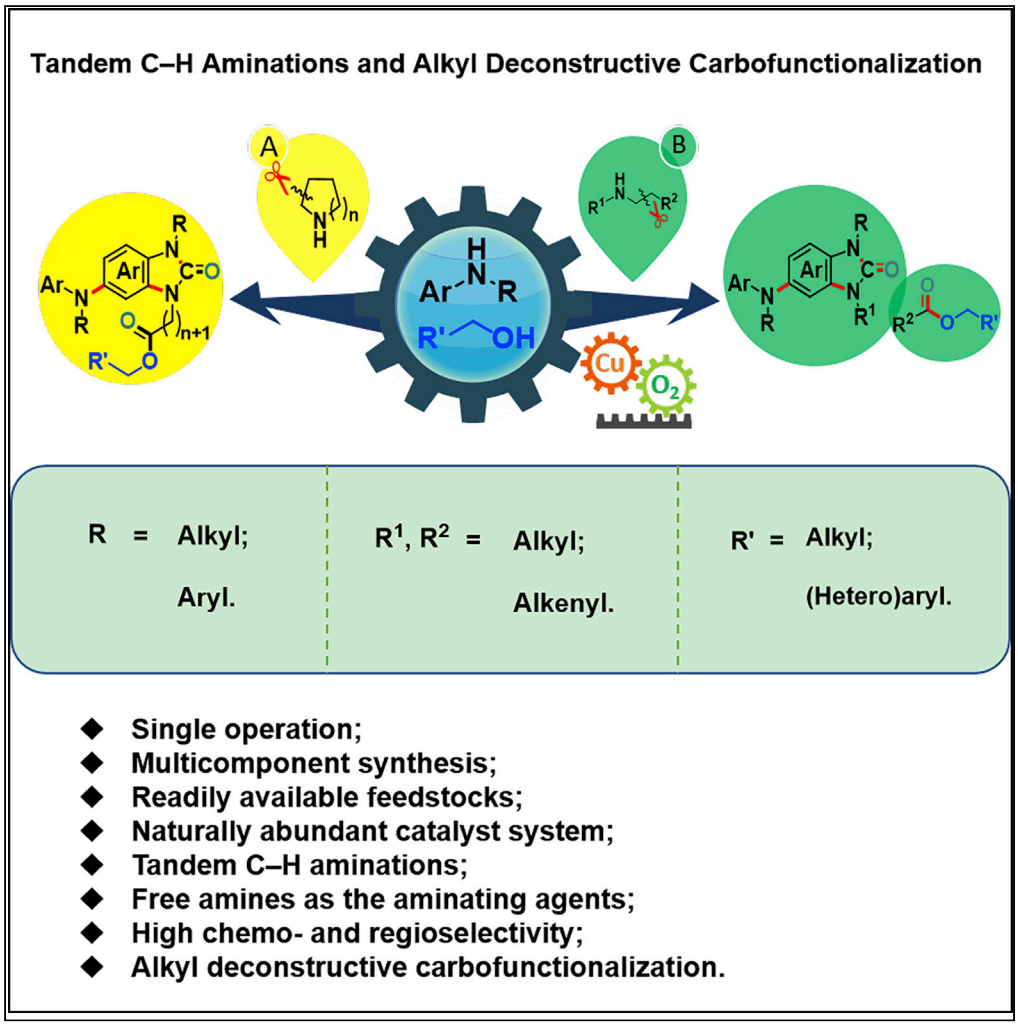

Taoyuan Liang, He Zhao, Lingzhen Gong, Huanfeng Jiang, Min Zhang

minzhang@scut.edu.cn

HIGHLIGHTS

Tandem C–H aminations

$C(sp^3)$–$C(sp^3)$ bond deconstructive carbofunctionalization

Multicomponent synthesis

High chemo- and regioselectivity

DATA AND SOFTWARE AVAILABILITY

www.ccdc.cam.ac.uk/getstructures

Liang et al., iScience *15*, 127–135
May 31, 2019
https://doi.org/10.1016/j.isci.2019.04.019

iScience

CellPress

Article

Synthesis of Multisubstituted Benzimidazolones via Copper-Catalyzed Oxidative Tandem C–H Aminations and Alkyl Deconstructive Carbofunctionalization

Taoyuan Liang,[1] He Zhao,[1] Lingzhen Gong,[1] Huanfeng Jiang,[1] and Min Zhang[1,2,*]

SUMMARY

Benzimidazolone constitutes the core structure of numerous pharmaceuticals, agrochemicals, inhibitors, pigments, herbicides, and fine chemicals. Amination of hydrocarbons is an attractive tool for the creation of nitrogen-containing products. However, the multiple steps, harsh conditions, and low atom efficiencies often present in these reactions remain challenging. We present a multicomponent synthesis of functional benzimidazolones from arylamines, dialkylamines, and alcohols, acting via the sequence of copper-catalyzed oxidative tandem C–H aminations and alkyl deconstructive carbofunctionalization. The catalytic transformation forms multiple bonds in one single operation, uses readily available feedstocks and a naturally abundant Cu/O_2 catalyst system, has broad substrate scope, avoids pre-installation of aminating agents and directing groups, and provides high chemo- and regioselectivity, resulting in direct functionalization of inert C–H and C–C bonds via single-electron oxidation-induced activation mode. This platform can be expected to provide structurally diverse products with interesting biological, chemical, and physical properties.

INTRODUCTION

Conventionally, the construction of functional organic products mainly relies on pre-preparation of active reactants followed by noble metal-catalyzed coupling steps, which can easily result in environmental pollution and low utilization efficiency of resources. In this context, there is a high demand for the development of novel catalytic transformations that, via direct functionalization of ubiquitous but poorly reactive C–H and C–C bonds in readily available feedstocks, generate the desired products in the presence of naturally abundant catalyst systems, as such transformations featuring high step and atom efficiency as well as sustainability would pave the ways to address the existing issues.

Among the various functionalizations of hydrocarbons, C–H amination constitutes a particularly attractive tool for the creation of nitrogen-containing products (Park et al., 2017; Kim and Chang, 2017; Beccalli et al., 2017; Boursalian et al., 2016). To date, a number of approaches have been elegantly explored for this purpose (Breslow and Gellman, 1983; Paudyal et al., 2016; Liang et al., 2018; Wertz et al., 2011; Yin et al., 2010; Kim et al., 2010; Gao et al., 2018; Wang et al., 2017a, 2017b; Tang et al., 2018; Wu et al., 2011, 2017; Wang et al., 2016, 2017a, 2017b; Margrey et al., 2017; Romero et al., 2015; Ouyang et al., 2017; Liu et al., 2017; Yang et al., 2017; Zhang et al., 2017). However, some key issues remain to be addressed in this field, such as the need for the pre-installation of specific aminating agents (e.g., nitrenes, N-atom with a leaving substituent, azoles) and directing groups, the use of waste-generating oxidants/additives, and harsh conditions. As such, the search for new C–H amination strategies involving free amines as the aminating agents in the absence of directing groups still remains a highly demanding goal. In terms of carbofunctionalization, much effort has been directed during the past decade toward the difunctionalization of alkenes (Qin et al., 2016; Shen et al., 2013, 2016; Li et al., 2016) and alkynes (Li et al., 2017; Urgoitia et al., 2017; Rubinstein et al., 2014; Rao et al., 2017). Moreover, carbofunctionalization via the cleavage of unsaturated C–C bonds (Sagadevan et al., 2017; Shen et al., 2013, 2016; Qin et al., 2016) has also been nicely established. In comparison, owing to a surrounding environment composed of four bonding atoms, regioselective alkyl deconstructive carbofunctionalization has at present remained a challenging but highly valuable topic in synthetic chemistry, as this process would offer the potential to develop novel transformations producing functional molecules that are difficult to prepare or inaccessible by conventional approaches (Liu et al., 2018). For instance in this regard, the Zhu group has reported a number of transformations on the cleavage of strained alkyl chains such as cyclobutanols (Ren et al., 2015, 2016; Yu et al., 2016; Zhao et al., 2015). Very recently, Roque et al. have demonstrated interesting examples on deconstructive functionalization of cyclic

[1]Key Lab of Functional Molecular Engineering of Guangdong Province, School of Chemistry and Chemical Engineering, South China University of Technology, Guangzhou, China

[2]Lead Contact

*Correspondence: minzhang@scut.edu.cn

https://doi.org/10.1016/j.isci.2019.04.019

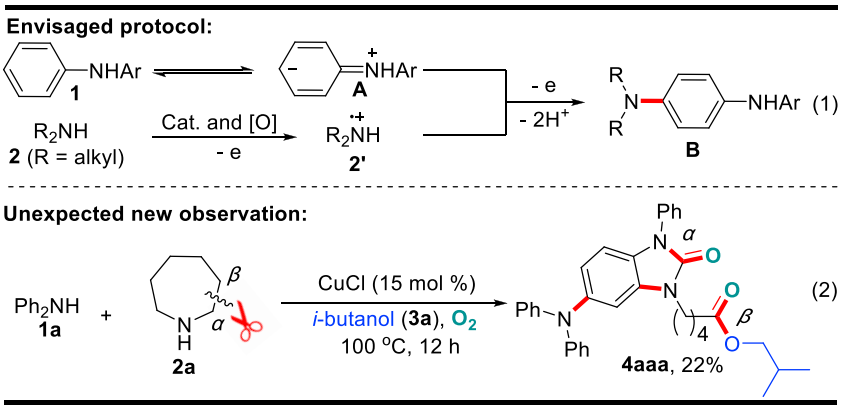

Scheme 1. Previous Work and the New Observation

tertiary amines (Roque et al., 2018a, 2018b). However, to the best of our knowledge, the elaboration of functional molecules, via the strategy combining direct C–H amination with deconstructive carbofunctionalization of unstrained alkyl chain, remains a new subject to be explored.

As our sustained effort has been directed toward the functionalization of N-heterocycles (Zhao et al., 2019; Xie et al., 2017, 2018, 2019; Chen et al., 2017), we have recently reported a site-specific fluoroalkylation of aniline derivatives with *in situ*-formed electrophilic radicals (Zhao et al., 2019). This work motivated us to conceive a protocol to aminate the *para*-site of relatively electron-poor diarylamine **1** with electron-rich dialkylamine **2**. As illustrated in Scheme 1, the presence of a suitable catalyst and oxidant is expected to lead to single electron oxidation (SEO) of **2** and generate radical cation **2′**, which then interacts with the zwitterionic form **A** of diarylamine **1** at the sterically less-hindered *para*-site, and generates the amination product **B** via further SEO and deprotonations. However, when we tested the reaction of diphenylamine **1a** and azepane **2a** in *i*-butanol by using $CuCl/O_2$ as a catalyst system, we observed that, instead of the anticipated aryl *para*-C–H amination product **B**, a novel functional benzimidazolone **4aaa** was isolated in 22% yield by combining two molecules of **1a**, one molecule of **2a**, and *i*-butanol **3a** (solvent). In such a reaction, three C–N and three C–O bonds are formed in one single operation. Especially, the aryl C–H aminations take place at positions 2 and 4 of diphenylamine **1a**, and the alkyl cleavage in amine **2a** occurs selectively between the α- and β-sties, which leads to α-carboamidation and β-carboesterification, respectively.

It is important to note that benzimidazolone constitutes the core structure of numerous pharmaceuticals, agrochemicals, inhibitors, pigments, herbicides, and fine chemicals (Monforte et al., 2010; Palin et al., 2008; Mastalerz and Oppel, 2012; Mir et al., 2012; Nale and Bhanage, 2015). To date, although there are a number of approaches reported for the synthesis of such compounds, including the cyclization of *o*-phenylenediamine with phosgene or CO surrogates (Scheme 2, path a), (Monforte et al., 2009; Kuethe et al., 2004; Diao et al., 2009) the cyclization of *o*-haloanilines involving C–N bond formation

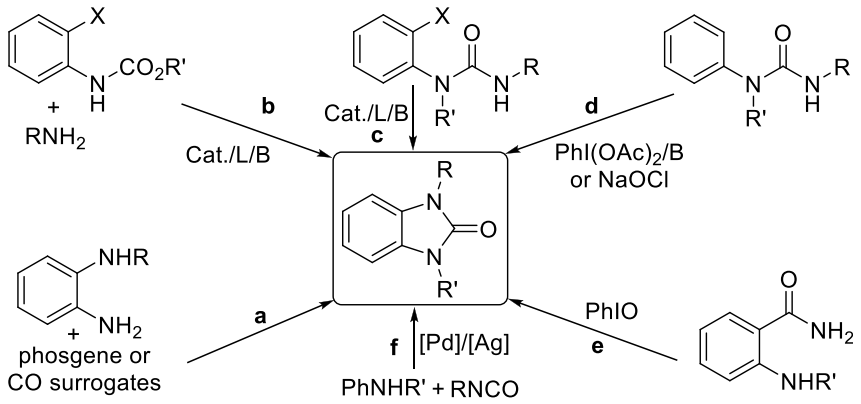

Scheme 2. Existing Main Approaches for the Synthesis of Benzimidazolones

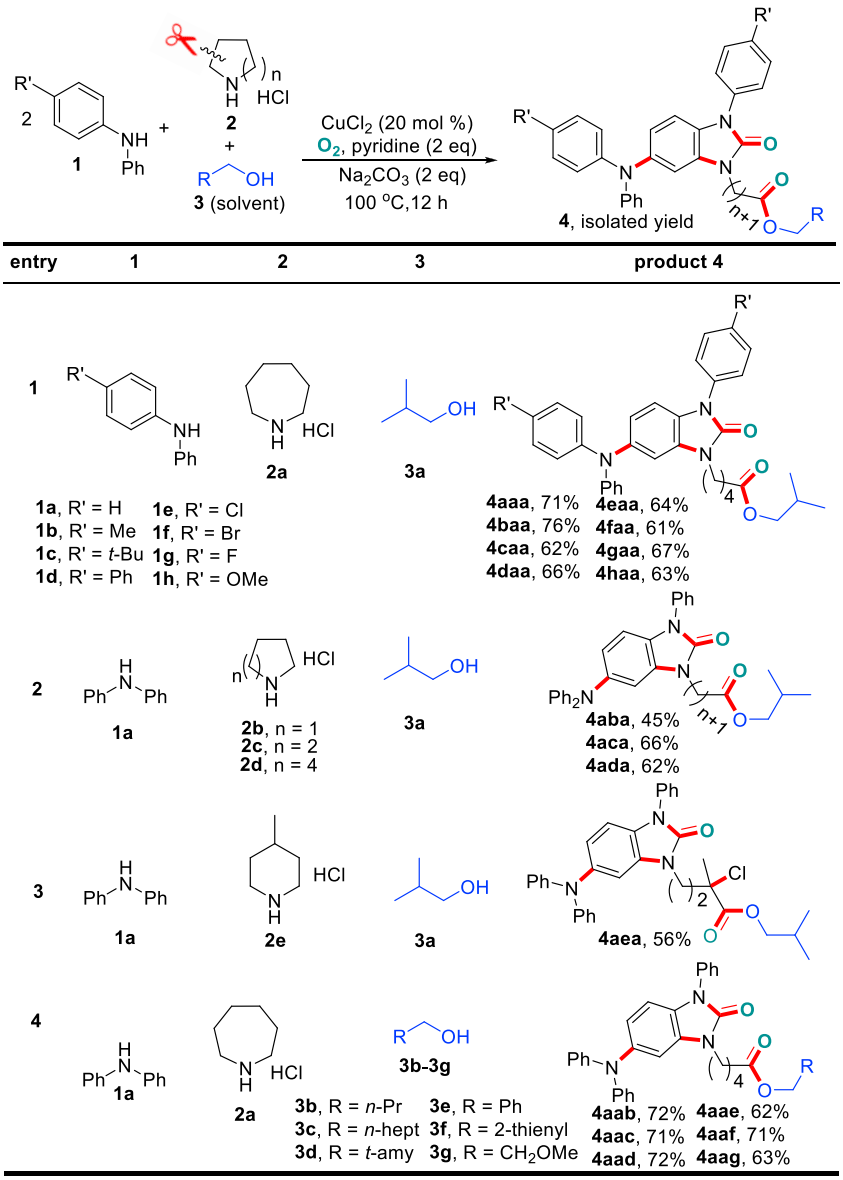

Scheme 3. Variation of the Three Coupling Partners

Also see Figures S1–S37.

(paths b and c) (Zou et al., 2007; An et al., 2016), the oxidative aryl C–H amidation of N-disubstituted ureas (path d) (Beyer et al., 2001; Li et al., 2008; Yu et al., 2015), PhIO-induced Hofmann rearrangement of amides followed by intramolecular nucleophilic attack by an *ortho*-amino group (path e) (Łukasik and Wróbel, 2016), and the addition of anilines to isocyanates followed by intramolecular oxidative C–H amidation (path f) (Youn and Kim, 2016; Allen and Tidwell, 2013), to the best of our knowledge, the direct construction of benzimidazolones incorporated with additional functionalities from easily available feedstocks is still lacking. On the basis of our new observation, we herein present, for the first time, a multicomponent synthesis of functional benzimidazolones via tandem C–H aminations and alkyl deconstructive carbofunctionalization.

RESULTS AND DISCUSSION

Initially, we focused on screening an efficient catalyst system by choosing the coupling of **1a** and **2a** in *i*-butanol (**3a**) as a model reaction. After evaluation of a series of reaction parameters (Table S1,

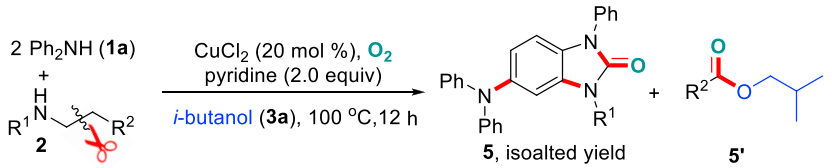

entry	2	product 5
1	**2f**: $HNEt_2$	**5af** (R^1 = Et), 78%
2	**2g**: HN(*n*-Pr)$_2$	**5ag** (R^1 = *n*-Pr), 86%
3	**2h**: HN(*n*-Bu)$_2$	**5ah** (R^1 = *n*-Bu), 74%
4	**2i**: HN(*i*-Bu)$_2$	**5ai** (R^1 = *i*-Bu), 62%
5	**2j**: HN(*n*-hexyl)$_2$	**5aj** (R^1 = *n*-hexyl), 75%
6	**2k**: 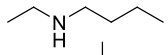	**5af**, 38% + **5ah**, 35%
7	**2l**: 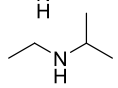	**5al** (R^1 = *i*-propyl), 35% (**X-ray diffraction**)
8	**2m**: 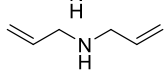	**5am** (R^1 = -$CH_2CH{=}CH_2$), 62%

Scheme 4. Variation of Open-Chain Dialkylamines

Standard condition deviation: without addition of Na_2CO_3. Also see Figures S38–S51 and S88 and Tables S2–S6.

Supplemental Information), an optimal isolated yield for product **4aaa** was obtained when the reaction charged with an O_2 balloon was performed at 100°C for 12 h with 20 mol % of $CuCl_2$, 2 equiv. of pyridine, and Na_2CO_3 (standard conditions), in which Na_2CO_3 was used to neutralize the combined HCl in the cyclic amine salts.

With the optimal conditions established, we then examined the generality of the synthetic protocol. First, various unsymmetrical diarylamines (**1b**-**1h**) in combination with cyclic amines **2a** in *i*-butanol **3a** were explored. As shown in Scheme 3, all the reactions proceeded smoothly and furnished the desired products (**4aaa**-**4haa**) in good isolated yields. The substituents with different electronic properties on the aryl ring of the diarylamines slightly influenced the product yields. Then, we tested the transformation of secondary cyclic amines with different ring sizes (**2b**-**2e**). Similarly all the substrates smoothly coupled with diphenylamine **1a** and *i*-butanol **3a** and provided the N-alkyl products with tunable chain lengths (**4aba**-**4aea**) in moderate to good yields. Interestingly, the use of 4-methylpiperidyl salt **2e** led to the generation of product **4aea,** which involves an additional chlorination at the tertiary α-site of the ester group, and the combined HCl in **2e** is believed to serve as the chlorine source. Furthermore, the variation of alcohols had no significant influence on the product formation. Thus different types of alcohols, including linear, branched, (hetero)aryl, and heteroatom-containing alcohols, efficiently reacted with **1a** and **2a** to give the desired products (**4aab**-**4aag**) in good yields. Owing to the excellent compatibility of the different coupling partners, the developed chemistry offers a versatile way for the synthesis of benzimidazolones with structural diversity.

The successful transformation of secondary cyclic amines (Scheme 3) subsequently encouraged us to apply the synthetic protocol to the open-chain dialkylamines. As shown in Scheme 4, a series of such substrates (**2f**-**2m**) in combination with diphenylamine **1a** and alcohol **3a** were tested. Gratifyingly, both linear and branched dialkylamines **2** underwent efficient alkyl cleavage between the α- and β-carbons, and the α-carboamidation generated the N-alkylated benzimidazolone products **5** (i.e., **5af**-**5aj**), whereas the β-carboesterofication led to the liberation of the ester by-products **5′**. It is noteworthy that unsymmetrical N-ethylbutan-1-amine (**2k**) generated two products (**5af** and **5ah**) with similar yields, whereas the reaction of N-ethylpropan-2-amine (**2l**) exclusively generated the N-propyl product **5al** with a 35% yield (as confirmed by single-crystal X-ray diffraction, CCDC: 1508570, for details, see Figure S88 and Tables S2–S6), and the C–C bond cleaved at the sterically less-hindered ethyl group. It is also of interest that diallylamine **2m** generated the product **5am** in 62% yield with the retention of the allylic functionality.

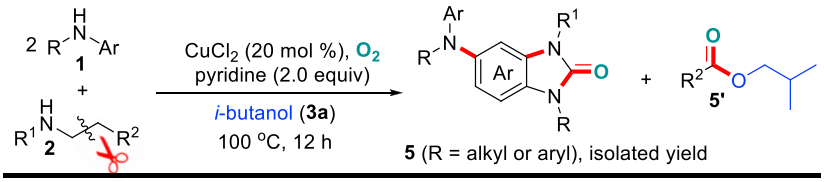

entry	1	2	product 5
1	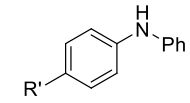 **1b**: R' = Me; **1e**: R' = Cl; **1c**: R' = *t*-Bu; **1f**: R' = Br; **1d**: R' = Ph; **1i**: R' = CN	**2f**	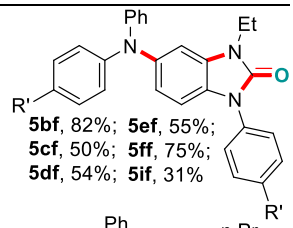 **5bf**, 82%; **5ef**, 55%; **5cf**, 50%; **5ff**, 75%; **5df**, 54%; **5if**, 31%
2	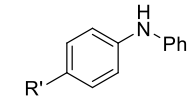 **1b**, R' = Me; **1k**, R' = CO_2Et; **1j**, R' = Et; **1l**, R' = CF_3	**2g**	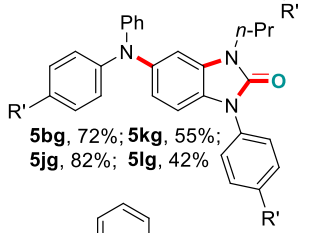 **5bg**, 72%; **5kg**, 55%; **5jg**, 82%; **5lg**, 42%
3	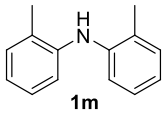 **1m**	**2f**	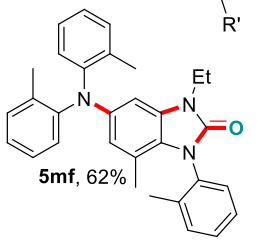 **5mf**, 62%
4	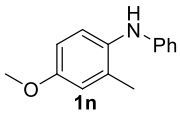 **1n**	**2f**	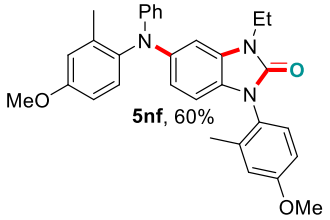 **5nf**, 60%
5	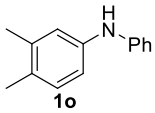 **1o**	**2g**	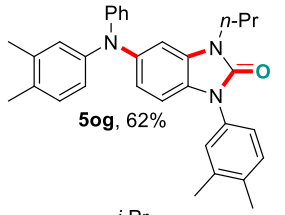 **5og**, 62%
6	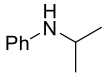 **1p**	**2f**	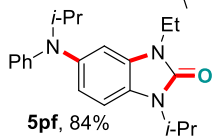 **5pf**, 84%

Scheme 5. Variation of Both Dialkyl- and Arylamines

Standard condition deviation: without addition of Na_2CO_3. Also see Figures S52–S83.

Subsequently, we focused on the variation of both diarylamines and open-chain dialkylamines (Scheme 5). Here, substrates **1** with different functionalities on the aryl ring, including –Me, –Et, –*t*-Bu, –Ph, –F, –Cl, –Br, –CN, $–CO_2Et$, $–NO_2$, and $–CF_3$, were well tolerated and afforded the desired products (**5bf**–**5ff**, **5if**, **5bg**, **5jg**, **5kg**, **5lg**, **5mf**–**5nf**, and **5og**) in moderate to excellent yields. The electronic properties of these substituents significantly influenced the product formation. In particular, the electron-rich diarylamines provided

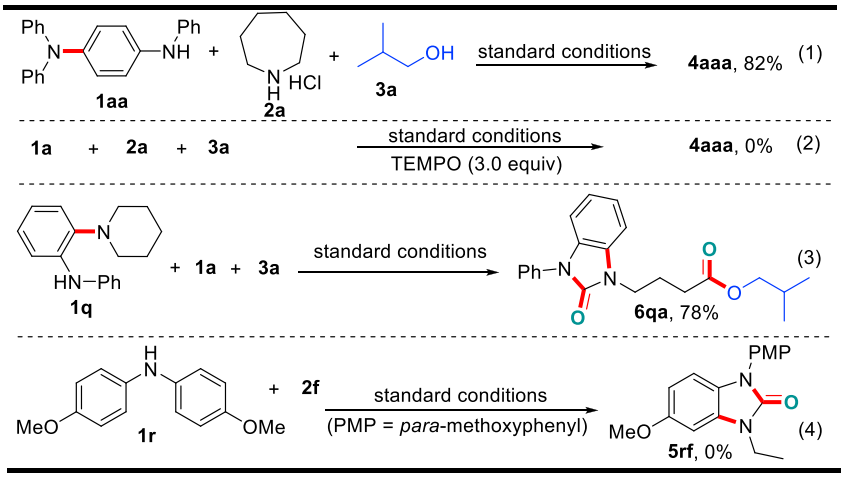

Scheme 6. Control Experiments
Also see Figures S84–S87.

much higher yields (**5bf**, **5bg**, **5jg**, **5mf**, **5og**, and **5pf**) than those of strong electron-withdrawing diarylamines (**5if**, **5kg**, and **5lg**). This phenomenon is explained as the result of electron-rich diarylamines favoring the oxidation process to form active intermediates. In addition to diarylamines, N-alkyl aniline **1p** was also favorable for the transformation and produced the desired product **5pf** in high yield.

In an effort to obtain some mechanistic insights into the reaction route, we conducted several control experiments as illustrated in Scheme 6, Equations 1–4 (also see Figures S84–S87). Interruption of the model reaction conducted under standard conditions after 1 h led to the generation of a small concentration of the homo-coupling product **1aa**, which arose from the *para*-C–H amination of diphenylamine **1a**. Thus we employed **1aa** to react with amine **2a** and alcohol **3a** under standard conditions, and benzimidazolone **4aaa** was generated in high yield (Equation 1). This result indicates that **1aa** is a key reaction intermediate. Then the addition of excess 2,2,6,6-tetramethyl-1-piperidinyloxy (TEMPO) to the model reaction completely suppressed the formation of product (Equation 2), indicating that the reaction involves radical intermediates. Furthermore, the reaction of N-phenyl-2-(piperidin-1-yl)aniline **1q** with **1a** and **3a** produced benzimidazolone **6qa** in a 78% yield (Equation 3), where diphenylamine **1a** was not incorporated in the terminal product. However, the *para*-site-blocked diarylamine (**1o**) was unable to couple with amine **2a** to yield product **5rf** (Equation 4). These results indicate that the first aryl *para*-C–H amination of **1a** occurs before the second aryl *ortho*-C–H amination with **2a** and product **4aaa** derives from tandem dual aryl C–H aminations followed by alkyl deconstructive intramolecular α-carboamidation and intermolecular β-carboesterification.

Based on the above findings, the possible reaction pathway is depicted in Figure 1. Owing to the lower oxidation potential, preferential SEO of dialkylamine **2** (from **2** to **2′**) followed by single-electron transfer from arylamine **1** to the resulting radical cation **2′** would form more stable diarylamino radical cation **1′**. Then, **1′** interacts with another molecule of diarylamine **1** and generates the first aryl *para*-C–H amination product **1-1** via further SEO and deprotonations. Similarly, the aryl radical cation arising from **1-1** interacts with the sterically less hindered dialkylamine **2** at the less congested *ortho*-site and gives rise to the 2,4-diamino intermediate **4-1**. Then, the oxidation of relatively electron-rich alkylamino motif of **4-1** followed by intramolecular nucleophilic addition gives the cyclization adduct **4-3**. Noteworthy, the preferential transformation from dimer **1-1** to **4-1** and **4-3** suppresses the formation of trimeric adducts of diarylamine **1**. Furthermore, the second round oxidation of the alkylamino unit generates iminium ion **4-4** and diamino alkene **4-5**, successively. The O_2-mediated oxidation of electron-rich C–C double bond in **4-5** would lead to selective C–C bond cleavage (from **4-5** to **4-6**) (Ando et al., 1975) and intramolecular α-carboamidation in conjunction with the formation of an aldehyde functionality at the β-site. Finally, the oxidative carboesterification of the aldehyde with alcohol **3** would produce product **4**. For the reaction applying open-chain dialkylamine **2**, the C(α)–C(β) cleavage leads to liberation of the ester by-product.

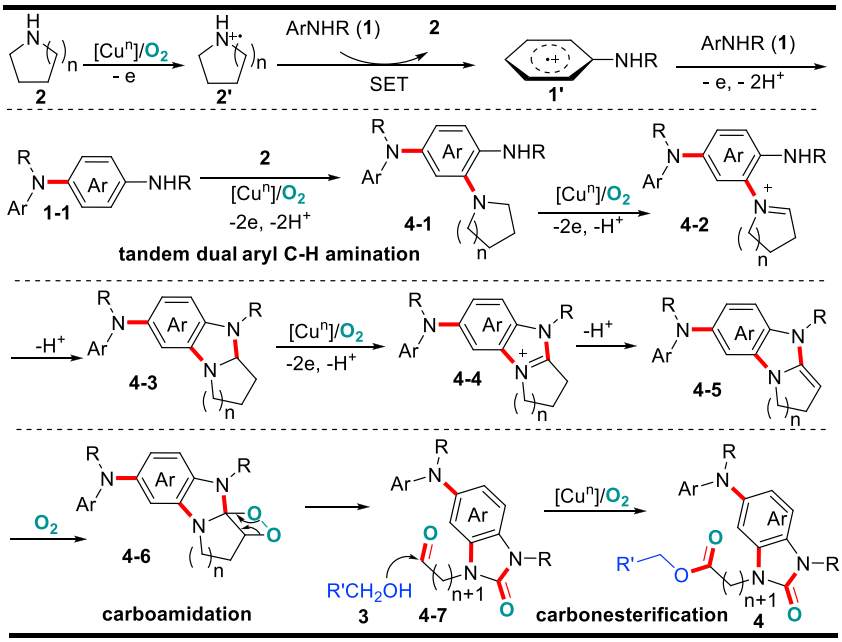

Figure 1. Plausible Reaction Pathway

Limitations of Study

Anilines and specific cyclic amines such as tetrahydroquinolines and indolines were not applicable in the present reactions and no benzimidazolones products were generated.

Conclusion

In summary, we have demonstrated, for the first time, a multicomponent synthesis of functional benzimidazolones via tandem C–H aminations and deconstructive carbofunctionalization of unstrained alkyl chain. The catalytic transformation proceeds with the striking features of the formation of three C–N and three C–O bonds in one single operation, the use of readily available feedstocks and a naturally abundant Cu/O_2 catalyst system, broad substrate scope, no need for pre-installation of specific aminating agents and directing groups, and high chemo- and regioselectivities, which offers an important basis in direct functionalization of inert C–H and C–C bonds via SEO-induced activation mode. The significant utility of benzimidazolones in combination with this novel platform that can be expected to provide structurally diverse products possessing original biological, chemical, and physical properties will incite extensive interest in the scientific community.

METHODS

All methods can be found in the accompanying Transparent Methods supplemental file.

DATA AND SOFTWARE AVAILABILITY

The crystallography data have been deposited at the Cambridge Crystallographic Data Center (CCDC) under accession number CCDC: 1508570 (**5al**) and can be obtained free of charge from www.ccdc.cam.ac.uk/getstructures.

SUPPLEMENTAL INFORMATION

Supplemental Information can be found online at https://doi.org/10.1016/j.isci.2019.04.019.

ACKNOWLEDGMENTS

The authors are grateful to the financial support of Science and Technology Program of GuangZhou (201607010306), National Natural Science Foundation of China (21472052), the "1000 Youth Talents Plan," Science Foundation for Distinguished Young Scholars of Guangdong Province (2014A030306018).

AUTHOR CONTRIBUTIONS

M.Z. conceived and designed the study and wrote the paper. T.L. performed the experiments and mechanism study and analyzed the data. L.G. synthesized some of the substrates. H.Z. performed the crystallographic studies, and H.J. gave some valuable suggestions on the reaction mechanism. All authors discussed the results and commented on the manuscript.

DECLARATION OF INTERESTS

The authors declare no competing financial interests, and the authors have a patent related to this work.

Received: March 1, 2019
Revised: March 27, 2019
Accepted: April 15, 2019
Published: May 31, 2019

REFERENCES

Allen, A.D., and Tidwell, T.T. (2013). Ketenes and other cumulenes as reactive intermediates. Chem. Rev. *113*, 7287–7342.

An, J., Alper, H., and Beauchemin, A.M. (2016). Copper-catalyzed cascade substitution/cyclization of *N*-Isocyanates: a synthesis of 1-aminobenzimidazolones. Org. Lett. *18*, 3482–3485.

Ando, W., Saiki, T., and Migita, T. (1975). Singlet oxygen reaction. IV. Photooxygenation of enamines involving a two-step cleavage of a 1,2-dioxetane intermediate. J. Am. Chem. Soc. *97*, 5028–5029.

Beccalli, E.M., Broggini, G., Martinelli, M., and Sottocornola, S. (2017). C–C, C–O, C–N bond formation on sp^2 carbon by Pd(II)-catalyzed reactions involving oxidant agents. Chem. Rev. *107*, 5318–5365.

Beyer, A., Reucher, C.M.M., and Bolm, C. (2001). Potassium hydroxide/dimethyl sulfoxide promoted intramolecular cyclization for the synthesis of benzimidazol-2-ones. Org. Lett. *13*, 2876–2879.

Boursalian, G.B., Ham, W.S., Mazzotti, A.R., and Ritter, T. (2016). Charge-transfer-directed radical substitution enables *para*-selective C–H functionalization. Nat. Chem. *8*, 810–815.

Breslow, R.S., and Gellman, H. (1983). Intramolecular nitrene carbon-hydrogen insertions mediated by transition-metal complexes as nitrogen analogs of cytochrome P-450 reactions. J. Am. Chem. Soc. *105*, 6728–6729.

Chen, X.-W., Zhao, H., Chen, C.-L., Jiang, H.-F., and Zhang, M. (2017). Hydrogen-transfer-mediated α-functionalization of 1,8-naphthyridines by a strategy overcoming the over-hydrogenation barrier. Angew. Chem. Int. Ed. *56*, 14232–14236.

Diao, X., Wang, Y., Jiang, Y., and Ma, D. (2009). Assembly of substituted 1*H*-benzimidazoles and 1,3-dihydrobenzimidazol-2-ones via CuI/l-Proline catalyzed coupling of aqueous ammonia with 2-Iodoacetanilides and 2-iodophenylcarbamates. J. Org.Chem. *74*, 7974–7977.

Gao, X., Wang, P., Zeng, L., Tang, S., and Lei, A. (2018). Cobalt(II)-catalyzed electrooxidative C–H amination of arenes with alkylamines. J. Am. Chem. Soc. *140*, 4195–4199.

Kim, H., and Chang, S. (2017). The use of ammonia as an ultimate amino source in the transition metal-catalyzed C–H amination. Acc. Chem. Res. *50*, 482–486.

Kim, J.Y., Cho, S.H., Joseph, J., and Chang, S. (2010). Cobalt-and manganese-catalyzed direct amination of azoles under mild reaction conditions and the mechanistic details. Angew. Chem. Int. Ed. *49*, 9899–9903.

Kuethe, J.T., Wong, A., and Davies, I.W. (2004). Synthesis of disubstituted imidazo[4,5-*b*]pyridin-2-ones. J. Org. Chem. *69*, 7752–7754.

Li, Z., Sun, H., Jiang, H., and Liu, H. (2008). Copper-catalyzed intramolecular cyclization to N-substituted 1,3-dihydrobenzimidazol-2-ones. Org. Lett. *10*, 3263–3266.

Li, Z., Garcia-Dominguez, A., and Nevado, C. (2016). Nickel-catalyzed stereoselective dicarbofunctionalization of alkynes. Angew. Chem. Int. Ed. *55*, 6938–6941.

Li, L., Li, Z.L., Gu, Q.S., Wang, N., and Liu, X.Y. (2017). A remote C–C bond cleavage–enabled skeletal reorganization: access to medium-/large-sized cyclic alkenes. Sci. Adv. *3*, e17014870.

Liang, T., Tan, Z., Zhao, H., Chen, X., Jiang, H., and Zhang, M. (2018). Aerobic copper-catalyzed synthesis of benzimidazoles from diaryl- and alkylamines via tandem triple C–H aminations. ACS Catal. *8*, 2242–2246.

Liu, Y.Y., Yang, X.H., Song, R.J., Luo, S., and Li, J.H. (2017). Oxidative 1,2-carboamination of alkenes with alkyl nitriles and amines toward γ-amino alkyl nitriles. Nat. Commun. *8*, 14720–14725.

Liu, Z., Zhang, X., Virelli, M., Zanoni, G., Anderson, E.A., and Bi, X. (2018). Silver-catalyzed regio- and stereoselective formal carbene insertion into unstrained C–Cσ-bonds of 1,3-dicarbonyls. iScience *8*, 54–60.

Margrey, K.A., Levens, A., and Nicewicz, D.A. (2017). Direct aryl C–H amination with primary amines using organic photoredox catalysis. Angew. Chem. Int. Ed. *56*, 15644–15648.

Mastalerz, M., and Oppel, I. (2012). Rational construction of an extrinsic porous molecular crystal with an extraordinary high specific surface area. Angew. Chem. Int. Ed. *51*, 5252–5255.

Mir, A.A., Matsumura, S., Hlil, A.R., and Hay, A.S. (2012). Synthesis and properties of polymers containing 2*H*-benzimidazol-2-one moieties: polymerization via N–C coupling reactions. ACSMacro Lett. *1*, 194–197.

Monforte, A.-M., Logoteta, P., Ferro, S., De Luca, L., Iraci, N., Maga, G., De Clercq, E., Pannecouque, C., and Chimirri, A. (2009). Design, synthesis, and structure–activity relationships of 1,3-dihydrobenzimidazol-2-one analogues as anti-HIV agents. Bioorg. Med. Chem. *17*, 5962–5967.

Monforte, A.-M., Logoteta, P., De Luca, L., Iraci, N., Ferro, S., Maga, G., DeClerq, E., Pannecouque, C., and Chimirri, A. (2010). Novel 1,3-dihydro-benzimidazol-2-ones and their analogues as potent non-nucleoside HIV-1 reverse transcriptase inhibitors. Bioorg. Med. Chem. *18*, 1702–1710.

Nale, D.B., and Bhanage, B.M. (2015). Copper-catalyzed efficient synthesis of a 2-benzimidazolone scaffold from 2-nitroaniline and dimethyl carbonate *via* a hydrosilylation reaction. Green. Chem. *17*, 2480–2486.

Ouyang, L., Li, J., Zheng, J., Huang, J., Qi, C., Wu, W., and Jiang, H. (2017). Access to α-amino acid esters through palladium-catalyzed oxidative amination of vinyl ethers with hydrogen peroxide as the oxidant and oxygen source. Angew. Chem. Int. Ed. *56*, 15926–15930.

Palin, R., Clark, J.K., Evans, L., Houghton, A.K., Jones, P.S., Prosser, A., Wishart, G., and Yoshiizumi, K. (2008). Structure–activity relationships and CoMFA of N-3 substituted phenoxypropyl piperidine benzimidazol-2-one analogues as NOP receptor agonists with analgesic properties. Bioorg. Med. Chem. *16*, 2829–2851.

Park, Y., Kim, Y., and Chang, S. (2017). Transition metal-catalyzed C–H amination: scope, mechanism, and applications. Chem. Rev. *117*, 9247–9301.

Paudyal, M.P., Adebesin, A.M., Burt, S.R., Ess, D.H., Ma, Z., Kürti, L., and Falck, J.R. (2016).

Dirhodium-catalyzed C–H arene amination using hydroxylamines. Science *353*, 1144–1147.

Qin, C., Su, Y., Shen, T., Shi, X., and Jiao, N. (2016). Splitting a substrate into three parts: gold-catalyzed nitrogenation of alkynes by C–C and C≡C bond cleavage. Angew. Chem. Int. Ed. *55*, 350–354.

Rao, C.Q., Mai, S.Y., and Song, Q.L. (2017). Cu-catalyzed synthesis of 3-formyl imidazo[1,2-*a*] pyridines and Imidazo[1,2-*a*]pyrimidines by employing ethyl tertiary amines as carbon sources. Org. Lett. *19*, 4726–4729.

Ren, R., Zhao, H., Huan, L., and Zhu, C. (2015). Manganese-catalyzed oxidative azidation of cyclobutanols: regiospecific synthesis of alkyl azides by C−C bond cleavage. Angew. Chem. Int. Ed. *54*, 12692–12696.

Ren, R., Wu, Z., Xu, Y., and Zhu, C. (2016). C−C bond-forming strategy by manganese-catalyzed oxidative ring-opening cyanation and ethynylation of cyclobutanol derivatives. Angew. Chem. Int. Ed. *55*, 2866–2869.

Romero, N.A., Margrey, K.A., Tay, N.E., and Nicewicz, D.A. (2015). Site-selective arene C−H amination via photoredox catalysis. Science *349*, 1326–1330.

Roque, J.B., Kuroda, Y., Gottemann, L.T., and Sarpong, R. (2018a). Deconstructive fluorination of cyclic amines by carbon-carbon cleavage. Science *361*, 171–174.

Roque, J.B., Kuroda, Y., Gottemann, L.T., and Sarpong, R. (2018b). Deconstructive diversification of cyclic amines. Nature *564*, 244–248.

Rubinstein, A., Jimenez-Lozanao, P., Carbo, J.J., Poblet, J.M., and Neumann, R. (2014). Aerobic carbon–carbon bond cleavage of alkenes to aldehydes catalyzed by first-row transition-metal-substituted polyoxometalates in the presence of nitrogen dioxide. J. Am. Chem. Soc. *136*, 10941–10948.

Sagadevan, A., Charpe, V.P., Ragupathi, A., and Hwang, K.C. (2017). Visible light copper photoredox-catalyzed aerobic oxidative coupling of phenols and terminal alkynes: regioselective synthesis of functionalized ketones via C≡C triple bond cleavage. J. Am. Chem. Soc. *139*, 2896–2899.

Shen, T., Wang, T., Qin, C., and Jiao, N. (2013). Silver-catalyzed nitrogenation of alkynes: a direct approach to nitriles through C≡C bond cleavage. Angew. Chem. Int. Ed. *52*, 6677–6680.

Shen, T., Zhang, Y., Liang, Y.F., and Jiao, N. (2016). Direct tryptophols synthesis from 2-vinylanilines and alkynes via C≡C triple bond cleavage and dioxygen activation. J. Am. Chem. Soc. *138*, 13147–13150.

Tang, S., Wang, S., Liu, Y., Cong, H., and Lei, A. (2018). Electrochemical oxidative C−H amination of phenols: access to triarylamine derivatives. Angew. Chem. Int. Ed. *57*, 4737–4741.

Urgoitia, G., SanMartin, R., Herrero, M.T., and Domínguez, E. (2017). Aerobic cleavage of alkenes and alkynes into carbonyl and carboxyl compounds. ACS Catal. *7*, 3050–3060.

Wang, P., Li, G.-C., Jain, P., Faimer, M.E., He, J., Shen, P.-X., and Yu, J.-Q. (2016). Ligand-promoted *meta*-C–H amination and alkynylation. J. Am. Chem. Soc. *138*, 14092–14099.

Wang, H.-W., Lu, Y., Zhang, B., He, J., Xu, H.-J., Kang, Y.-S., Sun, W.-Y., and Yu, J.-Q. (2017a). Ligand-promoted rhodium(III)-catalyzed *ortho*-C−H amination with free amines. Angew. Chem. Int. Ed. *56*, 7449–7453.

Wang, C.S., Wu, X.F., Dixneuf, P.H., and Soulé, J.F. (2017b). Copper-catalyzed oxidative dehydrogenative C(sp^3)−H bond amination of (cyclo)alkanes using NH-heterocycles as amine sources. ChemSusChem *10*, 3075–3082.

Wertz, S., Kodama, S., and Studer, A. (2011). Amination of benzoxazoles and 1,3,4-oxadiazoles using 2,2,6,6-tetramethylpiperidine-N-oxoammonium tetrafluoroborate as an organic oxidant. Angew. Chem. Int. Ed. *50*, 11511–11515.

Wu, T., Mu, X., and Liu, G. (2011). Palladium-catalyzed oxidative arylalkylation of activated alkenes: dual C−H bond cleavage of an arene and acetonitrile. Angew. Chem. Int. Ed. *50*, 12578–12581.

Wu, J., Zhou, Y., Zhou, Y., Chiang, C.-W., and Lei, A. (2017). Electro-oxidative C(sp^3)–H amination of azoles via intermolecular oxidative C(sp^3)–H/N–H cross-coupling. ACS Catal. *7*, 8320–8323.

Xie, F., Xie, R., Zhang, J.-X., Jiang, H.-F., Du, L., and Zhang, M. (2017). Direct reductive quinolyl *β*-C–H alkylation by multispherical cavity carbon-supported cobalt oxide nanocatalysts. ACS Catal. *7*, 4780–4785.

Xie, F., Chen, Q.H., Xie, R., Jiang, H.F., and Zhang, M. (2018). MOF-derived nanocobalt for oxidative functionalization of cyclic amines to quinazolinones with 2-aminoarylmethanols. ACS Catal. *8*, 5869–5874.

Xie, F., Lu, G.-P., Xie, R., Chen, Q.-H., Jiang, H.-F., and Zhang, M. (2019). MOF-derived subnanometer cobalt catalyst for selective C−H oxidative sulfonylation of tetrahydroquinoxalines with sodium sulfinates. ACS. Catal. *9*, 2718–2724.

Yang, Y., Song, R.J., Ouyang, X.H., Wang, C.Y., Li, J.H., and Luo, S. (2017). Iron-catalyzed intermolecular 1,2-difunctionalization of styrenes and conjugated alkenes with silanes and nucleophiles. Angew. Chem. Int. Ed. *56*, 7916–7919.

Yin, G., Wu, Y., and Liu, G.S. (2010). Scope and mechanism of allylic C−H amination of terminal alkenes by the palladium/PhI$(OPiv)_2$ catalyst system: insights into the effect of naphthoquinone. J. Am. Chem. Soc. *132*, 11978–11987.

Youn, S.W., and Kim, Y.H. (2016). Pd(II)/Ag(I)-promoted one-pot synthesis of cyclic ureas from (hetero)aromatic amines and isocyanates. Org. Lett. *18*, 6140–6143.

Yu, J., Gao, C., Song, Z., Yang, H., and Fu, H. (2015). Metal-free oxidative C–H amidation of N,N′-diarylureas with PhI$(OAc)_2$: synthesis of benzimidazol-2-one derivatives. Eur. J. Org. Chem. *26*, 5869–5875.

Yu, J., Yan, H., and Zhu, C. (2016). Synthesis of multiply substituted polycyclic aromatic hydrocarbons by iridium-catalyzed annulation of ring-fused benzocyclobutenol with alkyne through C−C bond cleavage. Angew. Chem. Int. Ed. *55*, 1143–1146.

Zhang, W., Chen, P., and Liu, G. (2017). Enantioselective palladium(II)-catalyzed intramolecular aminoarylation of alkenes by dual N−H and aryl C−H bond cleavage. Angew. Chem. Int. Ed. *56*, 5336–5340.

Zhao, H., Fan, X., Yu, J., and Zhu, C. (2015). Silver-catalyzed ring-opening strategy for the synthesis of *β*- and *γ*-fluorinated ketones. J. Am. Chem. Soc. *137*, 3490–3493.

Zhao, H., Zhao, S., Li, X., Deng, Y.-Y., Jiang, H.-F., and Zhang, M. (2019). Cobalt-catalyzed selective functionalization of aniline derivatives with hexafluoroisopropanol. Org. Lett. *21*, 218–222.

Zou, B., Yuan, Q., and Ma, D. (2007). Cascade coupling/cyclization process to N-substituted 1,3-dihydrobenzimidazol-2-ones. Org. Lett. *9*, 4291–4294.

Łukasik, E., and Wróbel, Z. (2016). Aryliminophosphoranes as key intermediates in the one-pot synthesis of 1-aryl-1,3-dihydro-2*H*-benzimidazol-2-ones from *N*-aryl-2-nitrosoanilines and carbon dioxide under mild metal-free conditions. Synthesis *48*, 1159–1166.

ISCI, Volume *15*

Supplemental Information

Synthesis of Multisubstituted Benzimidazolones via Copper-Catalyzed Oxidative Tandem C–H Aminations and Alkyl Deconstructive Carbofunctionalization

Taoyuan Liang, He Zhao, Lingzhen Gong, Huanfeng Jiang, and Min Zhang

Copies of product NMR spectra

Figure S1. ^{1}H-NMR (400 MHz, $CDCl_3$) spectrum of **4aaa**, related to **Scheme 3**.

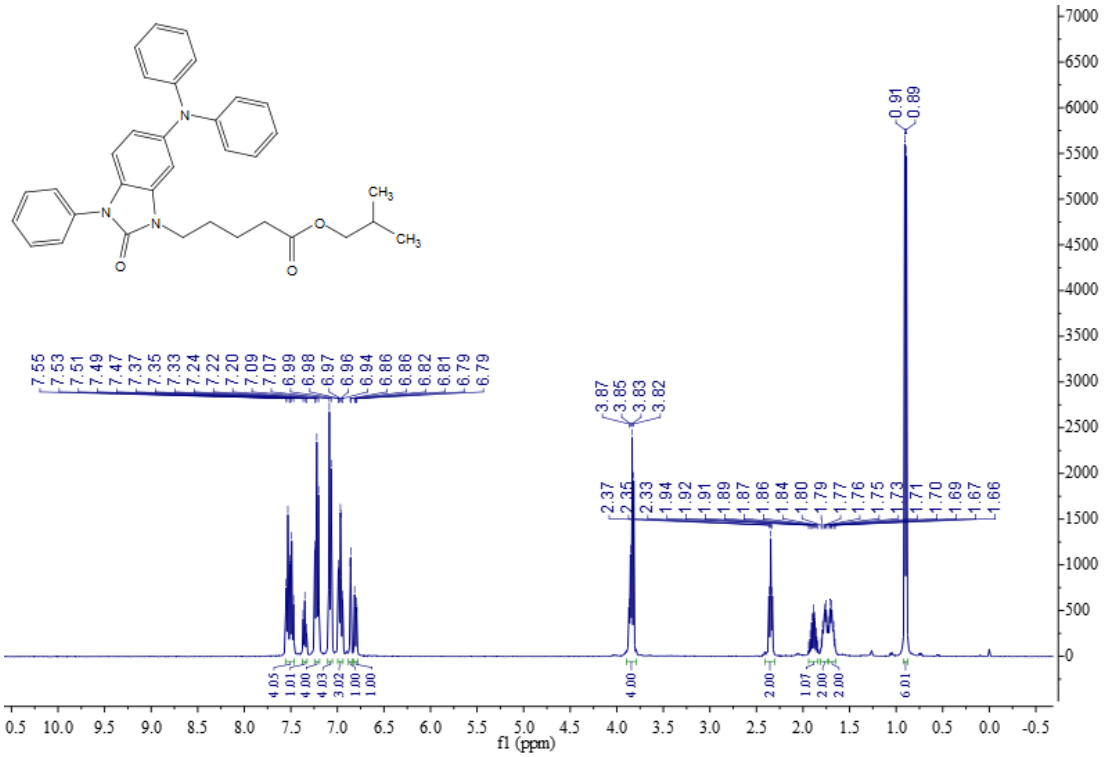

Figure S2. ^{13}C-NMR (100 MHz, $CDCl_3$) spectrum of **4aaa**, related to **Scheme 3**.

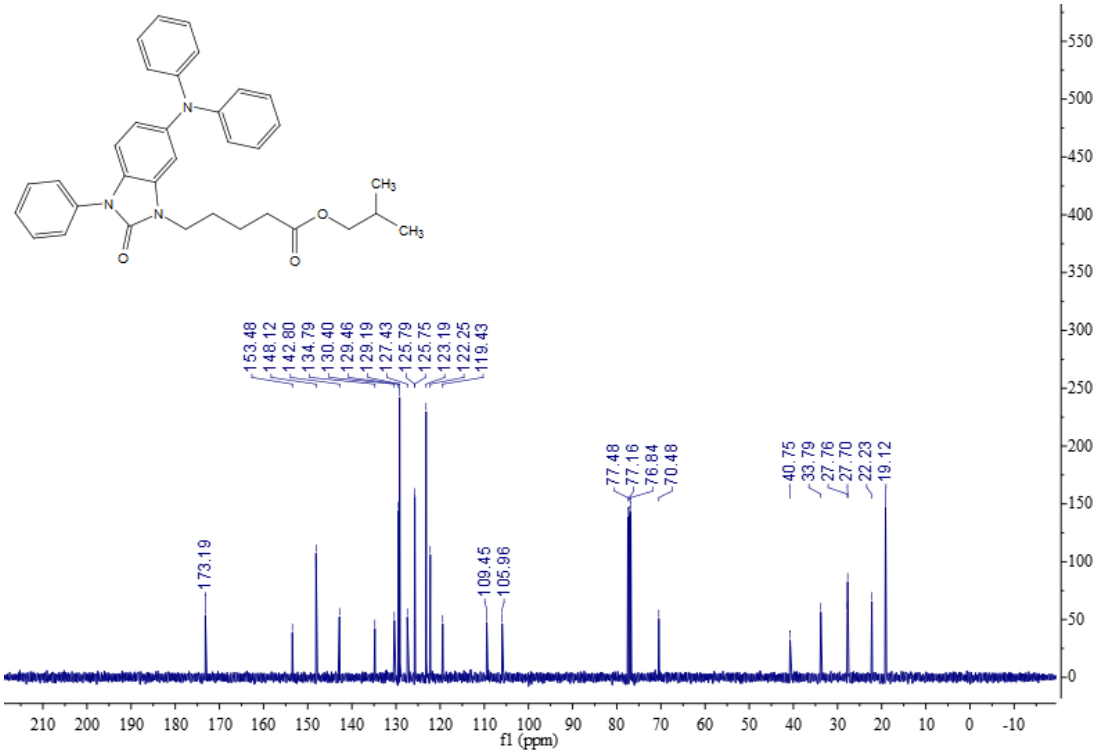

Figure S3. ^{1}H-NMR (400 MHz, $CDCl_3$) spectrum of **4baa**, related to **Scheme 3**.

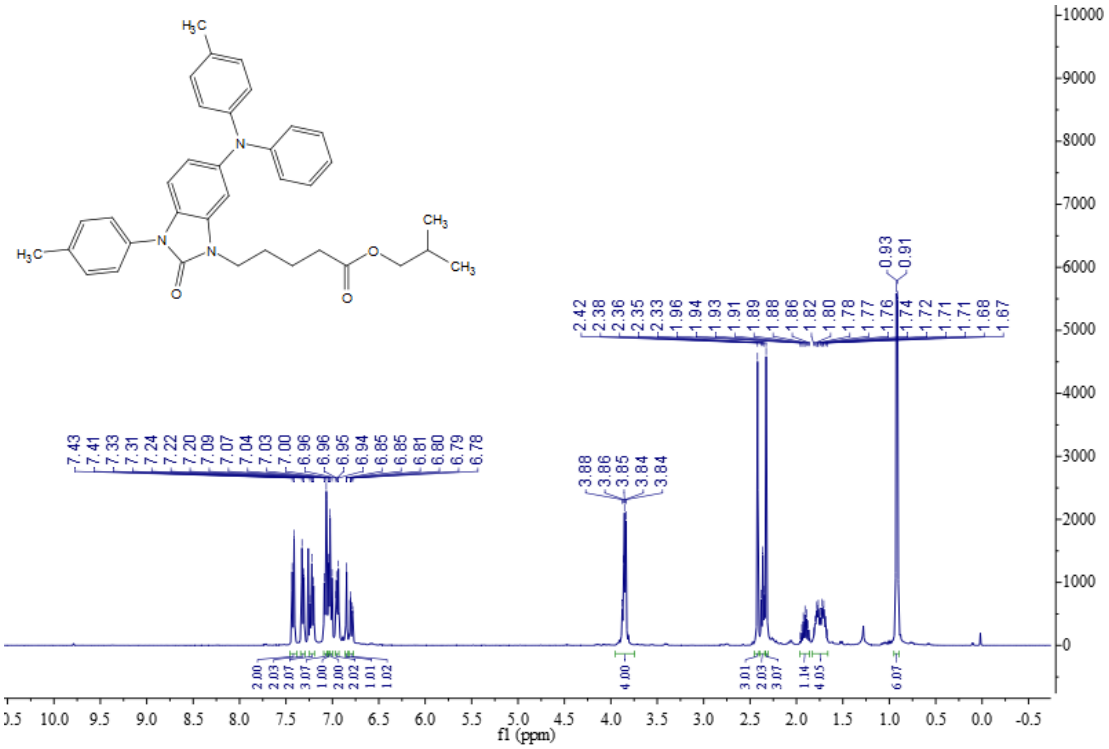

Figure S4. ^{13}C-NMR (100 MHz, $CDCl_3$) spectrum of **4baa**, related to **Scheme 3**.

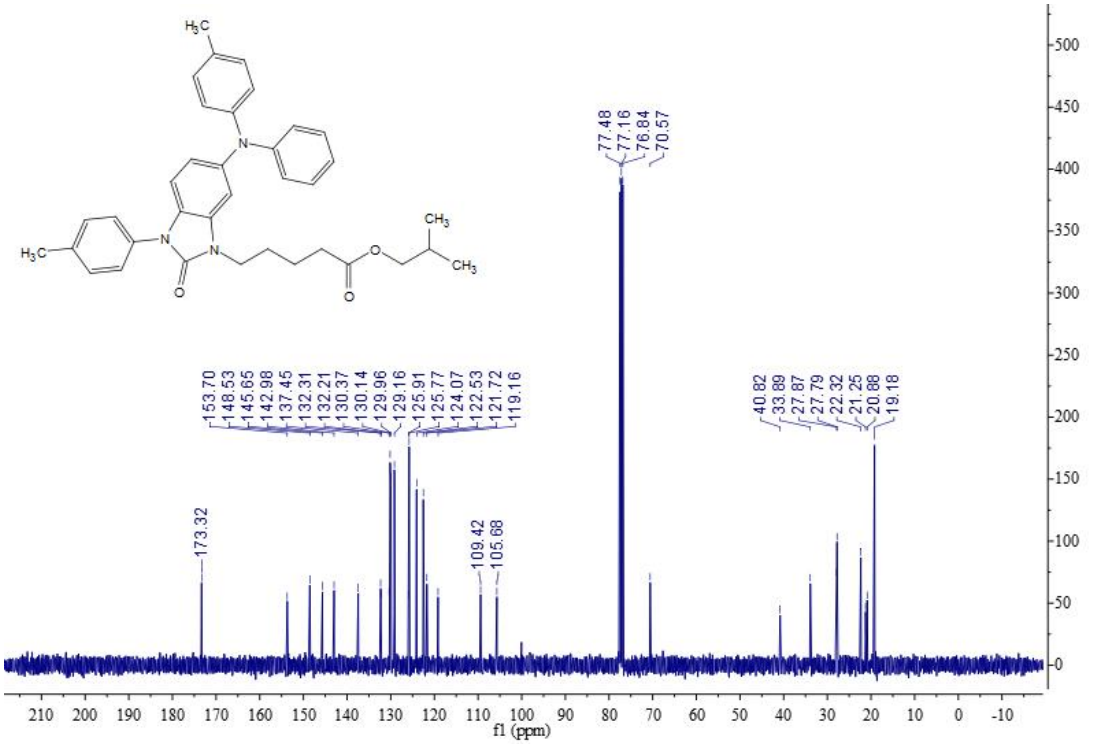

Figure S5. ^{1}H-NMR (400 MHz, $CDCl_3$) spectrum of **4caa**, related to **Scheme 3**.

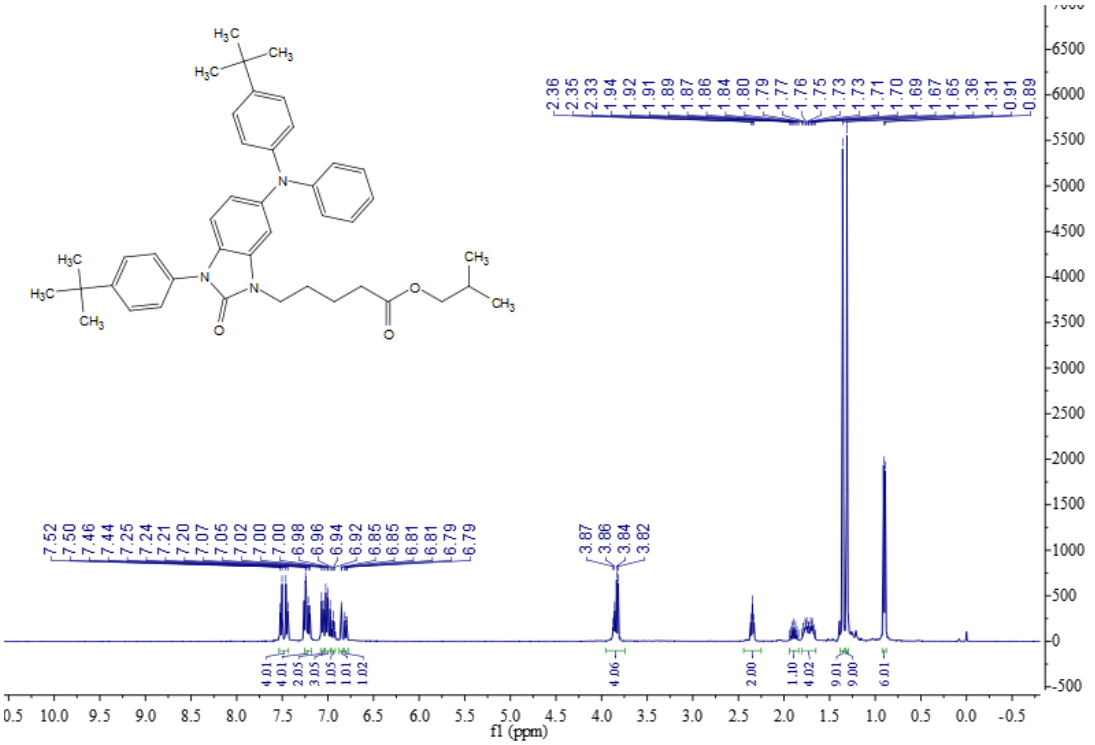

Figure S6. ^{13}C-NMR (100 MHz, $CDCl_3$) spectrum of **4caa**, related to **Scheme 3**.

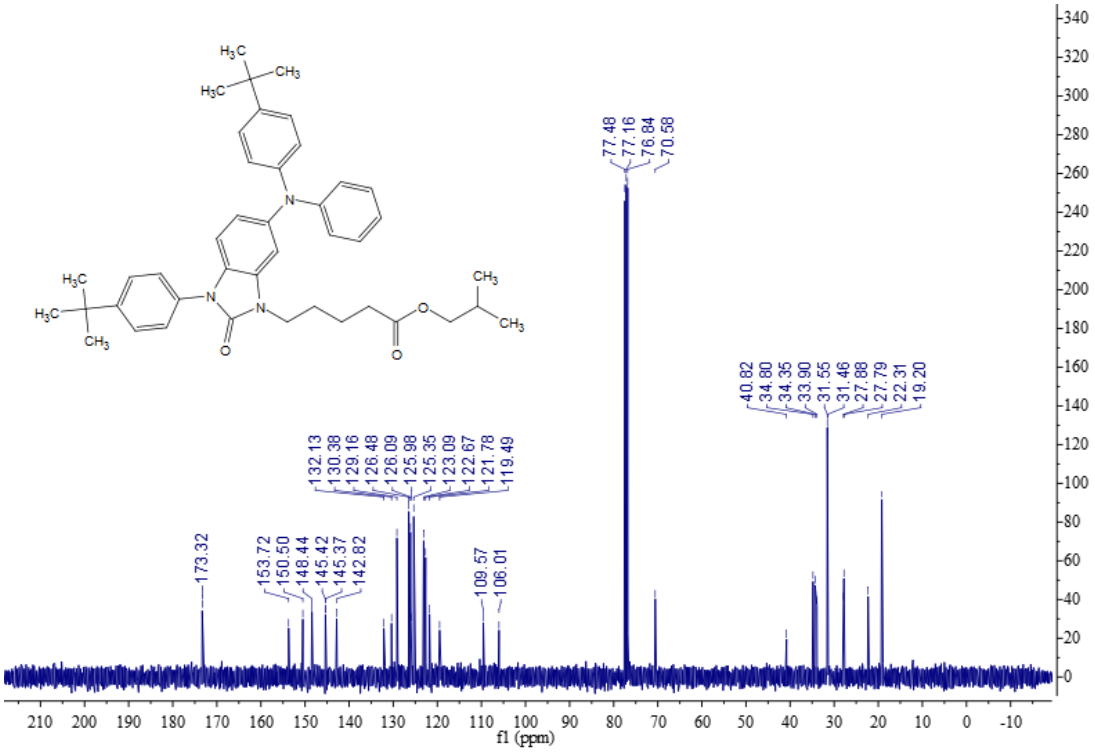

Figure S7. ^{1}H-NMR (400 MHz, $CDCl_3$) spectrum of **4daa**, related to **Scheme 3**.

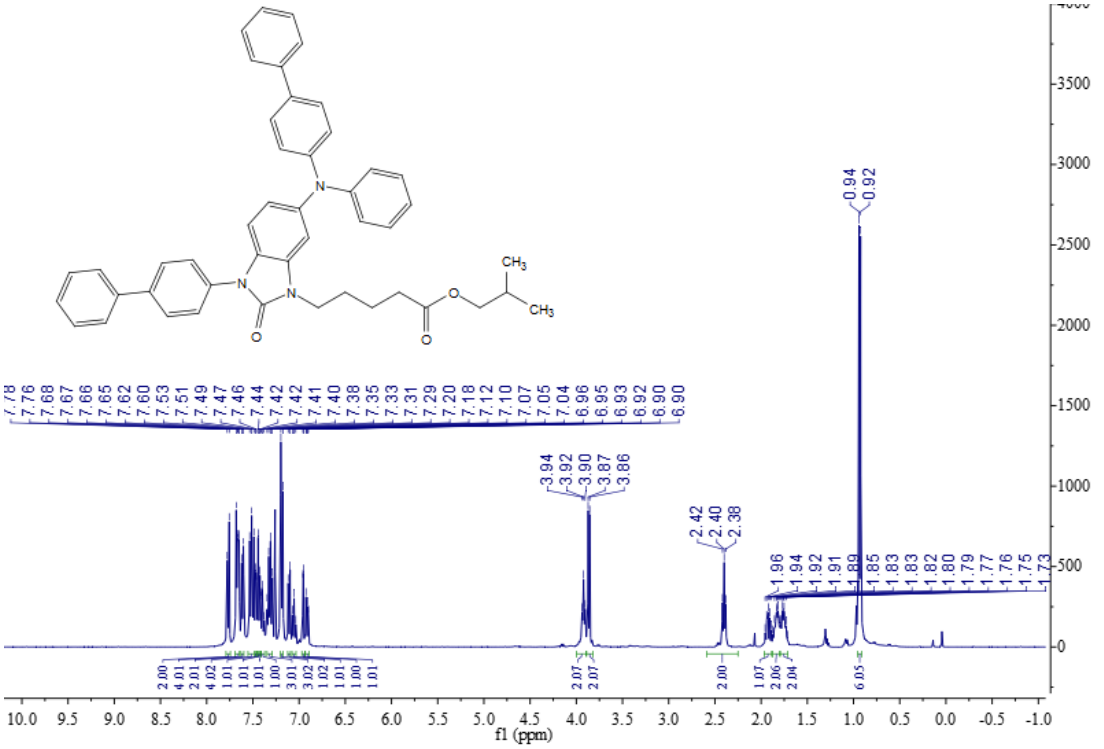

Figure S8. ^{13}C-NMR (100 MHz, $CDCl_3$) spectrum of **4daa**, related to **Scheme 3**.

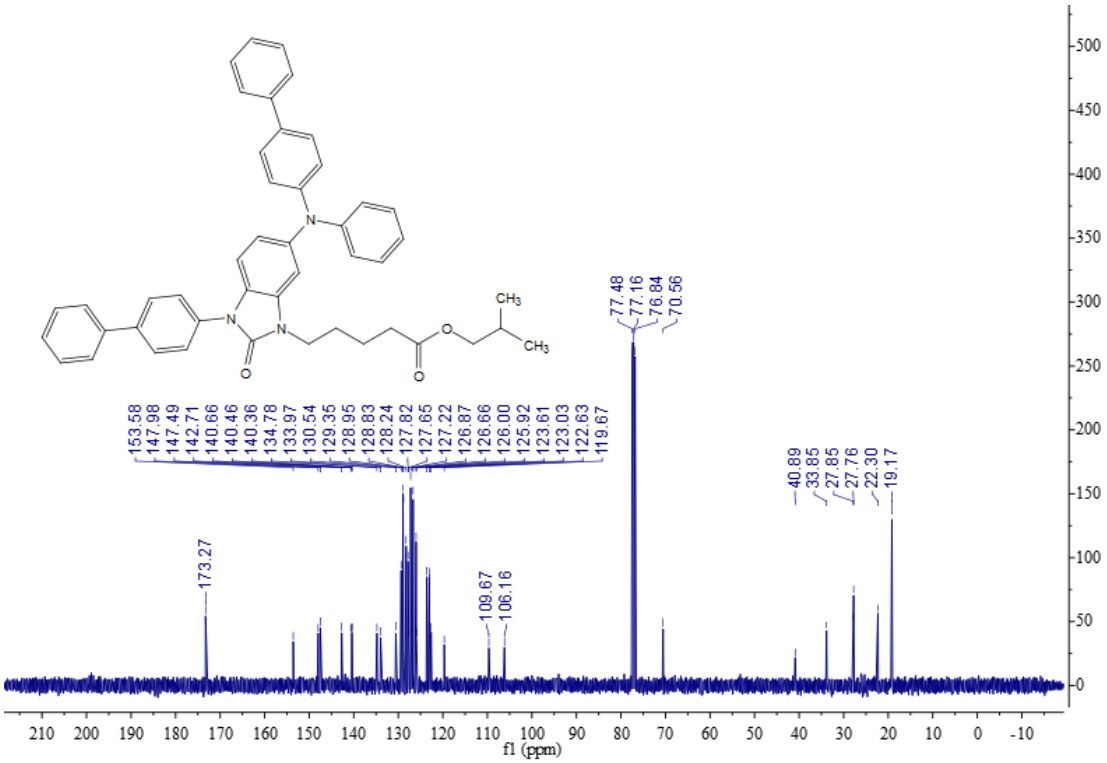

Figure S9. ^{1}H-NMR (400 MHz, $CDCl_3$) spectrum of **4eaa**, related to **Scheme 3**.

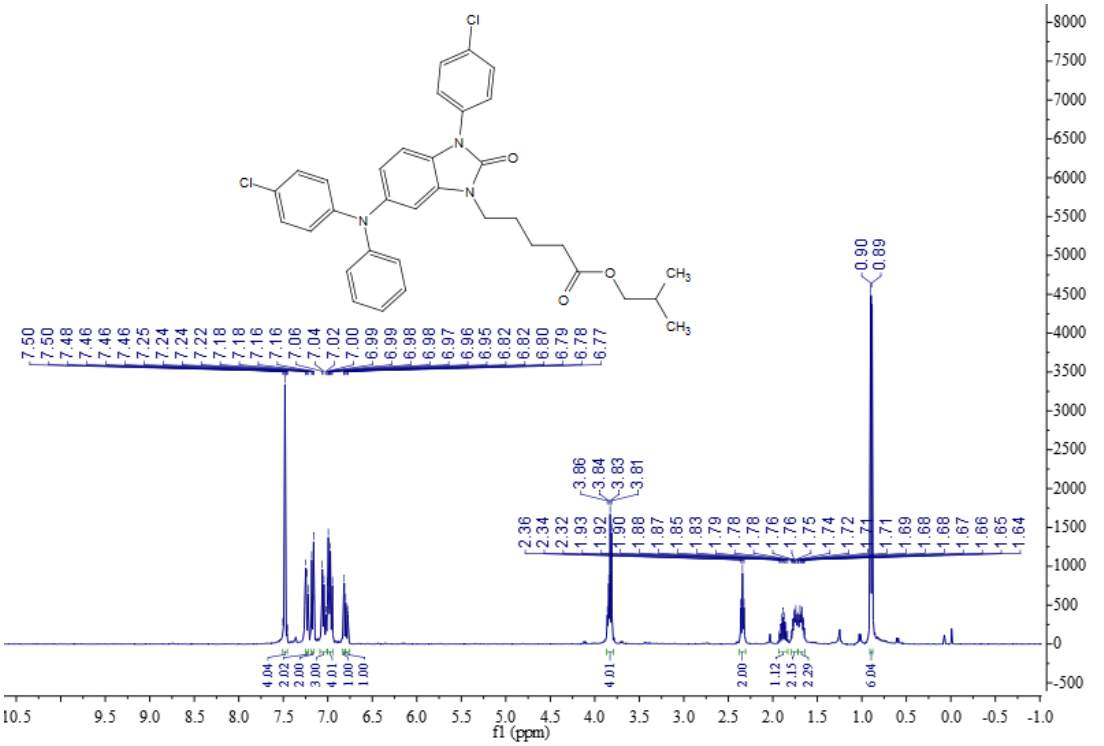

Figure S10. ^{13}C-NMR (100 MHz, $CDCl_3$) spectrum of **4eaa**, related to **Scheme 3**.

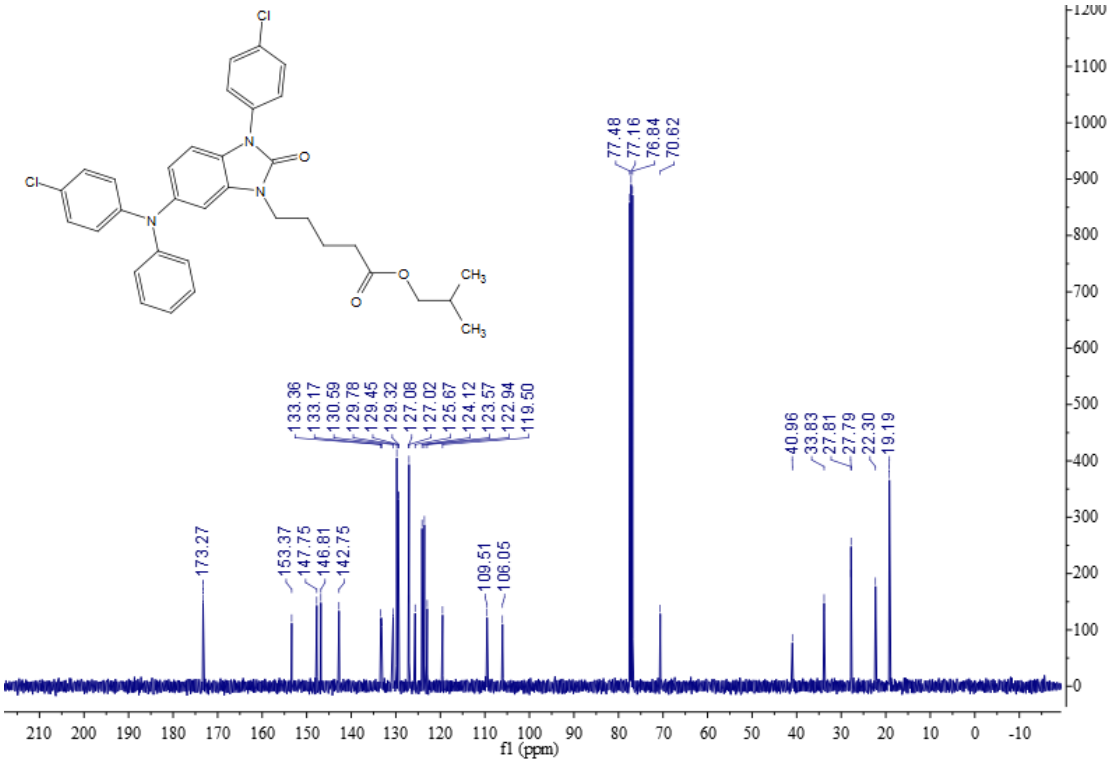

Figure S11. ^{1}H-NMR (400 MHz, $CDCl_3$) spectrum of **4faa**, related to **Scheme 3**.

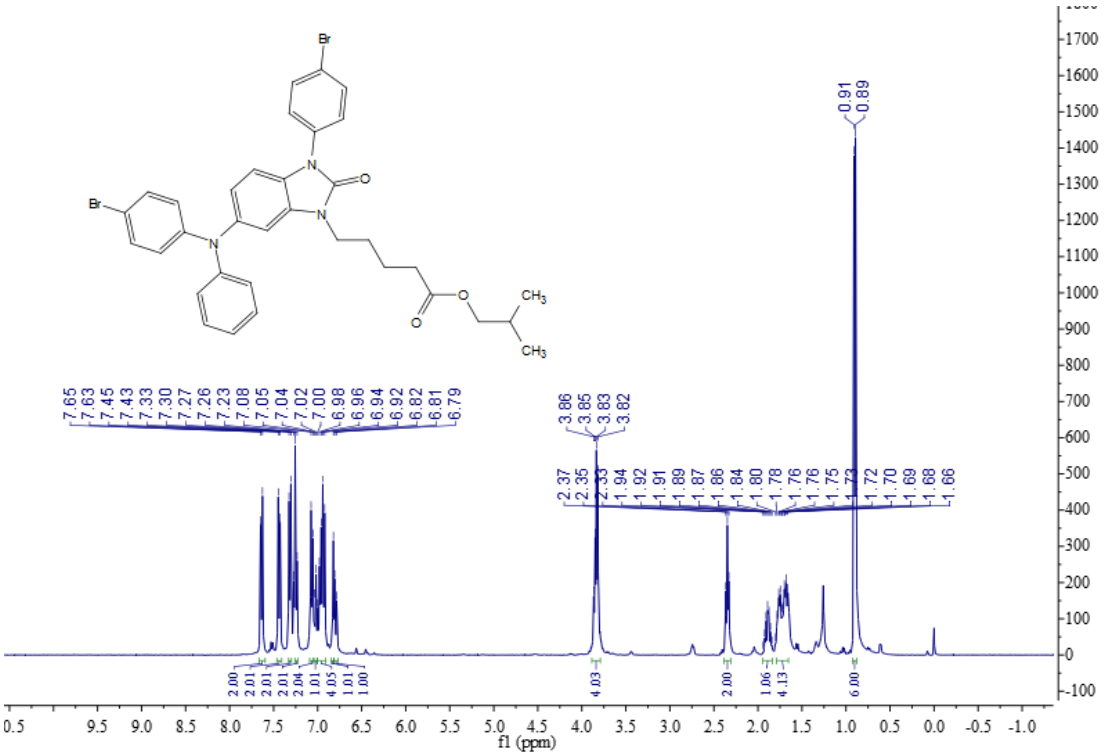

Figure S12. ^{13}C-NMR (100 MHz, $CDCl_3$) spectrum of **4faa**, related to **Scheme 3**.

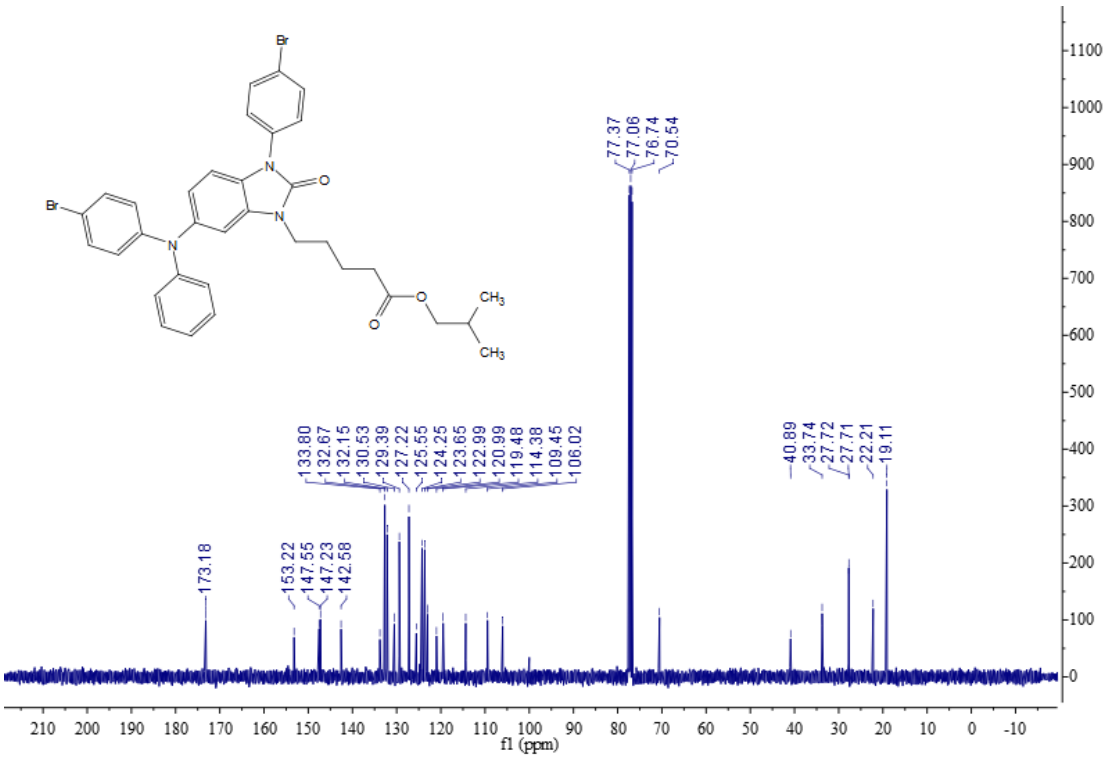

Figure S13. ^{1}H-NMR (400 MHz, $CDCl_3$) spectrum of **4gaa**, related to **Scheme 3**.

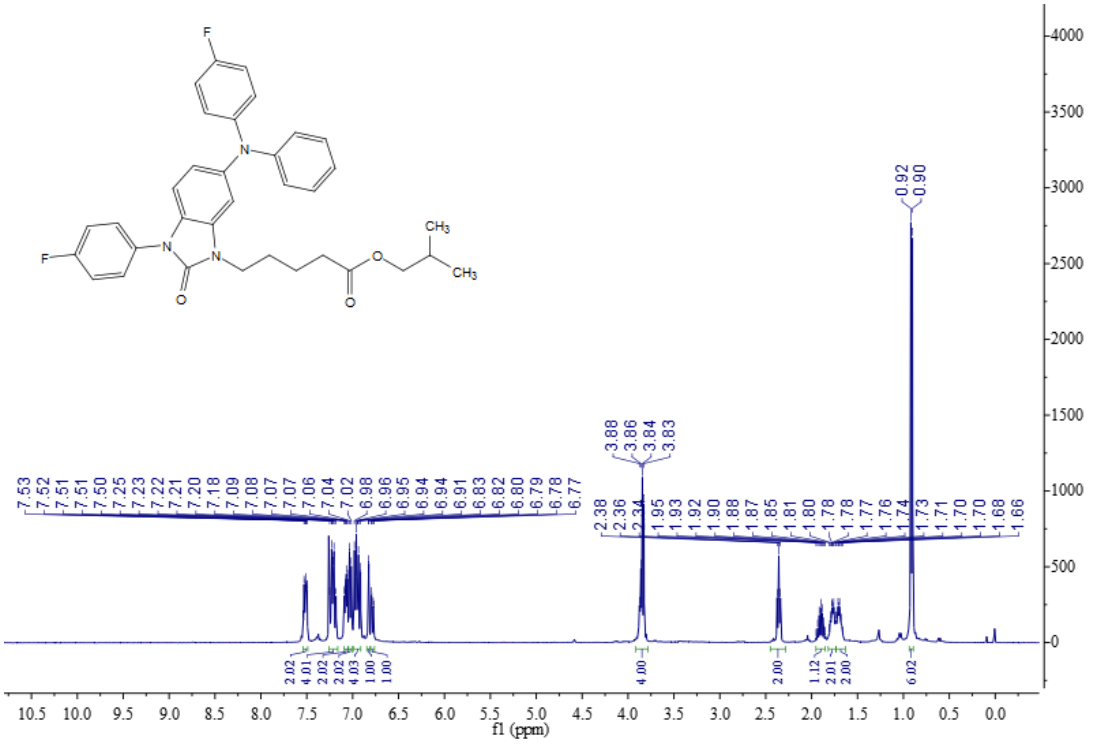

Figure S14. ^{13}C-NMR (100 MHz, $CDCl_3$) spectrum of **4gaa**, related to **Scheme 3**.

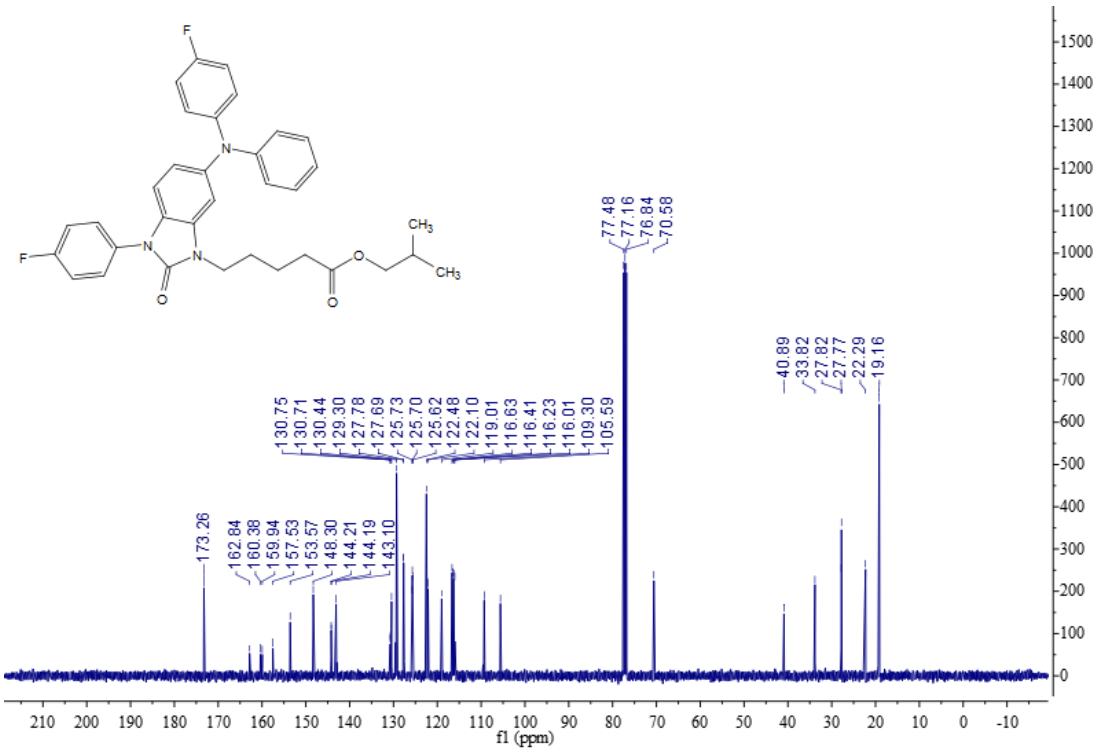

Figure S15. ^{19}F-NMR (376 MHz, $CDCl_3$) spectrum of **4gaa**, related to **Scheme 3**.

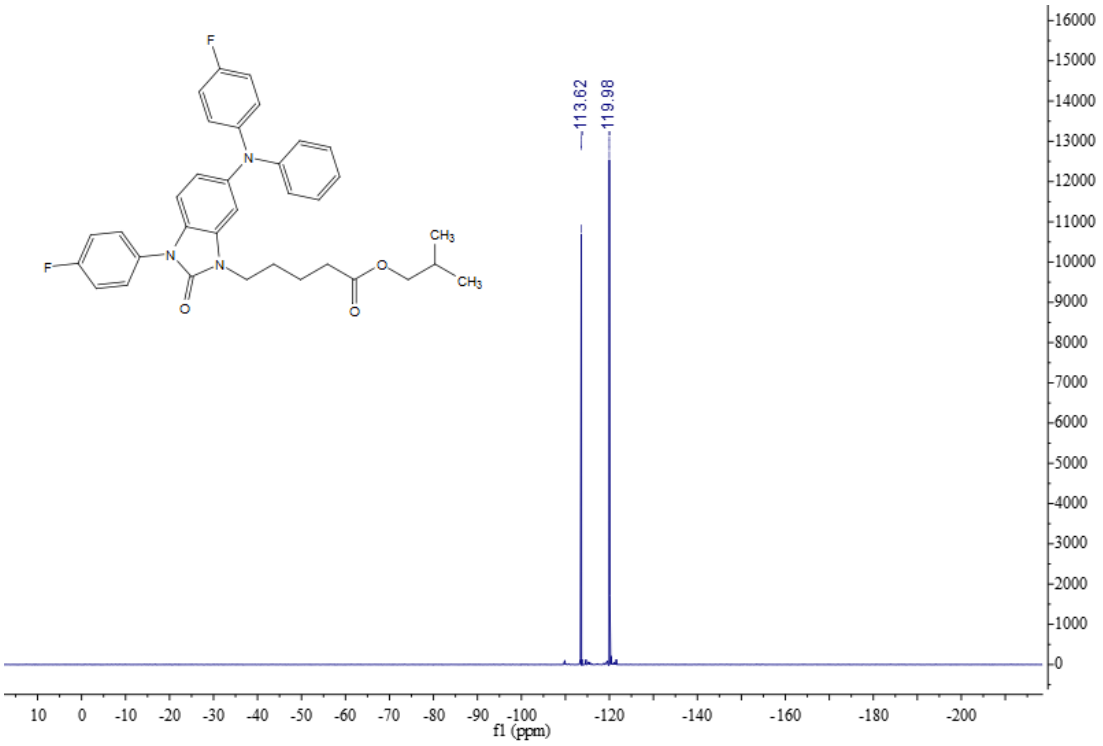

Figure S16. ^{1}H-NMR (400 MHz, $CDCl_3$) spectrum of **4haa**, related to **Scheme 3**.

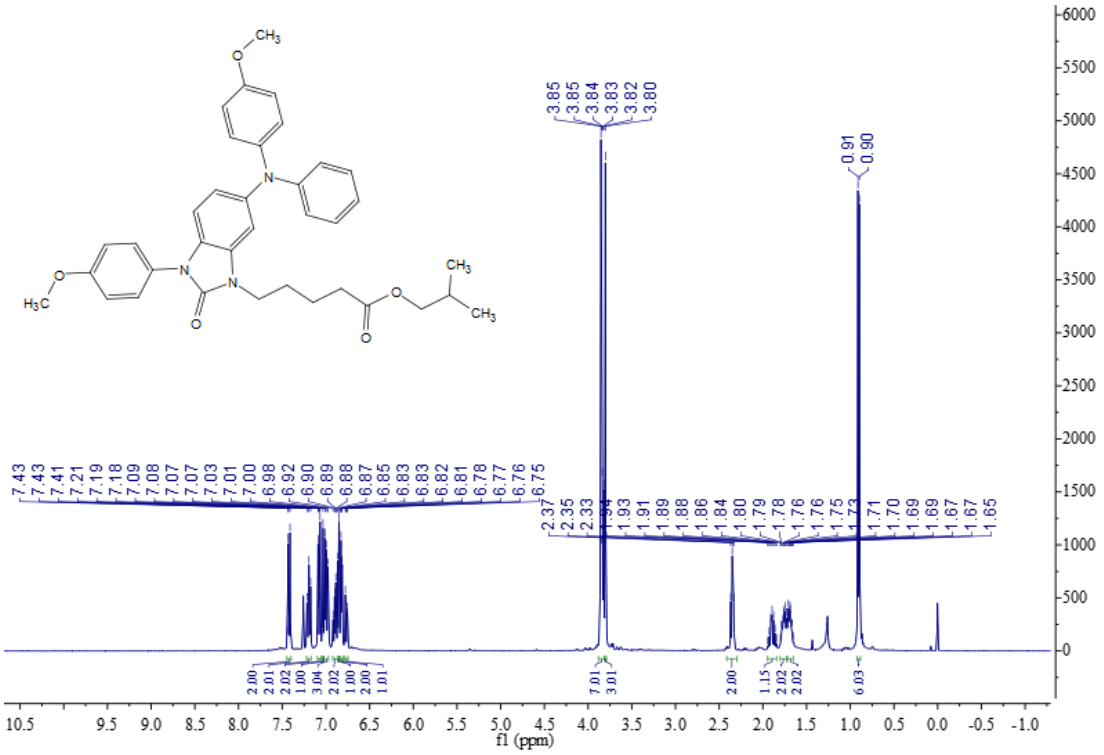

Figure S17. ^{13}C-NMR (100 MHz, $CDCl_3$) spectrum of **4haa**, related to **Scheme 3**.

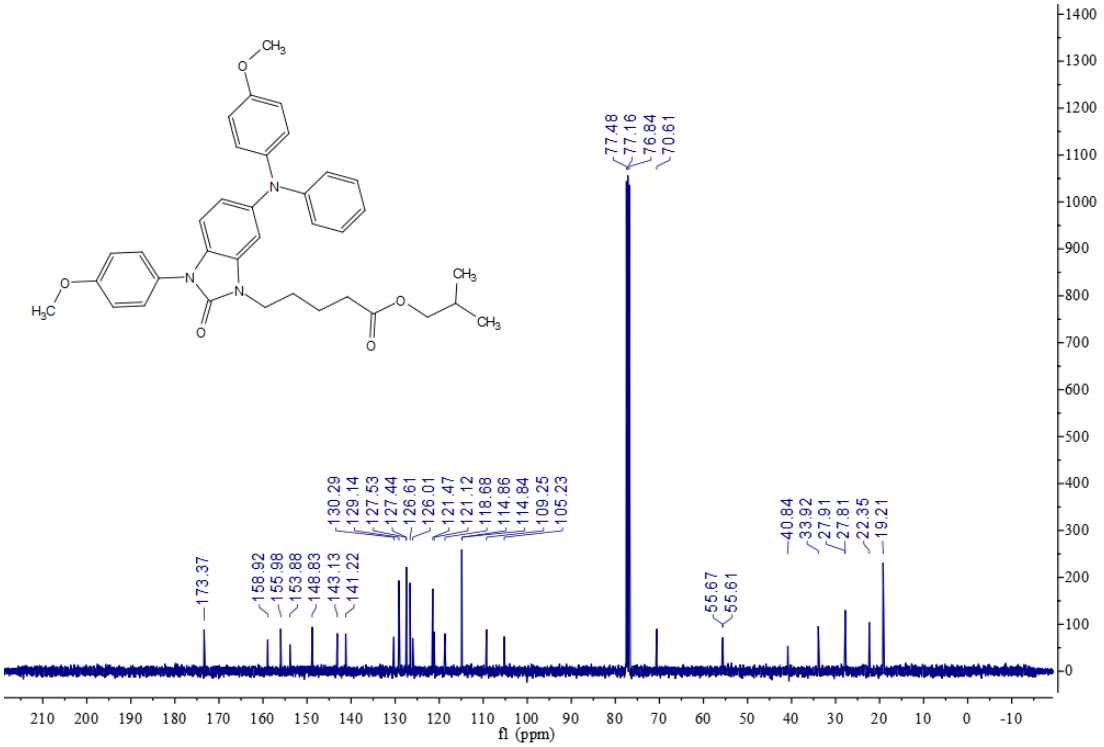

Figure S18. ^{1}H-NMR (400 MHz, $CDCl_3$) spectrum of **4aba**, related to **Scheme 3**.

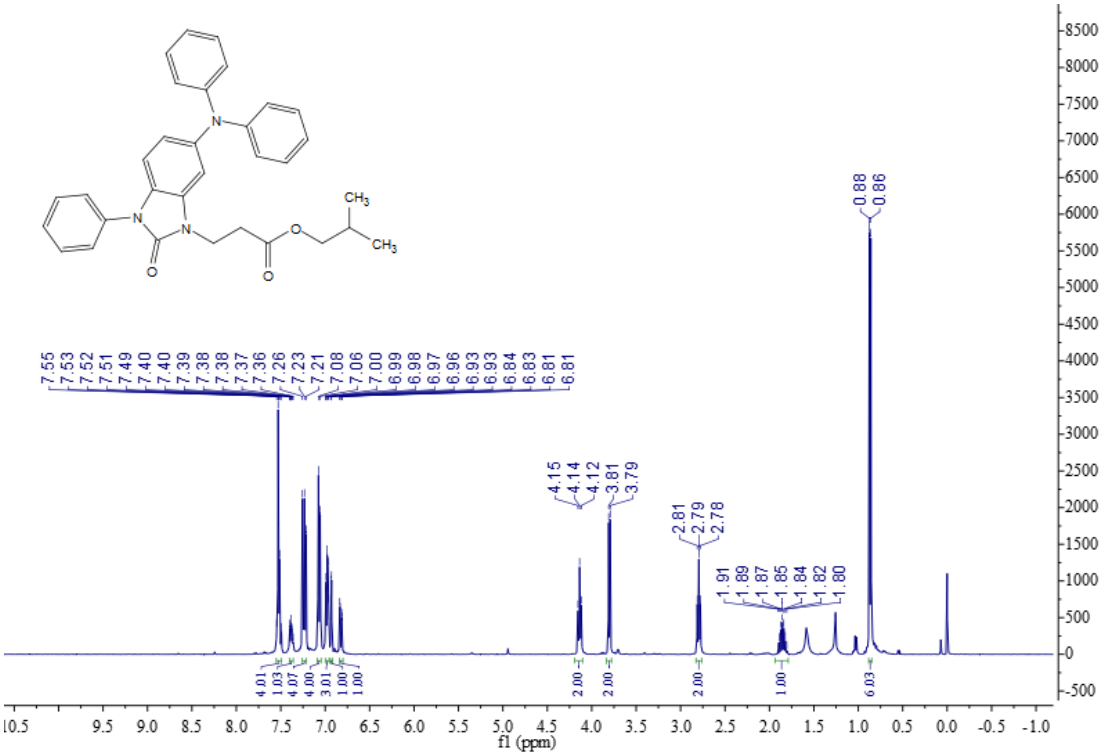

Figure S19. ^{13}C-NMR (100 MHz, $CDCl_3$) spectrum of **4aba**, related to **Scheme 3**.

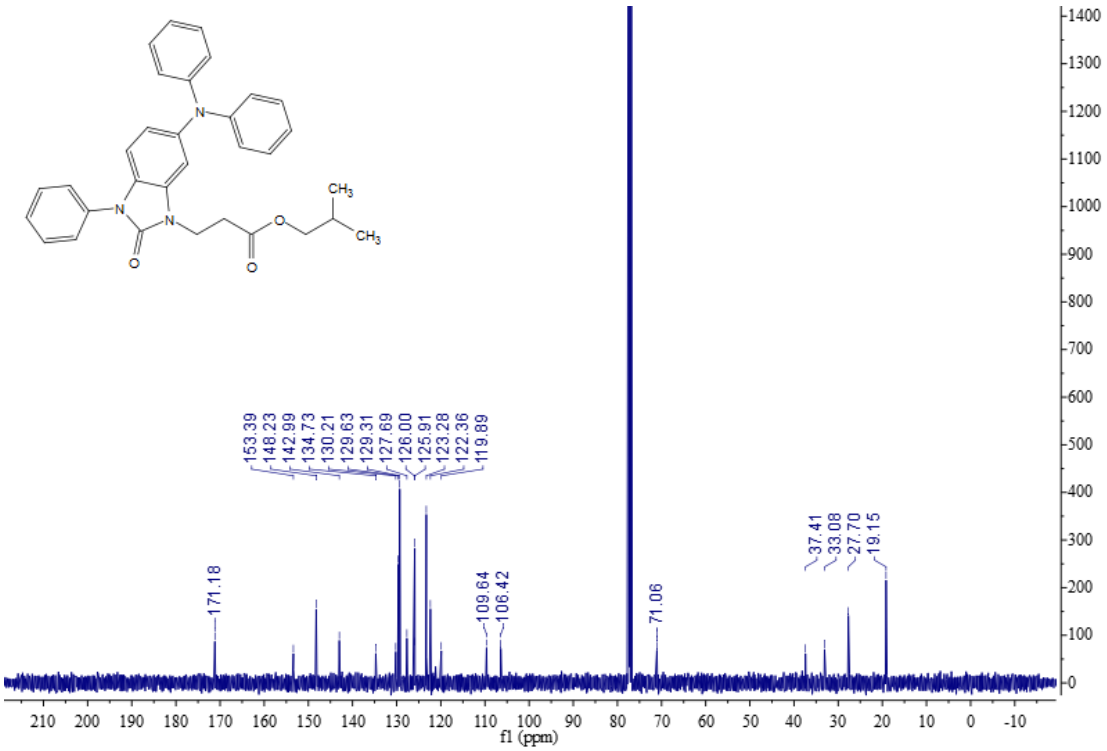

Figure S20. ^{1}H-NMR (400 MHz, $CDCl_3$) spectrum of **4aca**, related to **Scheme 3**.

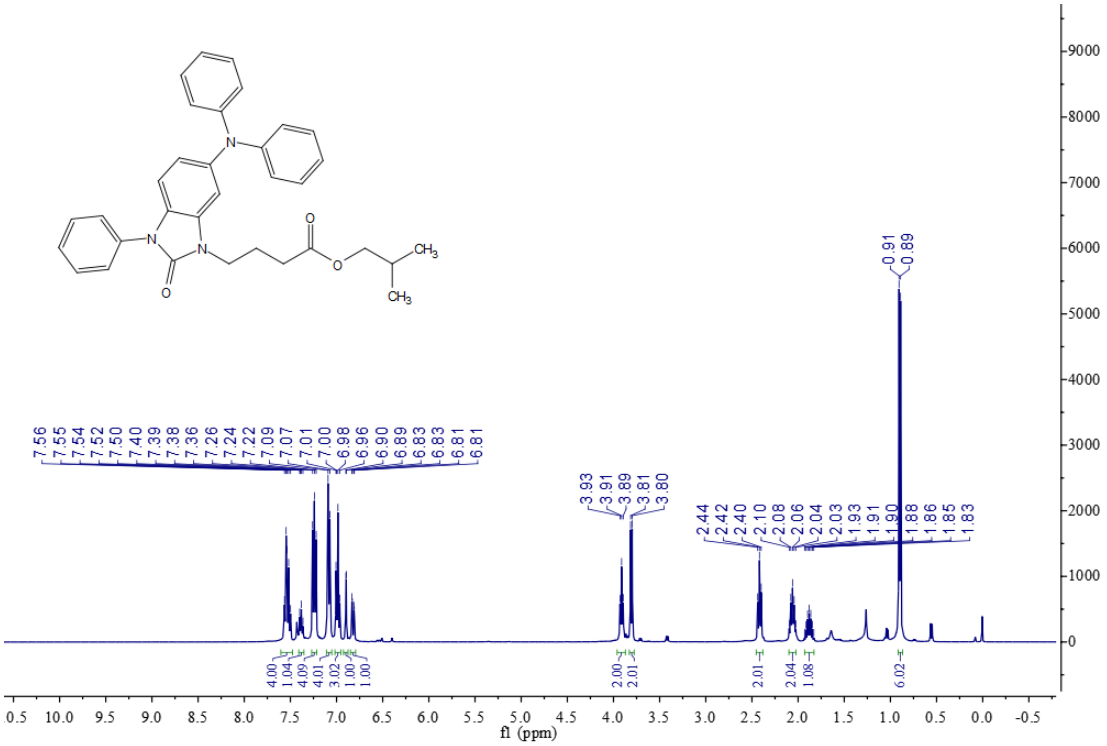

Figure S21. ^{13}C-NMR (100 MHz, $CDCl_3$) spectrum of **4aca**, related to **Scheme 3**.

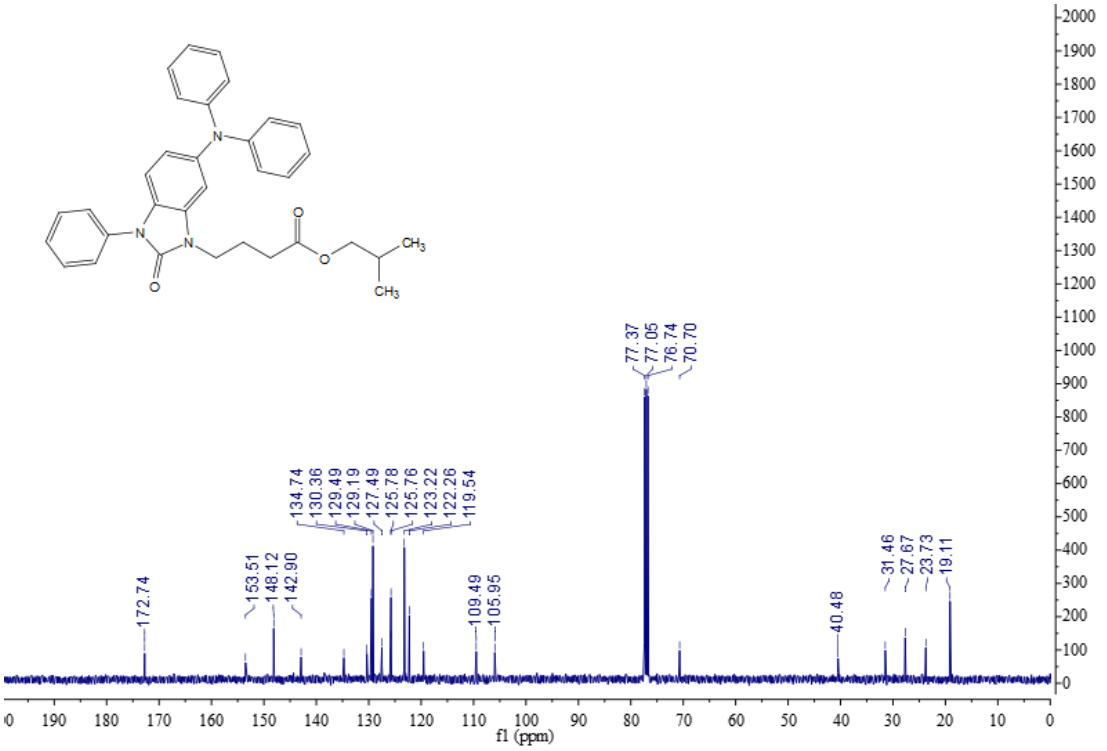

Figure S22. ^{1}H-NMR (400 MHz, $CDCl_3$) spectrum of **4ada**, related to **Scheme 3**.

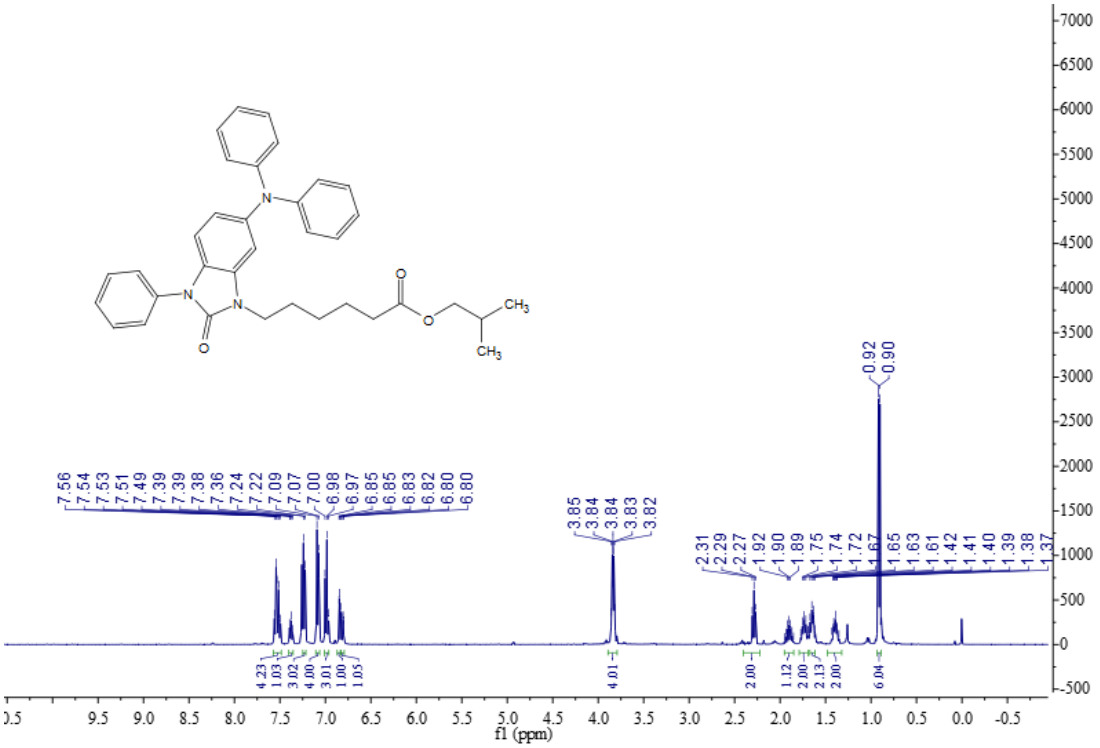

Figure S23. ^{13}C-NMR (100 MHz, $CDCl_3$) spectrum of **4ada**, related to **Scheme 3**.

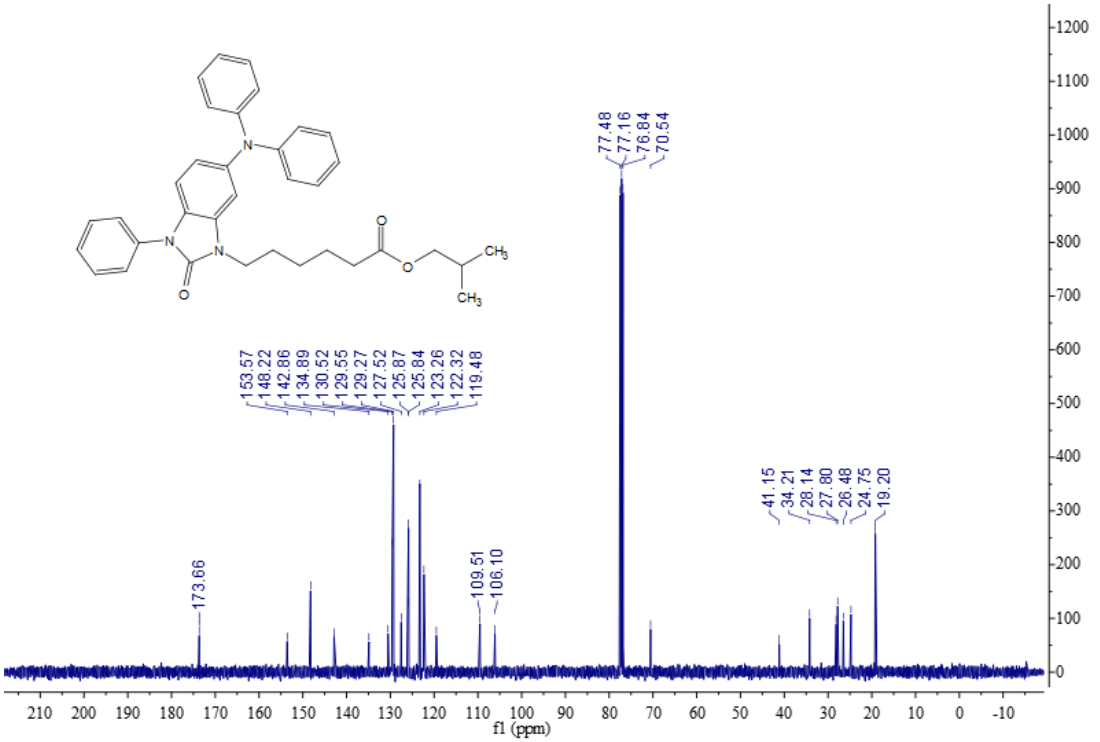

Figure S24. ^{1}H-NMR (400 MHz, $CDCl_3$) spectrum of **4aea**, related to **Scheme 3**.

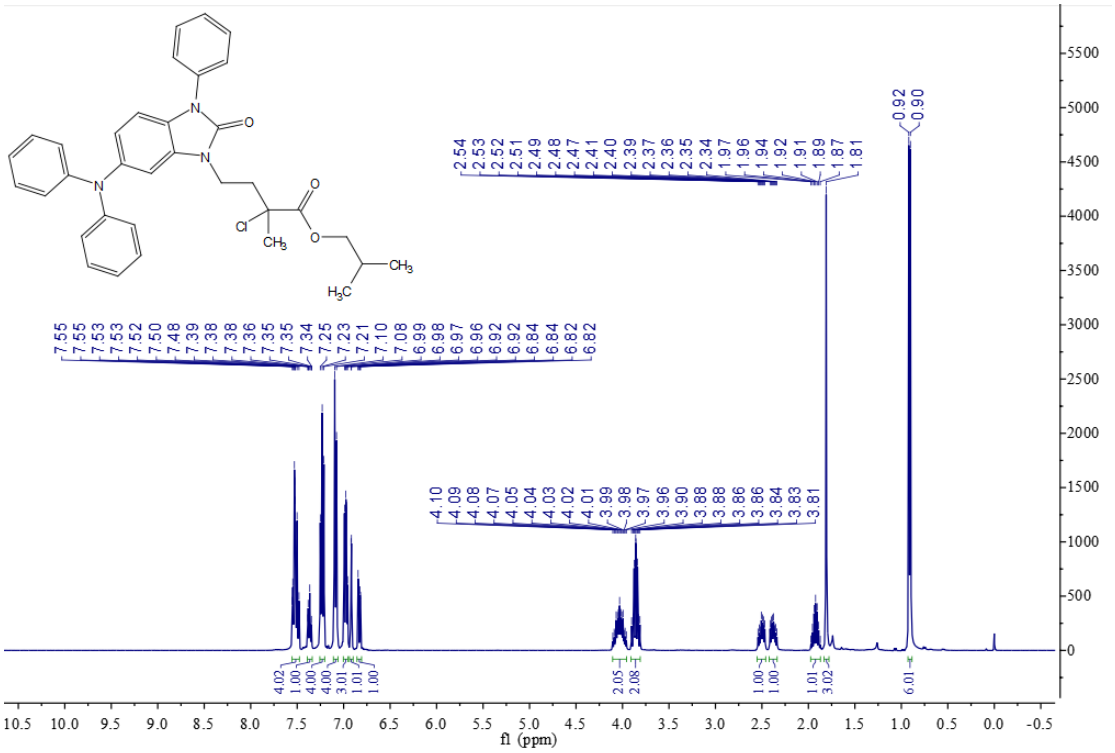

Figure S25. ^{13}C-NMR (100 MHz, $CDCl_3$) spectrum of **4aea**, related to **Scheme 3**.

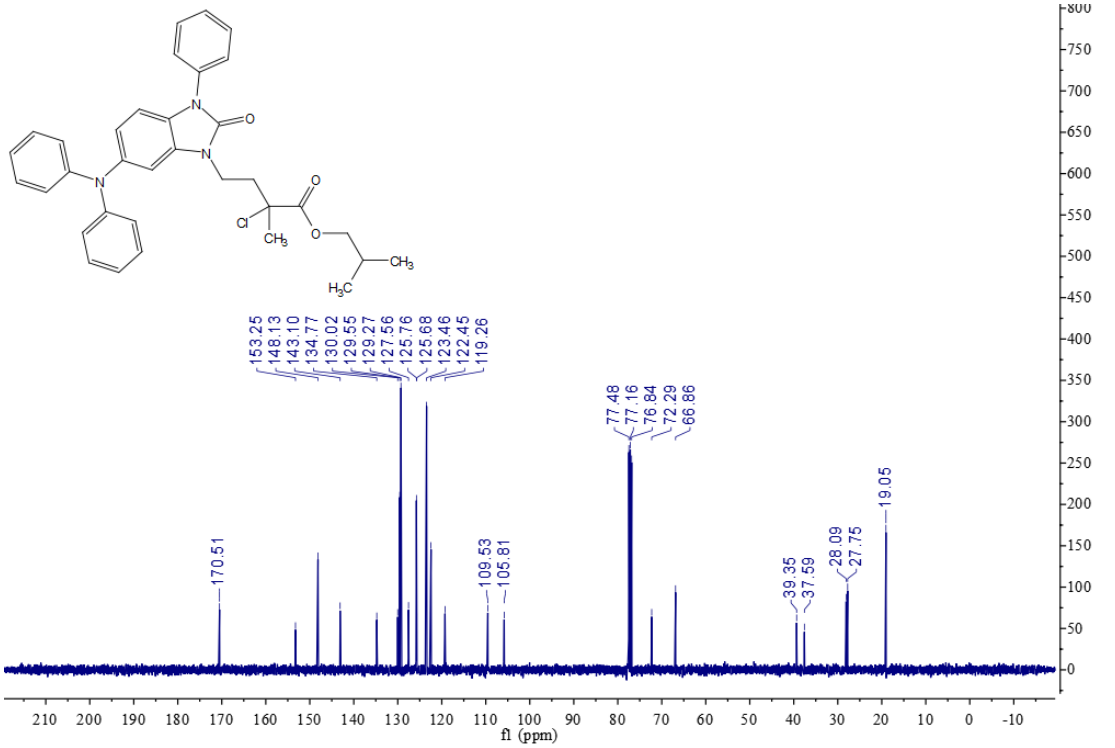

Figure S26. ^{1}H-NMR (400 MHz, $CDCl_3$) spectrum of **4aab**, related to **Scheme 3**.

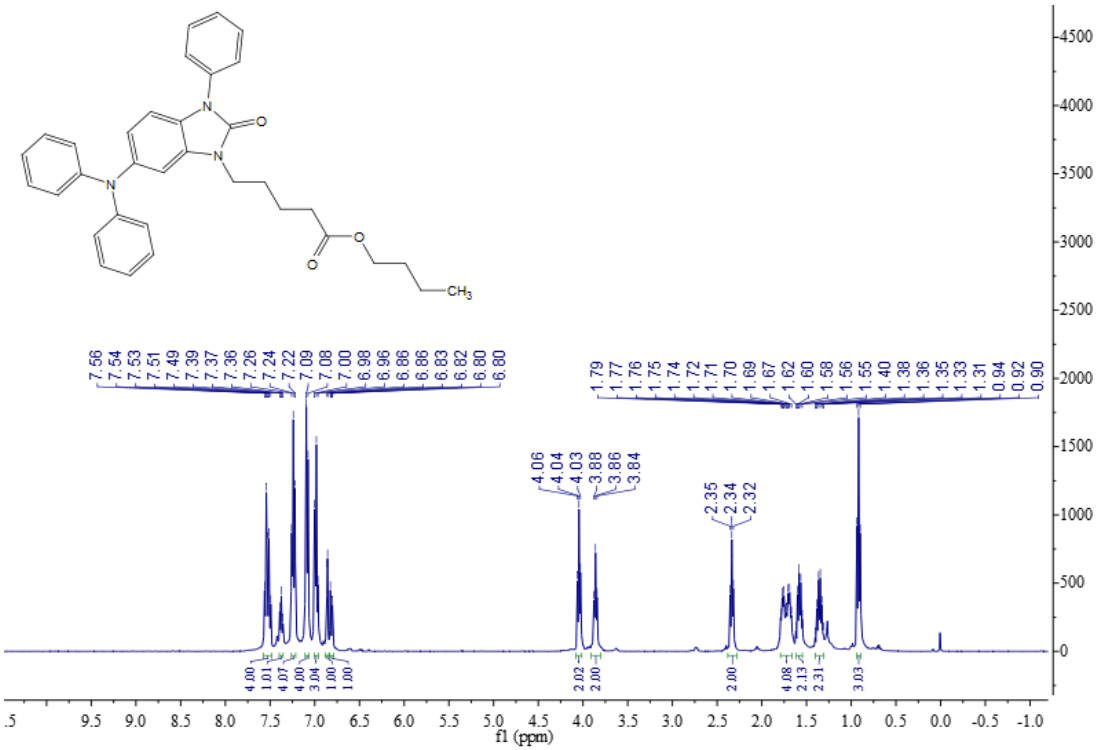

Figure S27. ^{13}C-NMR (100 MHz, $CDCl_3$) spectrum of **4aab**, related to **Scheme 3**.

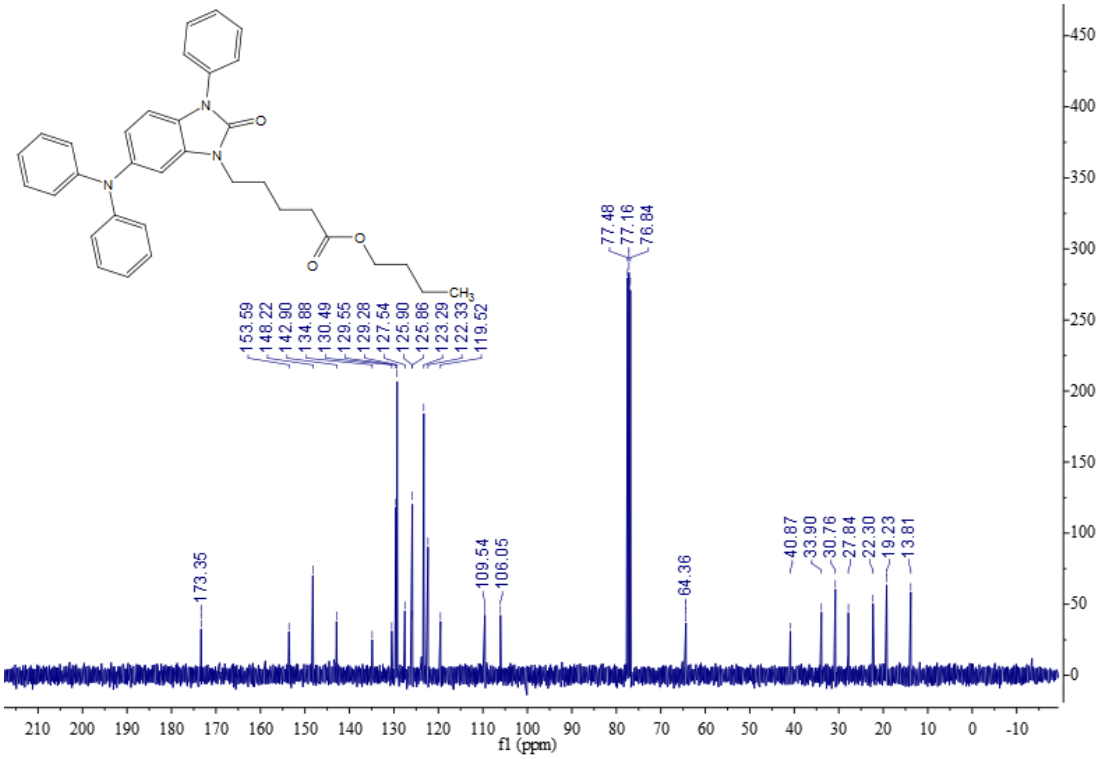

Figure S28. ^{1}H-NMR (400 MHz, $CDCl_3$) spectrum of **4aac**, related to **Scheme 3**.

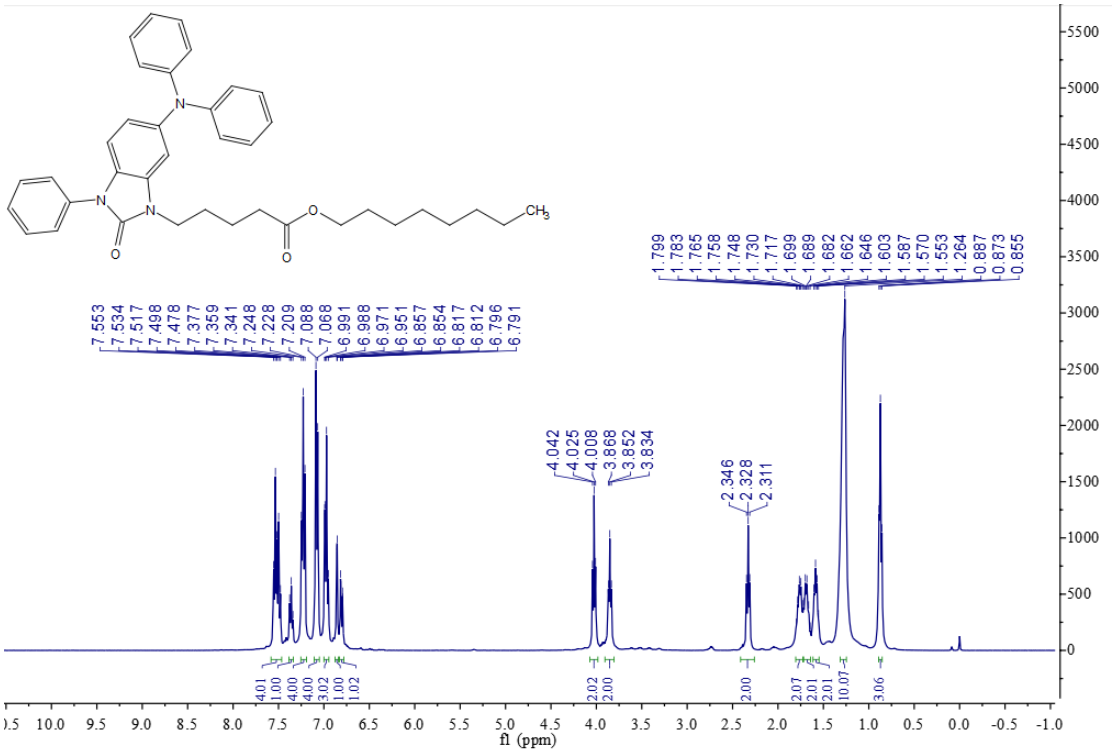

Figure S29. ^{13}C-NMR (100 MHz, $CDCl_3$) spectrum of **4aac**, related to **Scheme 3**.

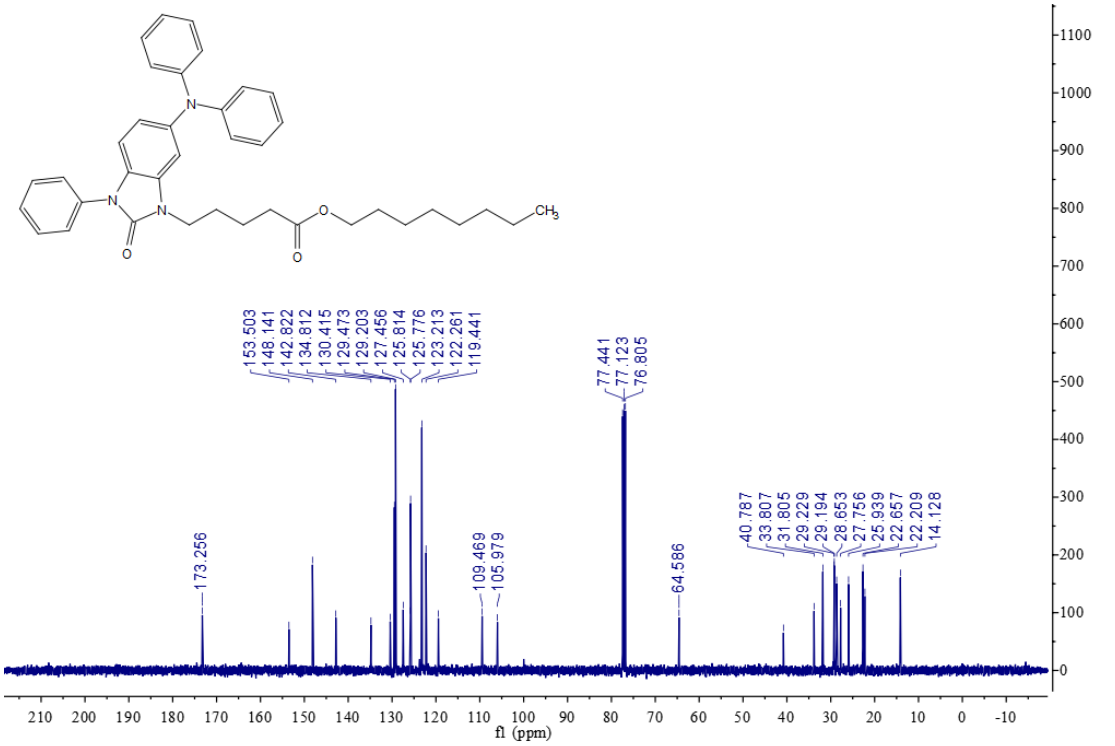

Figure S30. ^{1}H-NMR (400 MHz, $CDCl_3$) spectrum of **4aad**, related to **Scheme 3**.

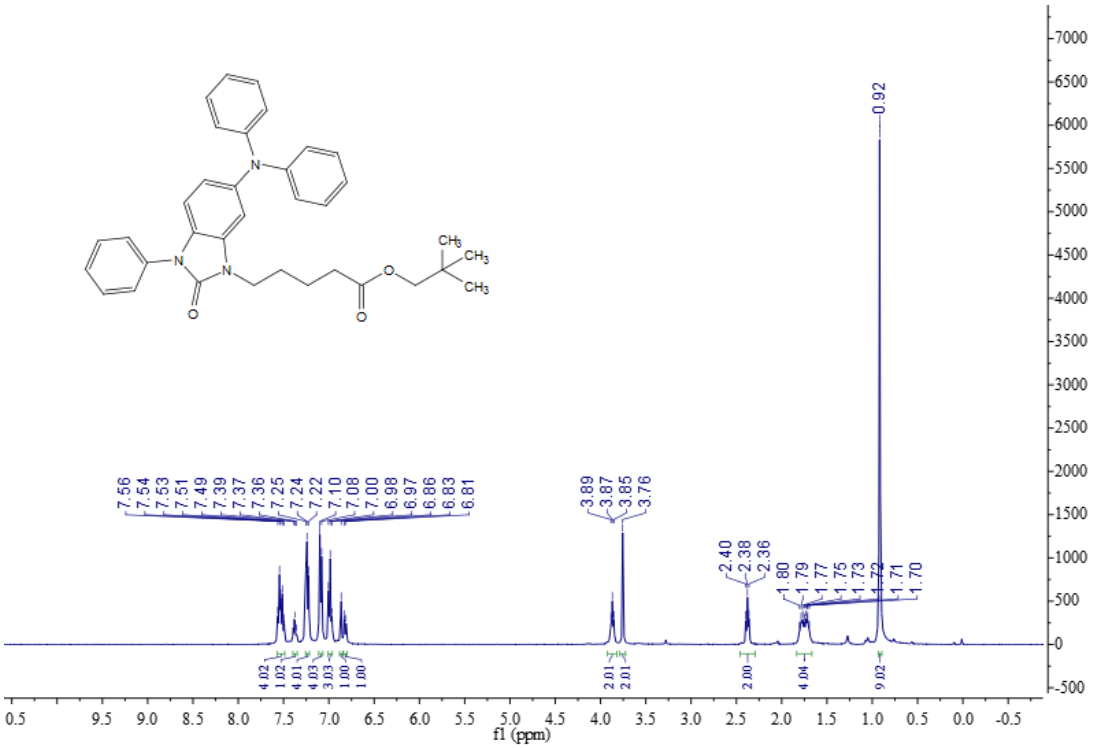

Figure S31. ^{13}C-NMR (100 MHz, $CDCl_3$) spectrum of **4aad**, related to **Scheme 3**.

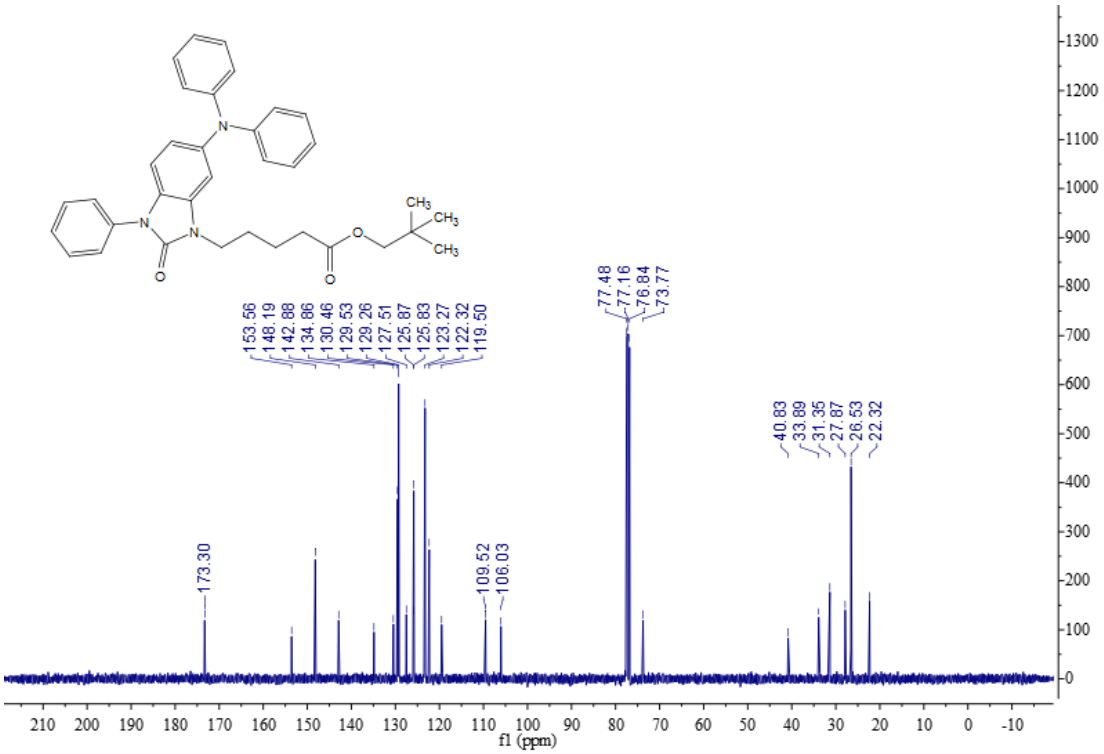

Figure S32. ^{1}H-NMR (400 MHz, $CDCl_3$) spectrum of **4aae**, related to **Scheme 3**.

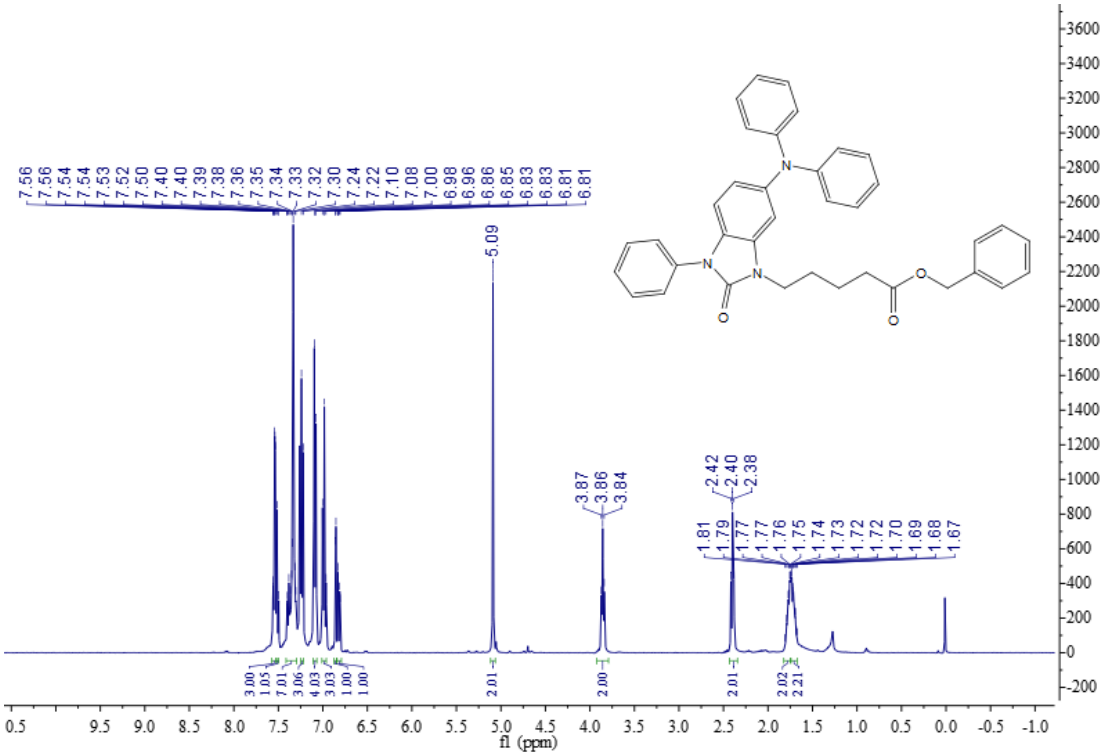

Figure S33. ^{13}C-NMR (100 MHz, $CDCl_3$) spectrum of **4aae**, related to **Scheme 3**.

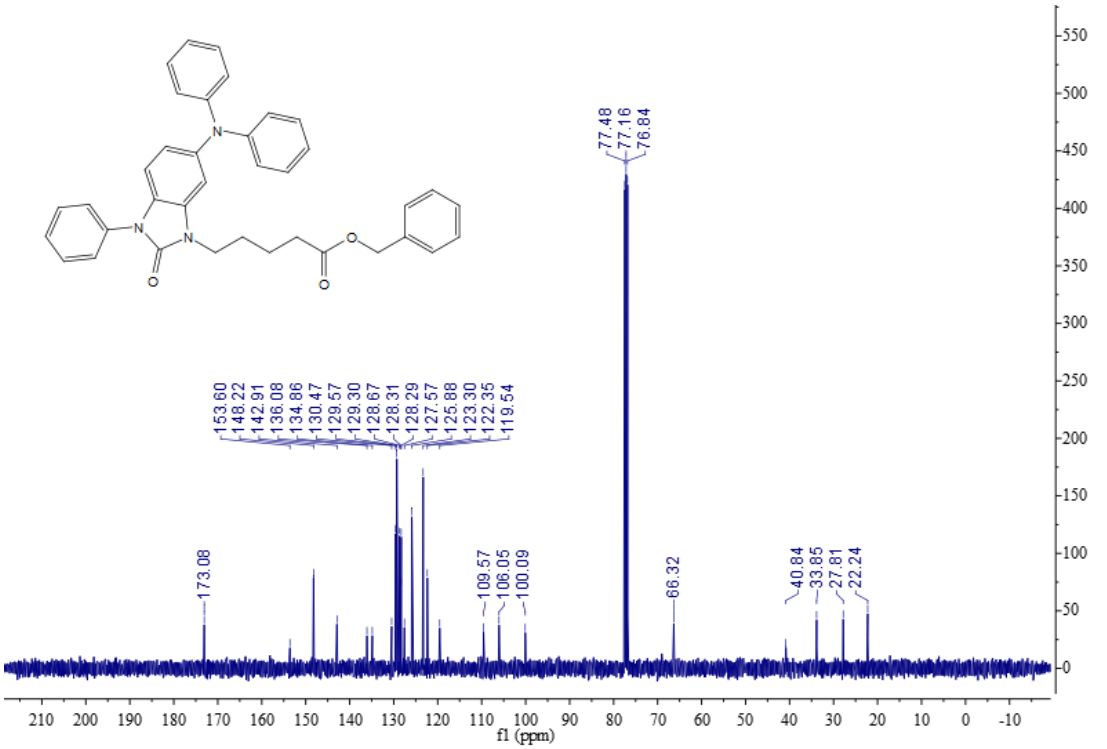

Figure S34. ^{1}H-NMR (400 MHz, $CDCl_3$) spectrum of **4aaf**, related to **Scheme 3**.

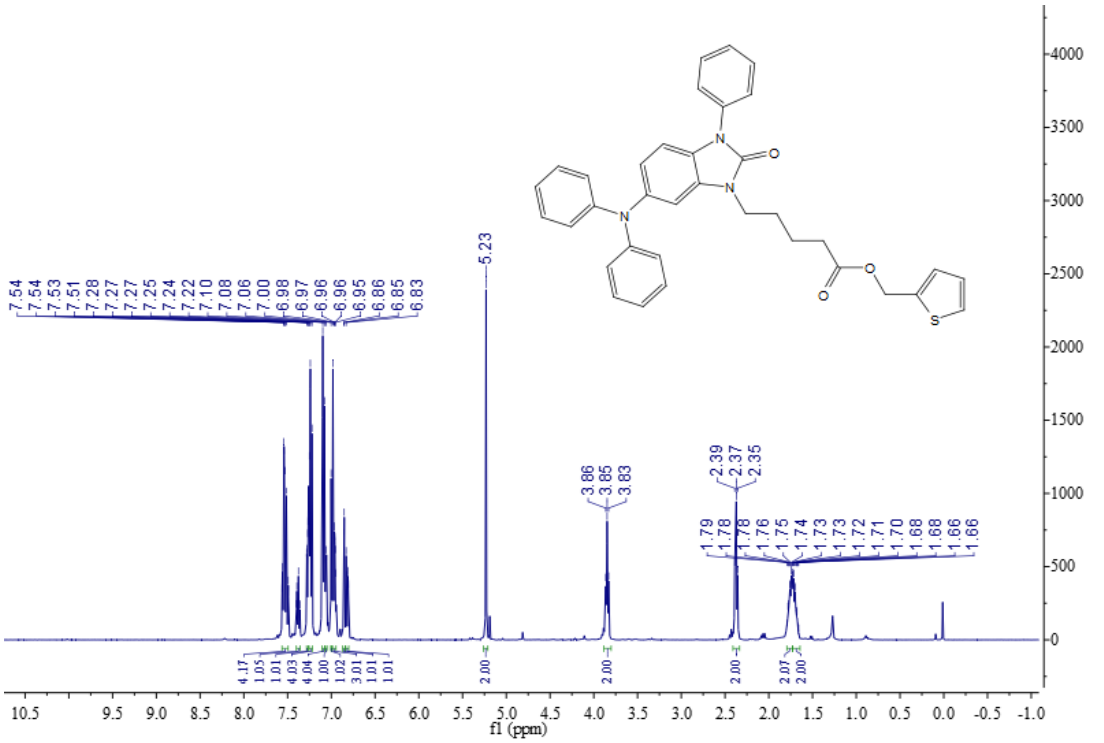

Figure S35. ^{13}C-NMR (100 MHz, $CDCl_3$) spectrum of **4aaf**, related to **Scheme 3**.

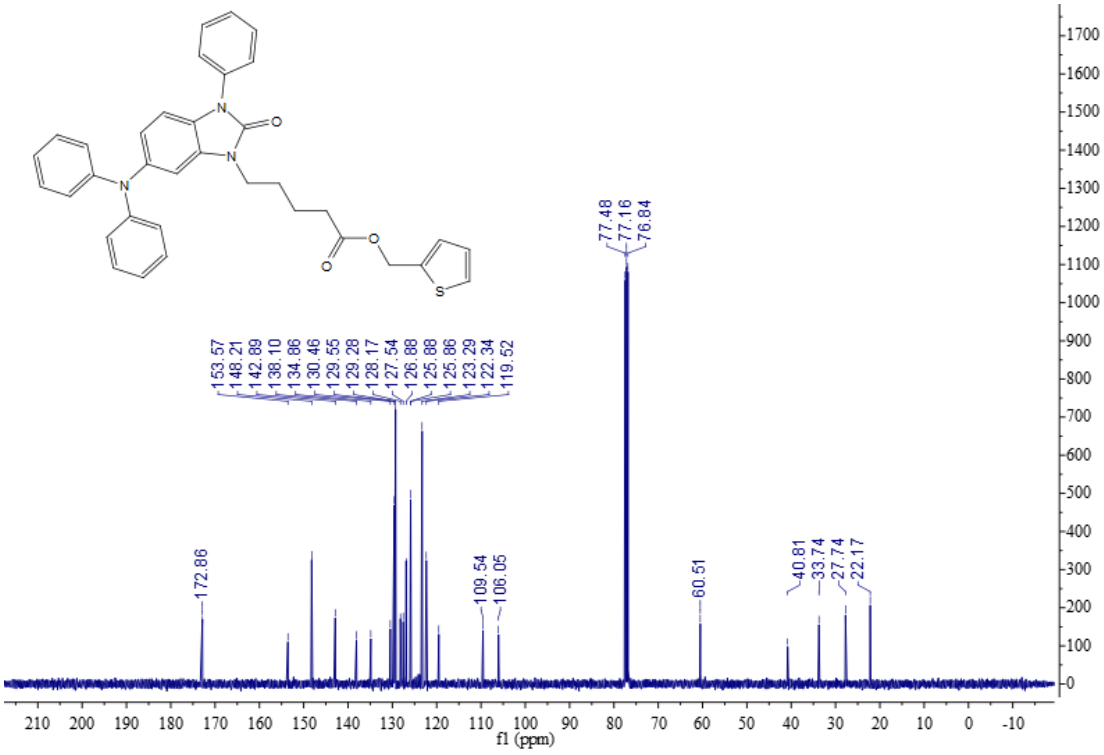

Figure S36. ^{1}H-NMR (400 MHz, $CDCl_3$) spectrum of **4aag**, related to **Scheme 3**.

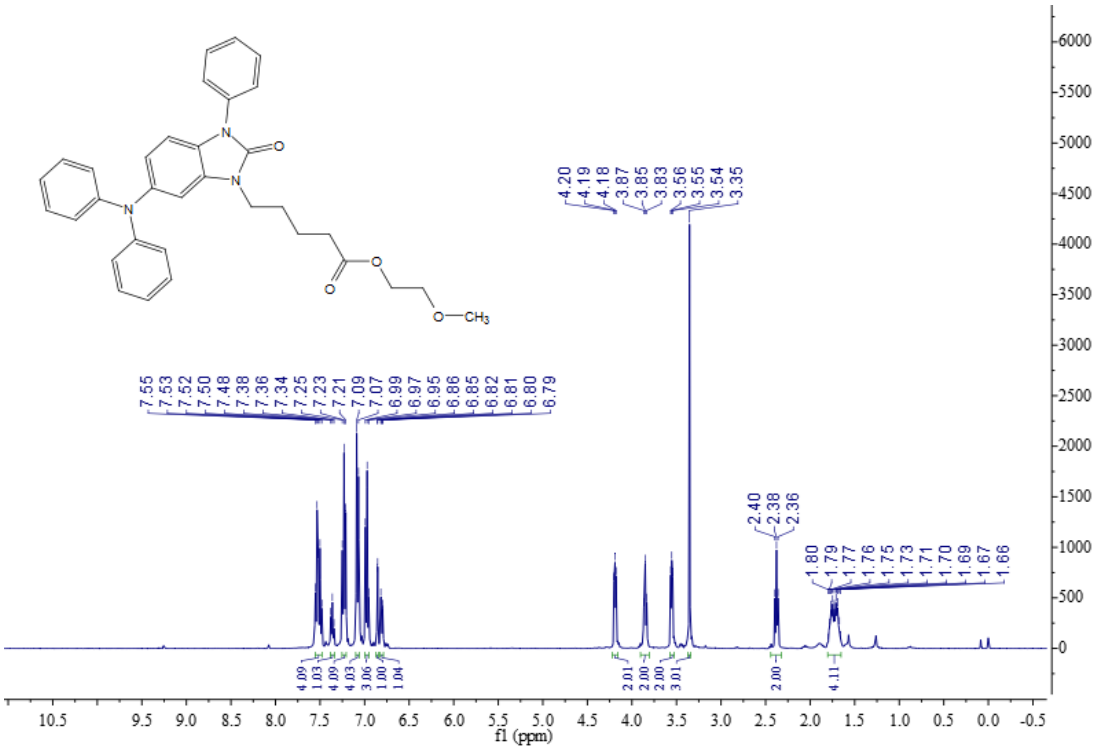

Figure S37. ^{13}C-NMR (100 MHz, $CDCl_3$) spectrum of **4aag**, related to **Scheme 3**.

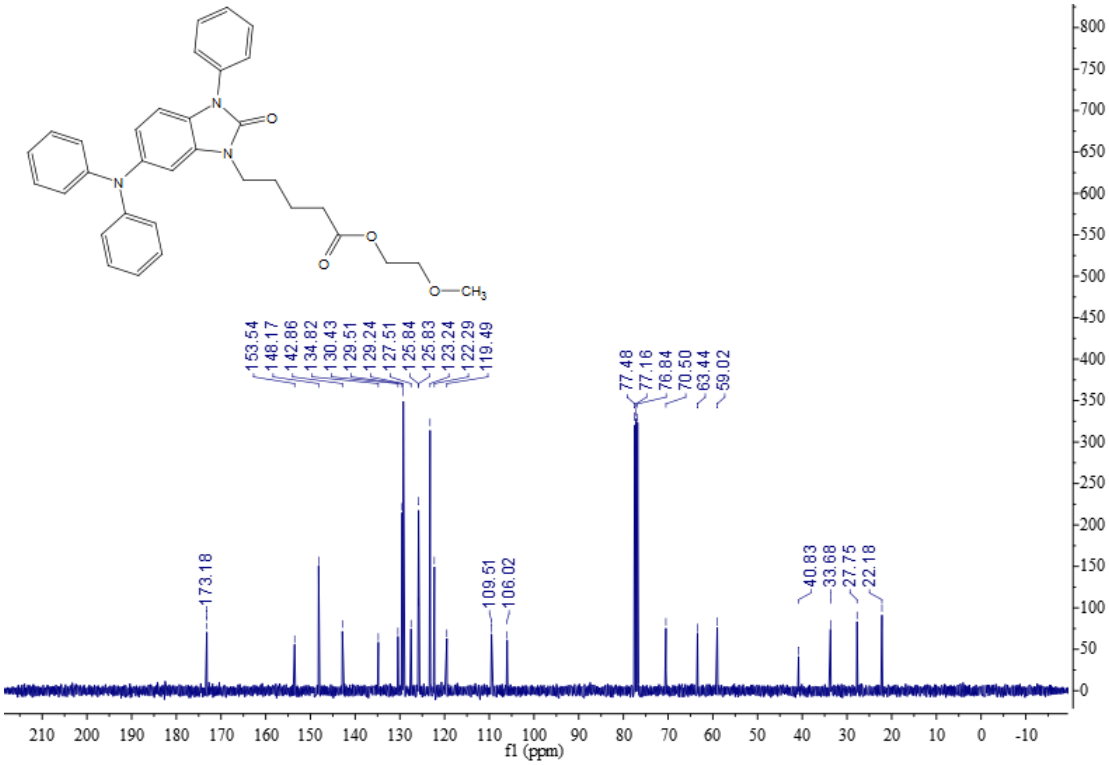

Figure S38. ^{1}H-NMR (400 MHz, $CDCl_3$) spectrum of **5af**, related to **Scheme 4**.

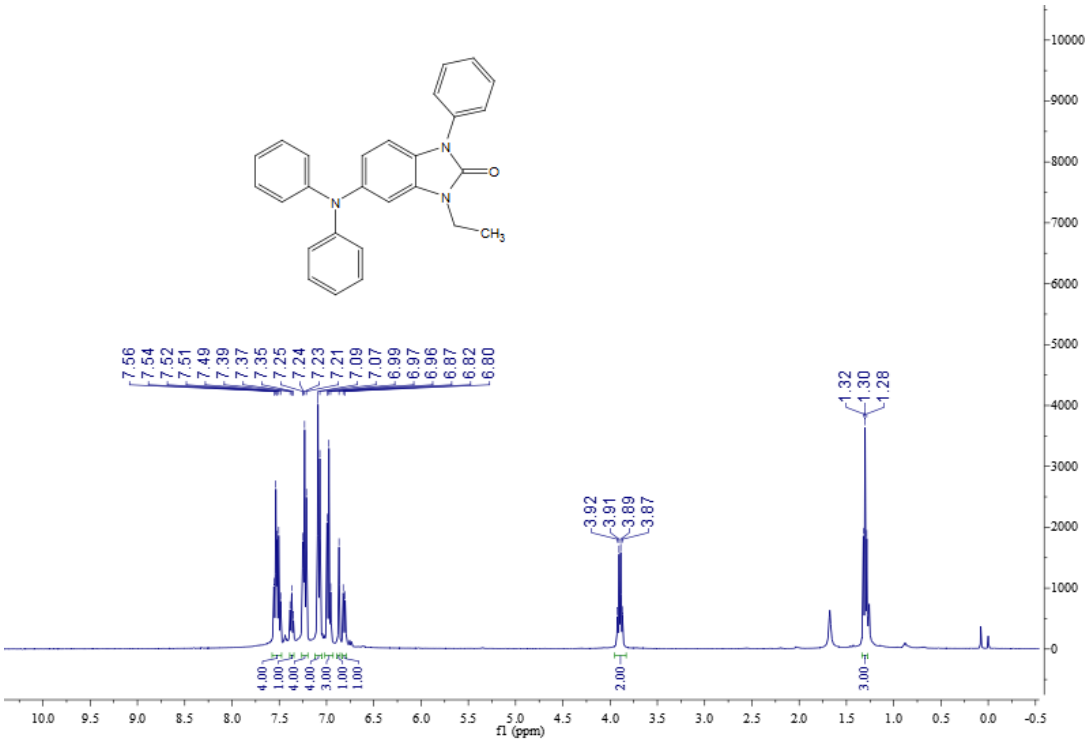

Figure S39. ^{13}C-NMR (100 MHz, $CDCl_3$) spectrum of **5af**, related to **Scheme 4**.

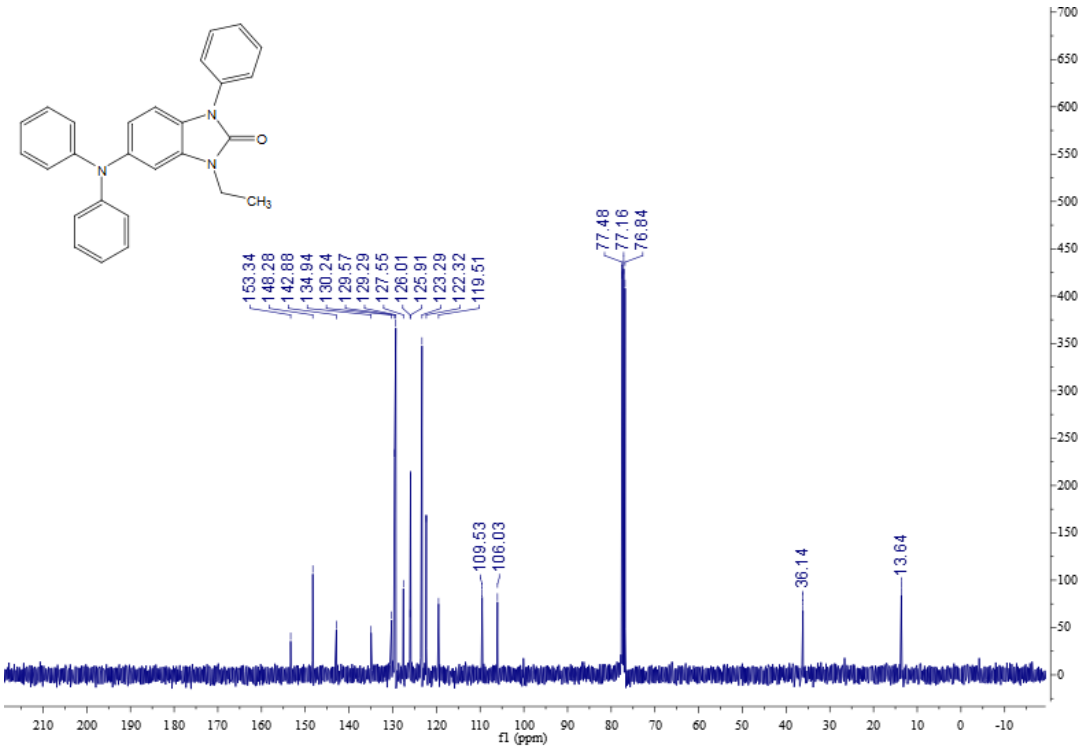

Figure S40. ^{1}H-NMR (400 MHz, $CDCl_3$) spectrum of **5ag**, related to **Scheme 4**.

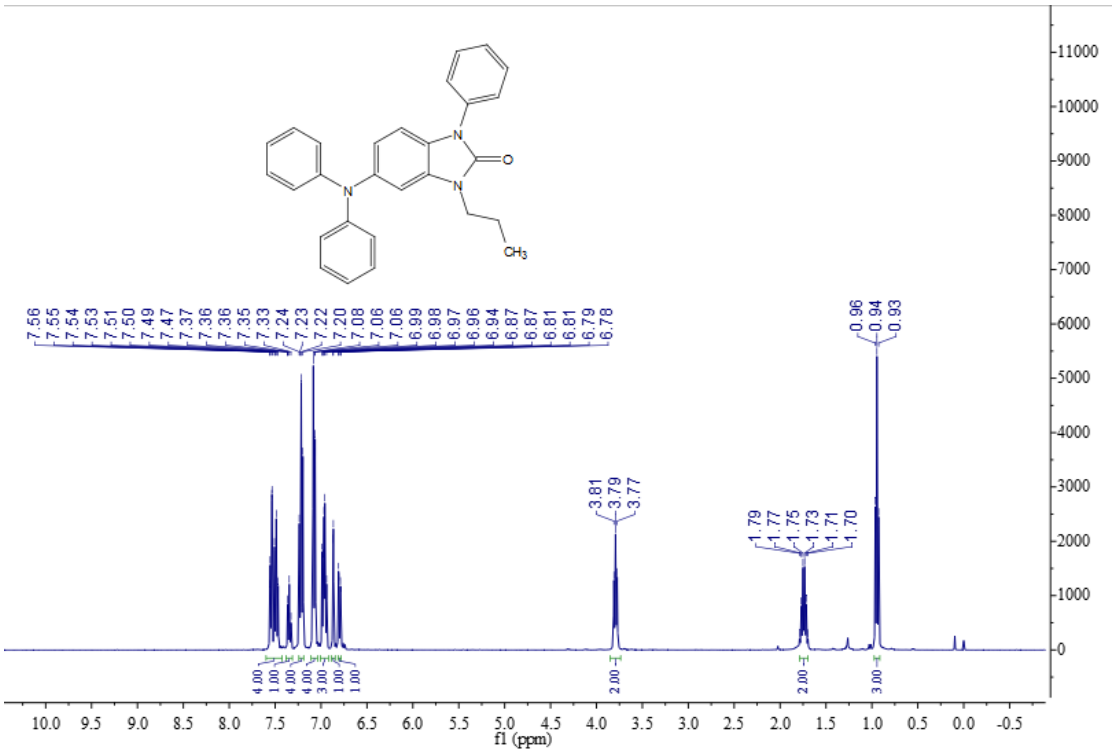

Figure S41. ^{13}C-NMR (100 MHz, $CDCl_3$) spectrum of **5ag**, related to **Scheme 4**.

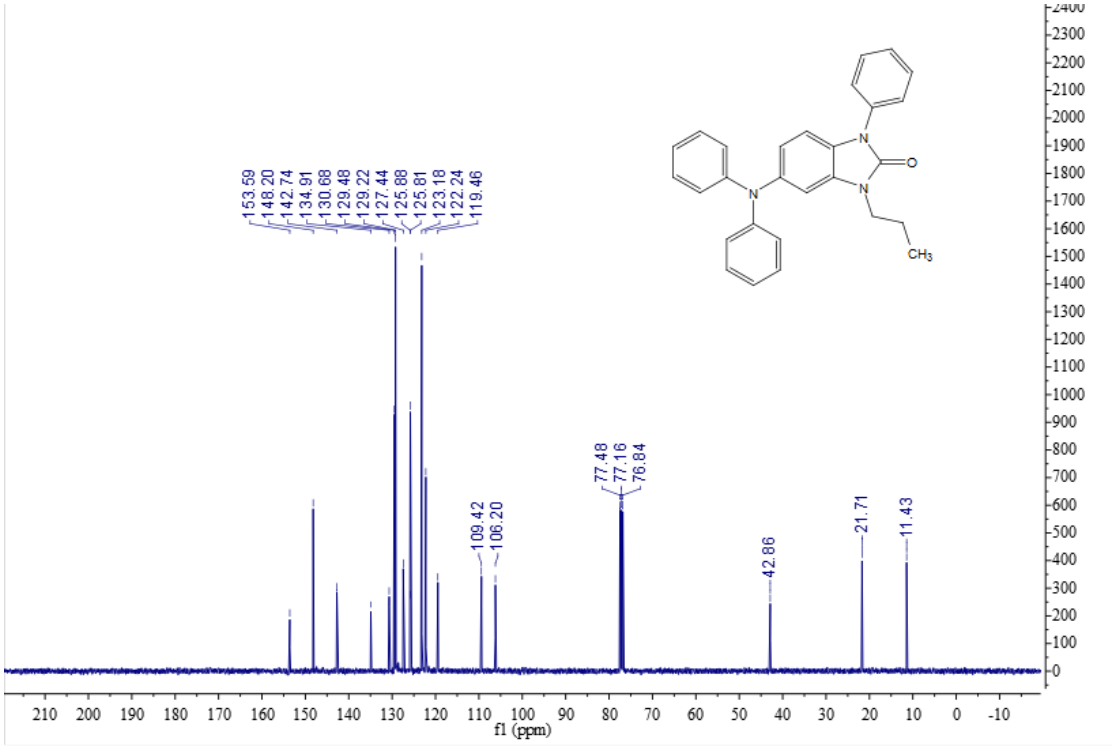

Figure S42. ^{1}H-NMR (400 MHz, $CDCl_3$) spectrum of **5ah**, related to **Scheme 4**.

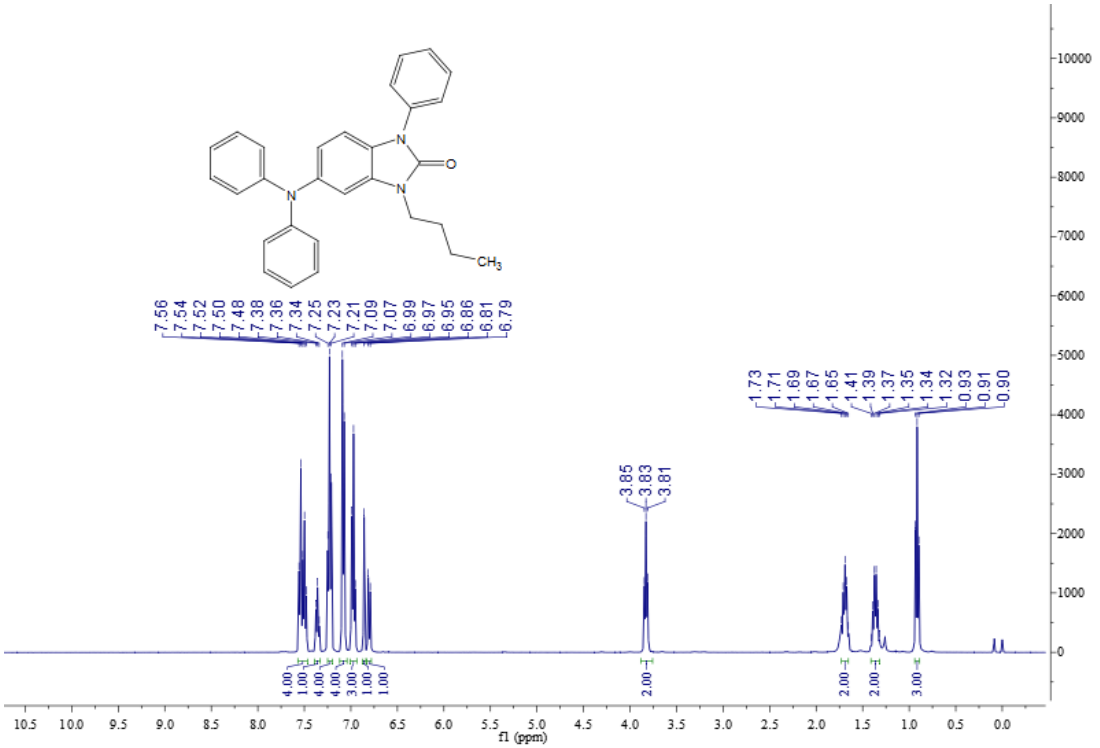

Figure S43. ^{13}C-NMR (100 MHz, $CDCl_3$) spectrum of **5ah**, related to **Scheme 4**.

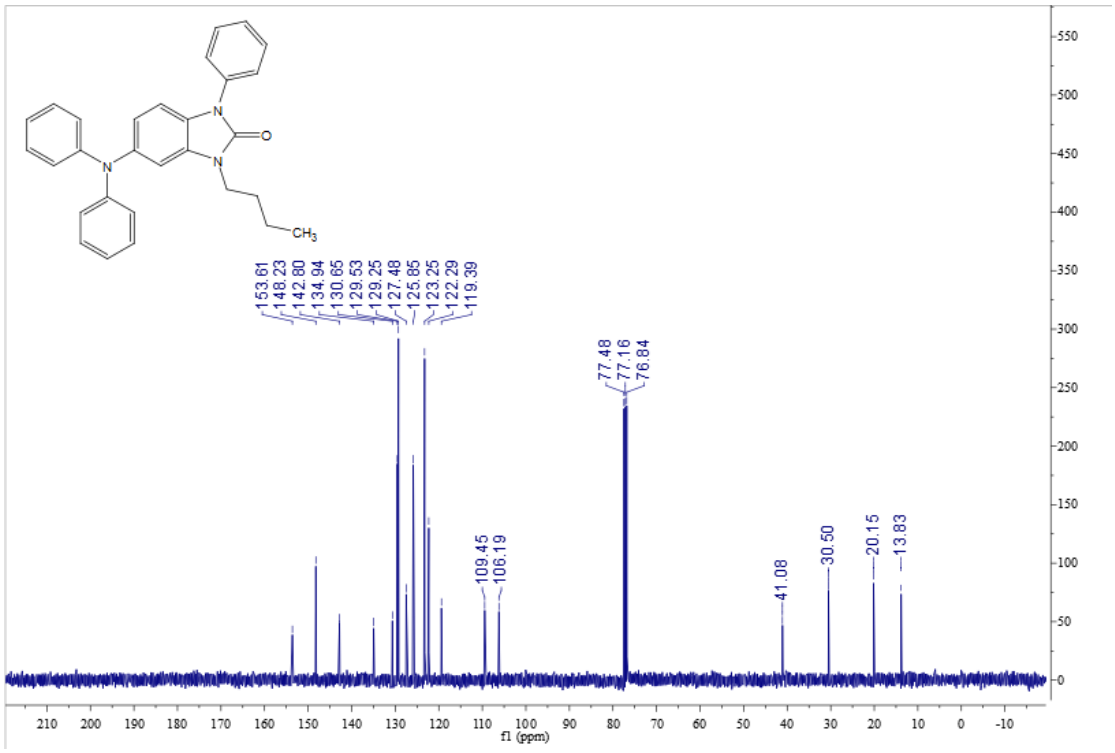

Figure S44. ^{1}H-NMR (400 MHz, $CDCl_3$) spectrum of **5ai**, related to **Scheme 4**.

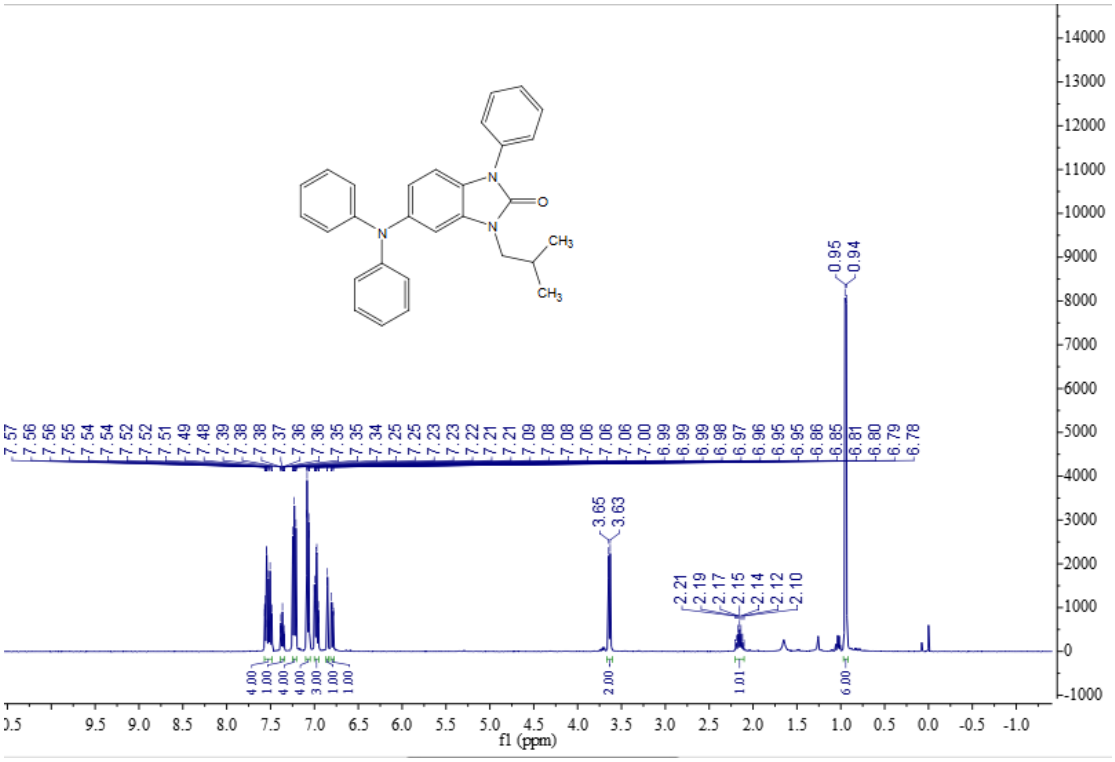

Figure S45. ^{13}C-NMR (100 MHz, $CDCl_3$) spectrum of **5ai**, related to **Scheme 4**.

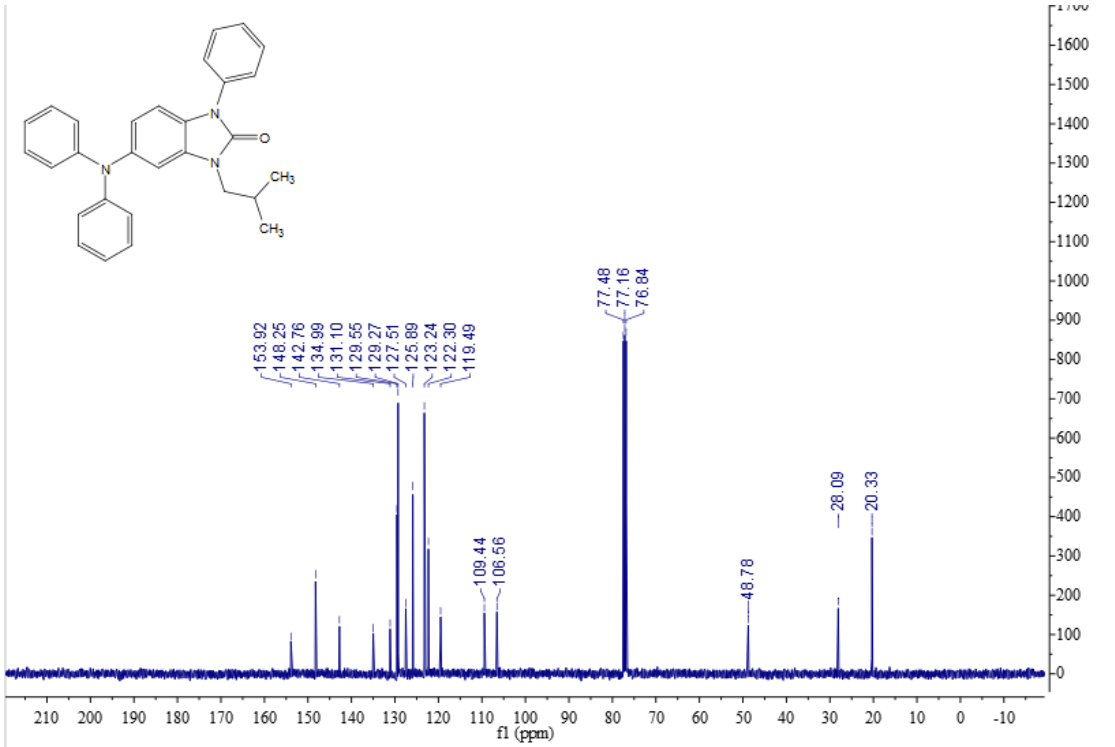

Figure S46. ^{1}H-NMR (400 MHz, $CDCl_3$) spectrum of **5aj**, related to **Scheme 4**.

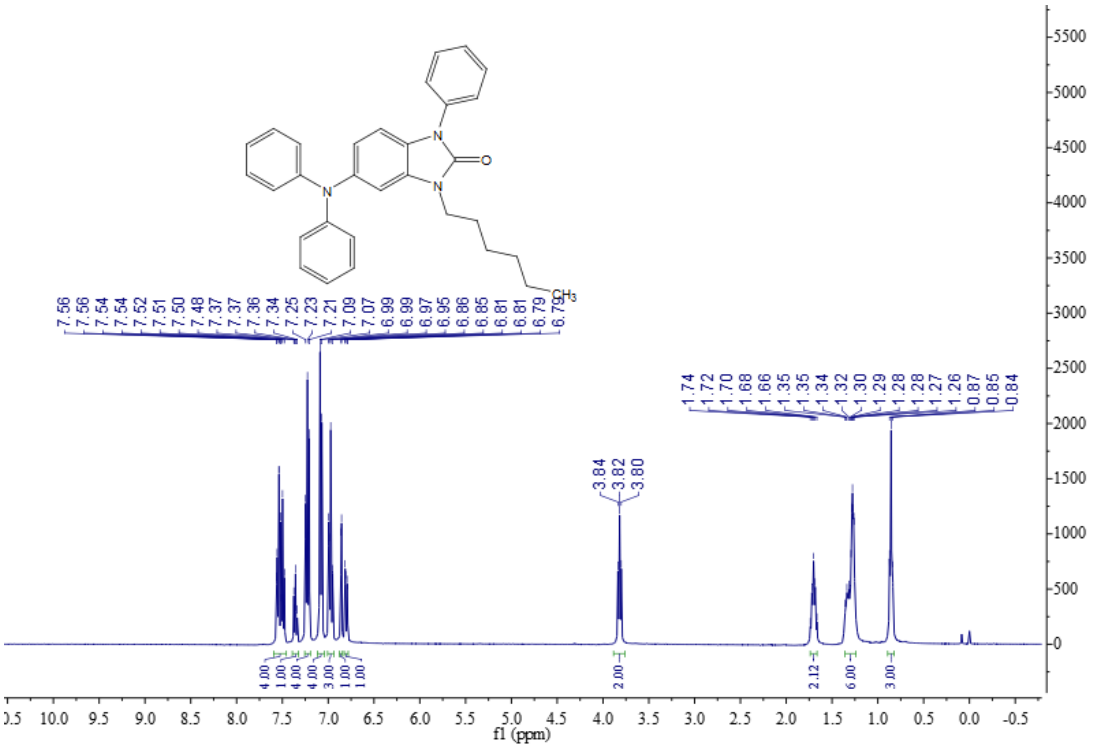

Figure S47. ^{13}C-NMR (100 MHz, $CDCl_3$) spectrum of **5aj**, related to **Scheme 4**.

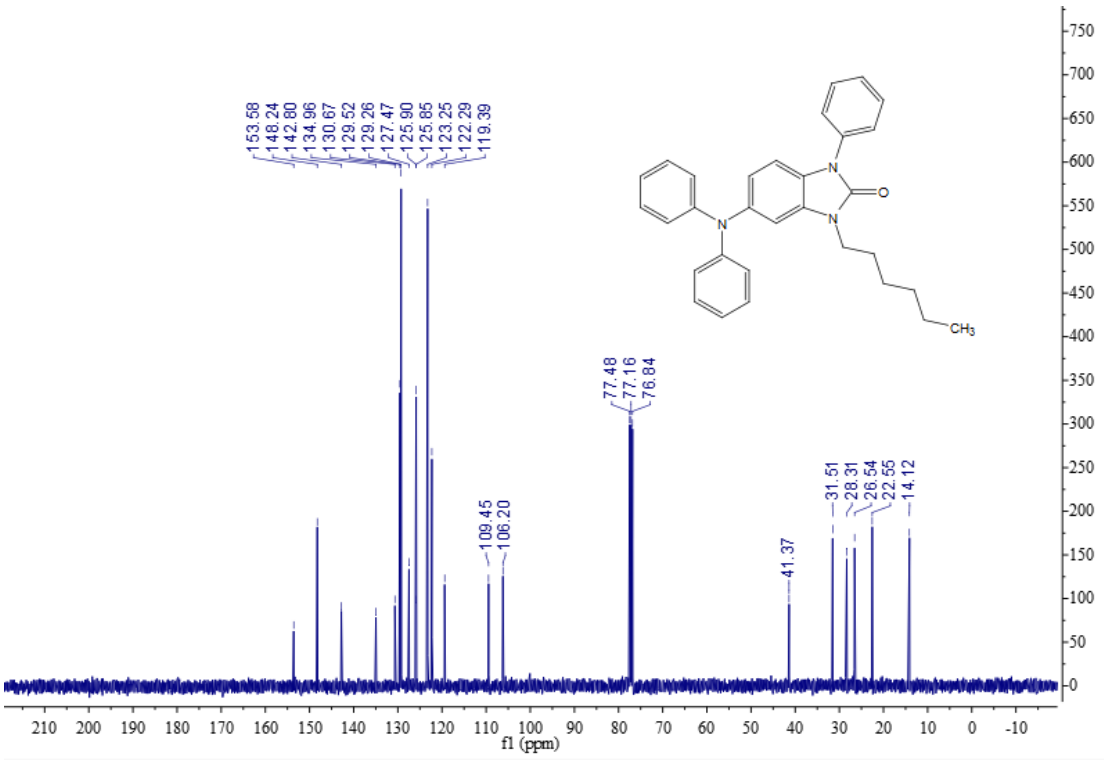

Figure S48. ^{1}H-NMR (400 MHz, $CDCl_3$) spectrum of **5al**, related to **Scheme 4**.

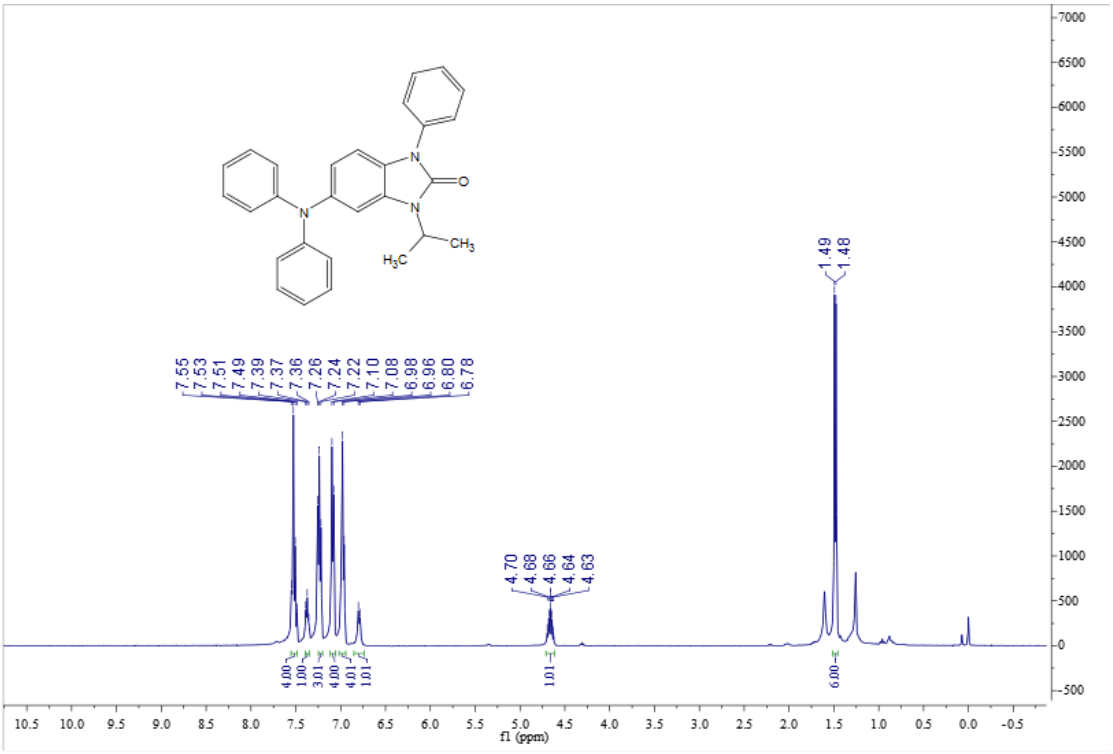

Figure S49. ^{13}C-NMR (100 MHz, $CDCl_3$) spectrum of **5al**, related to **Scheme 4**.

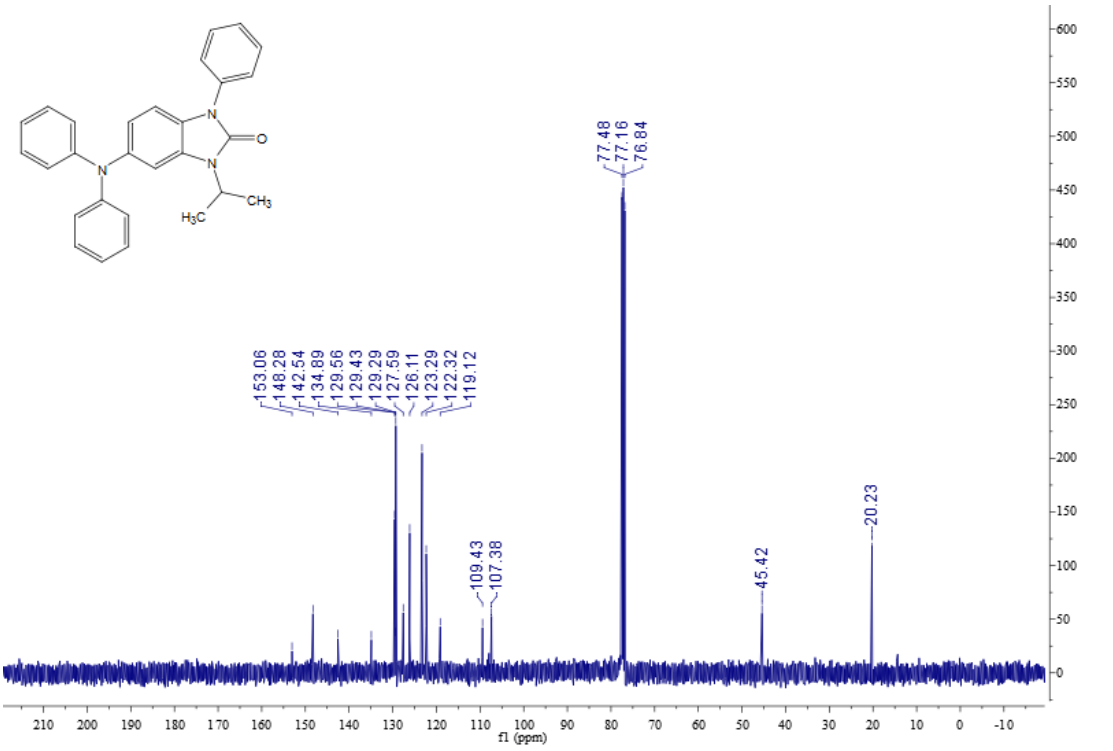

Figure S50. ^{1}H-NMR (400 MHz, $CDCl_3$) spectrum of **5am**, related to **Scheme 4**.

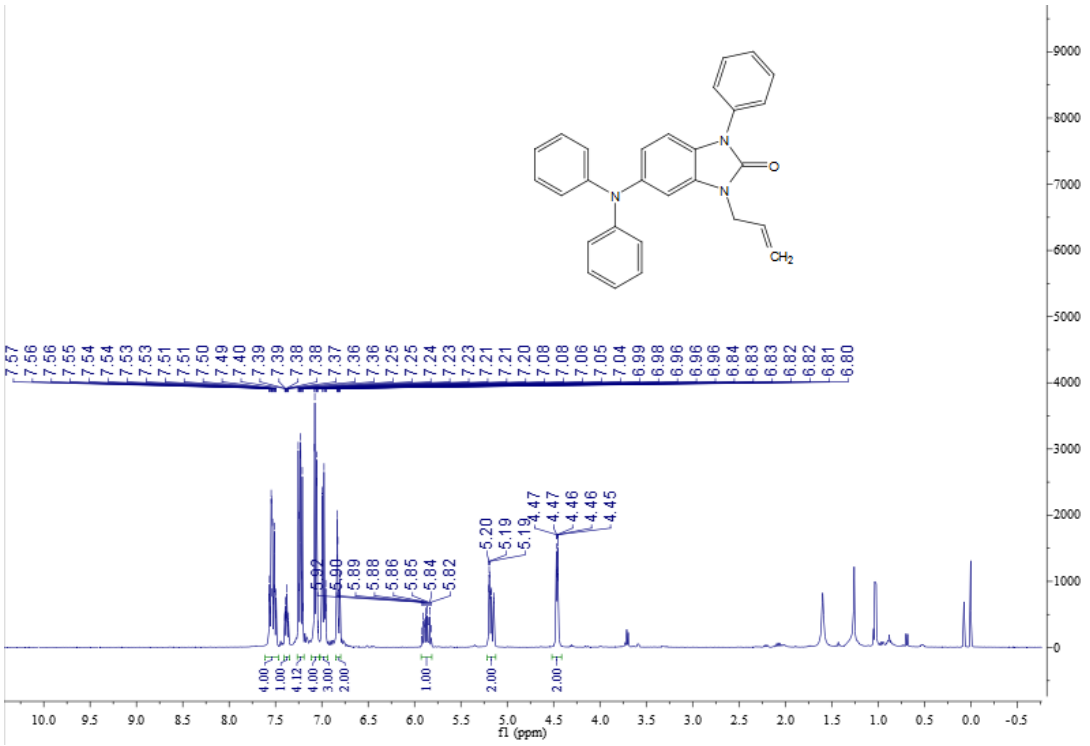

Figure S51. ^{13}C-NMR (100 MHz, $CDCl_3$) spectrum of **5am**, related to **Scheme 4**.

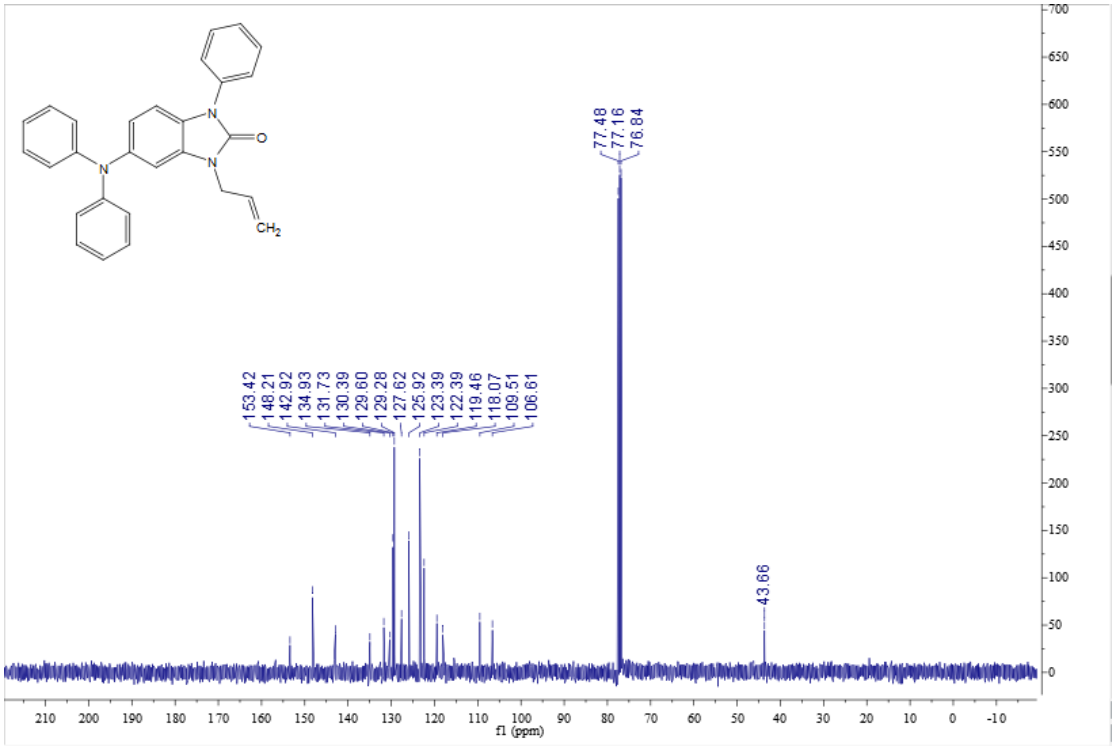

Figure S52. ^{1}H-NMR (400 MHz, $CDCl_3$) spectrum of **5bf**, related to **Scheme 5**.

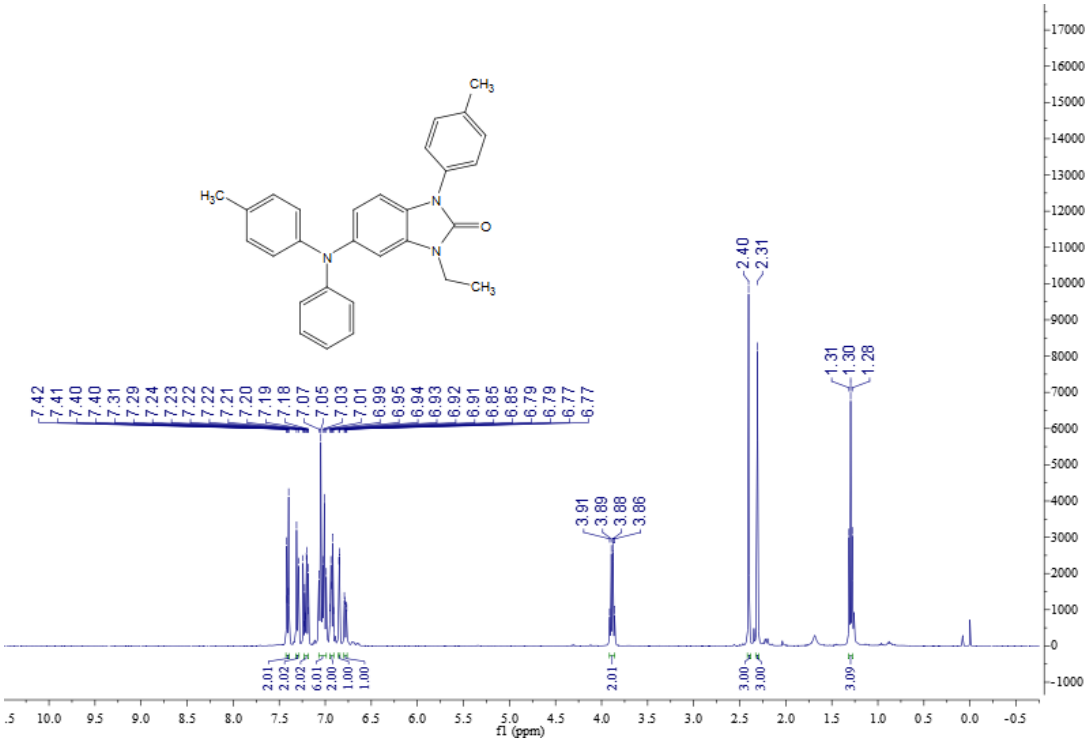

Figure S53. ^{13}C-NMR (100 MHz, $CDCl_3$) spectrum of **5bf**, related to **Scheme 5**.

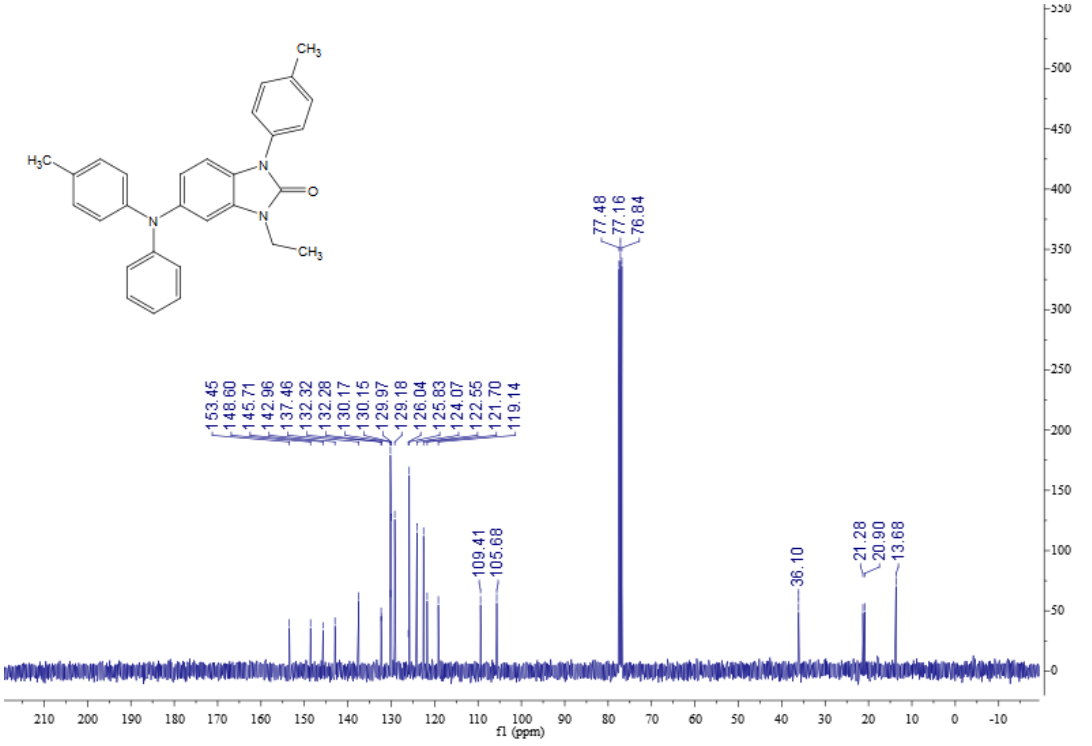

Figure S54. ^{1}H-NMR (400 MHz, $CDCl_3$) spectrum of **5cf**, related to **Scheme 5**.

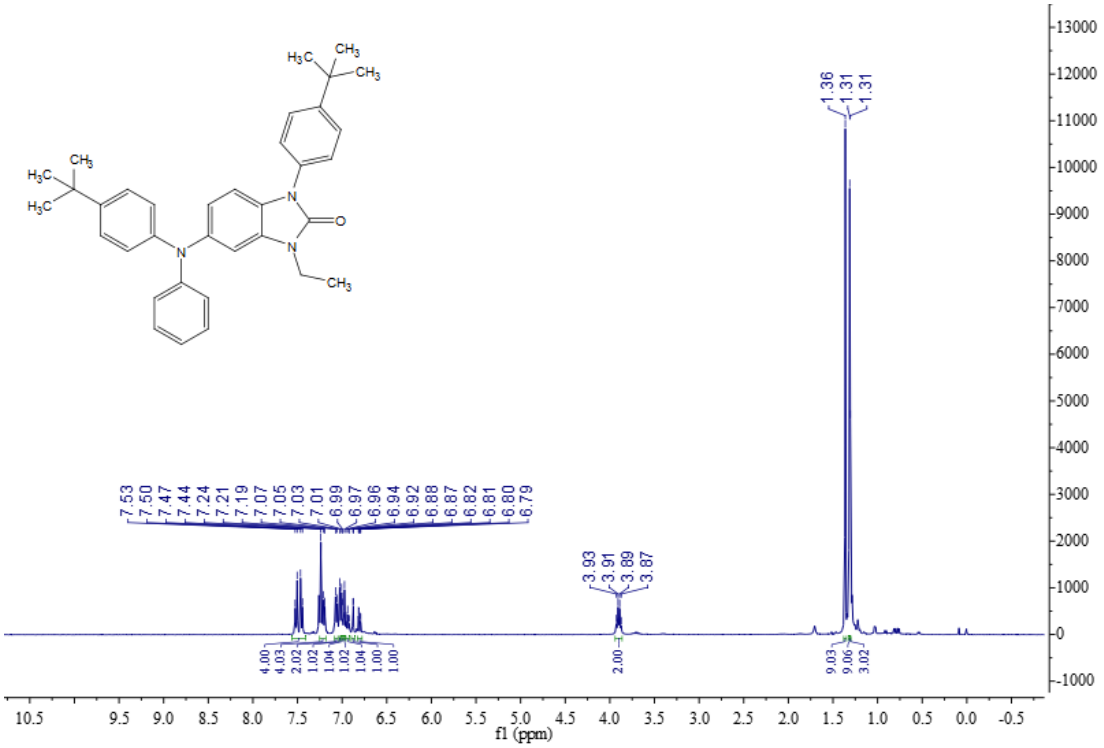

Figure S55. ^{13}C-NMR (100 MHz, $CDCl_3$) spectrum of **5cf**, related to **Scheme 5**.

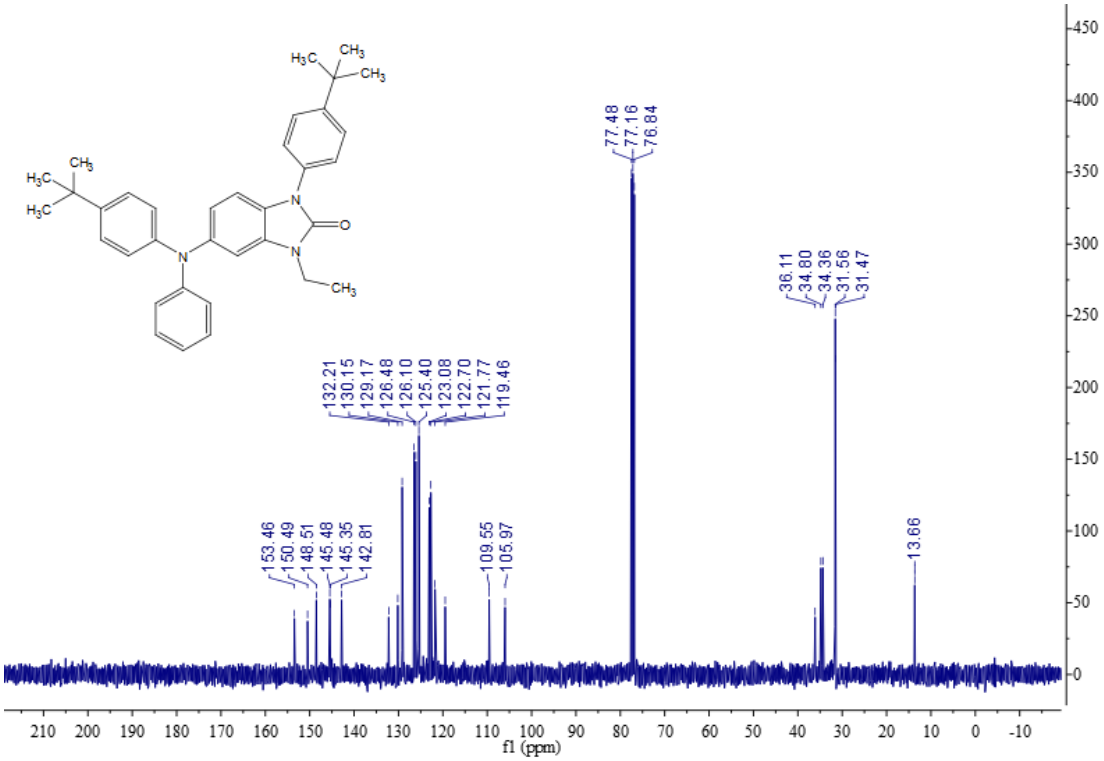

Figure S56. ^{1}H-NMR (400 MHz, $CDCl_3$) spectrum of **5df**, related to **Scheme 5**.

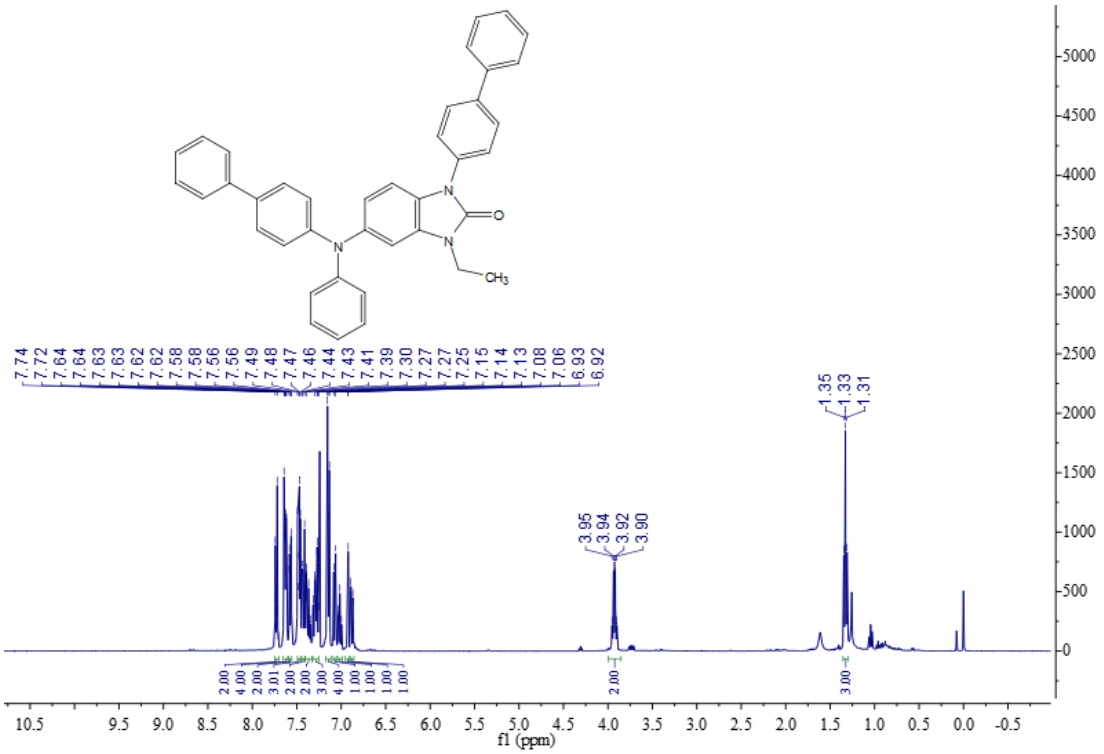

Figure S57. ^{13}C-NMR (100 MHz, $CDCl_3$) spectrum of **5df**, related to **Scheme 5**.

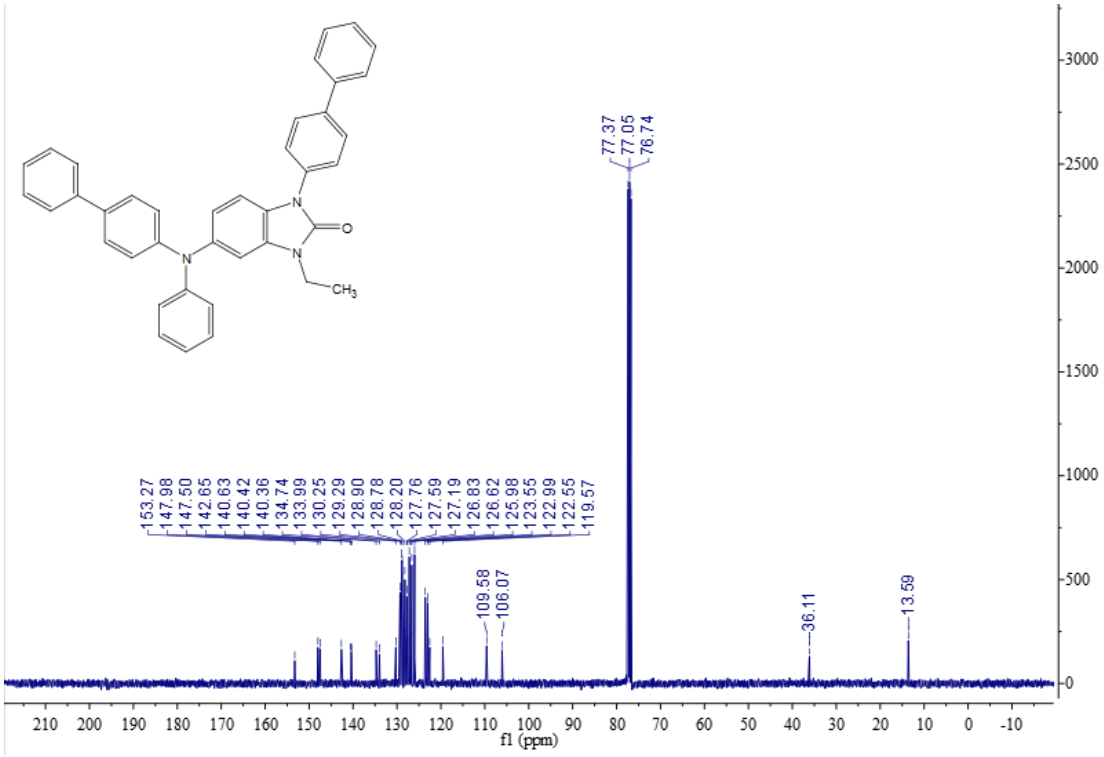

Figure S58. ^{1}H-NMR (400 MHz, $CDCl_3$) spectrum of **5ef**, related to **Scheme 5**.

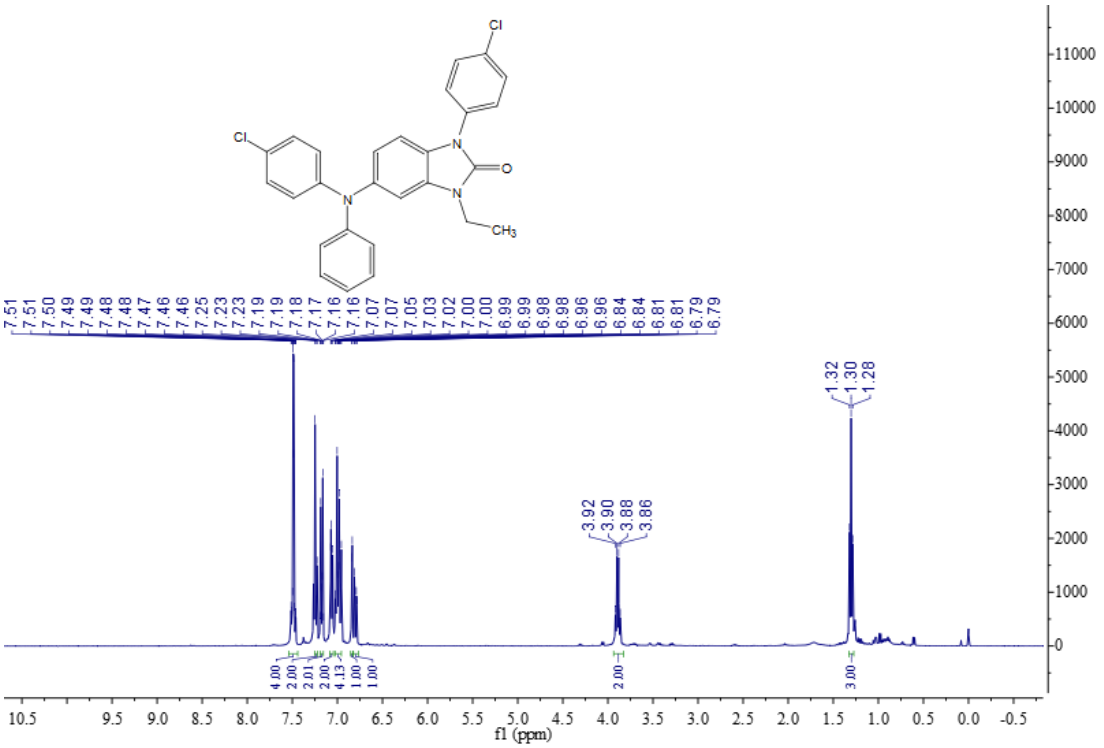

Figure S59. ^{13}C-NMR (100 MHz, $CDCl_3$) spectrum of **5ef**, related to **Scheme 5**.

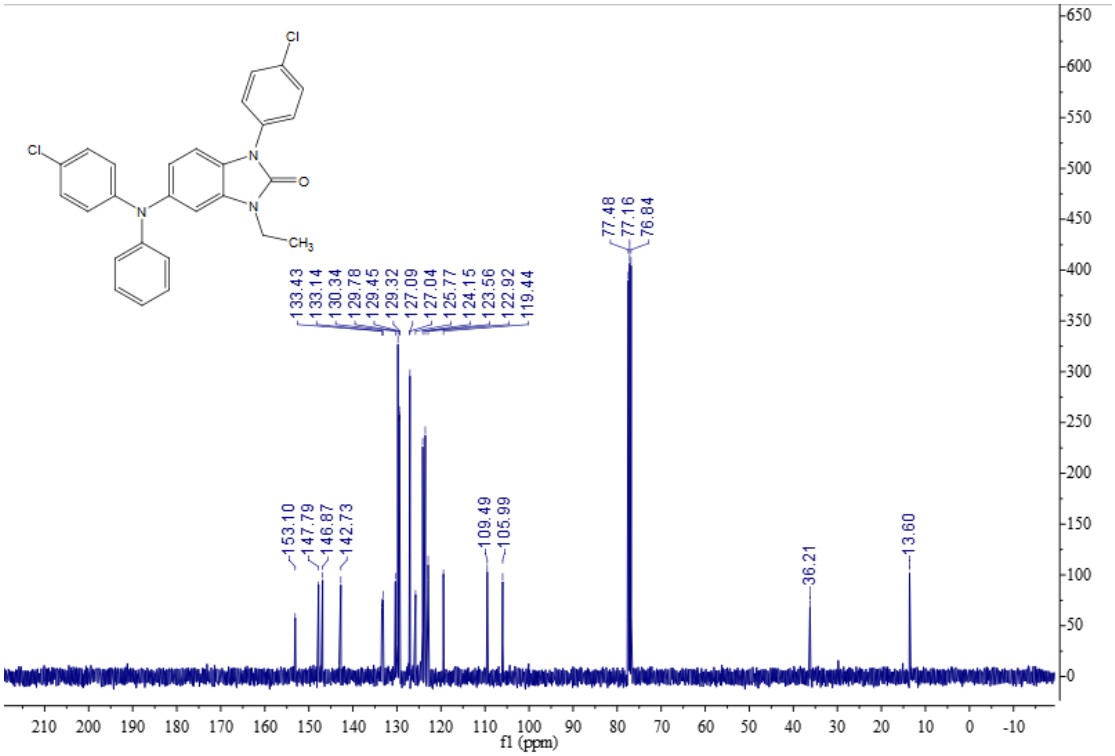

Figure S60. ^{1}H-NMR (400 MHz, $CDCl_3$) spectrum of **5ff**, related to **Scheme 5**.

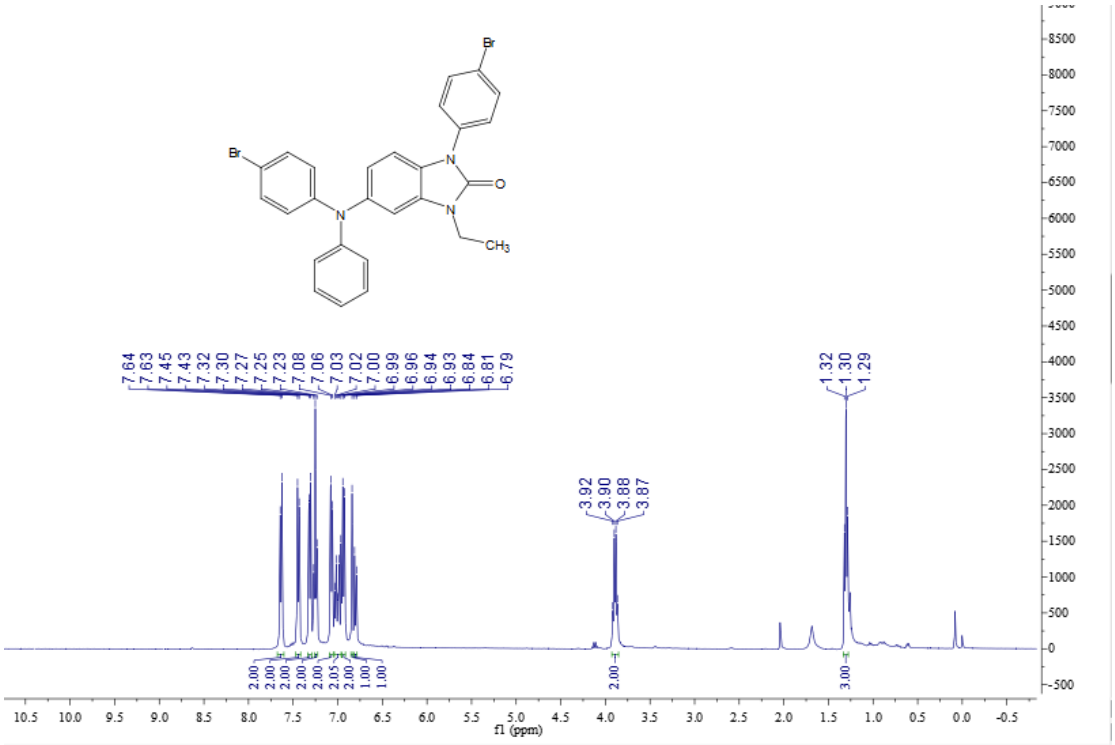

Figure S61. ^{13}C-NMR (100 MHz, $CDCl_3$) spectrum of **5ff**, related to **Scheme 5**.

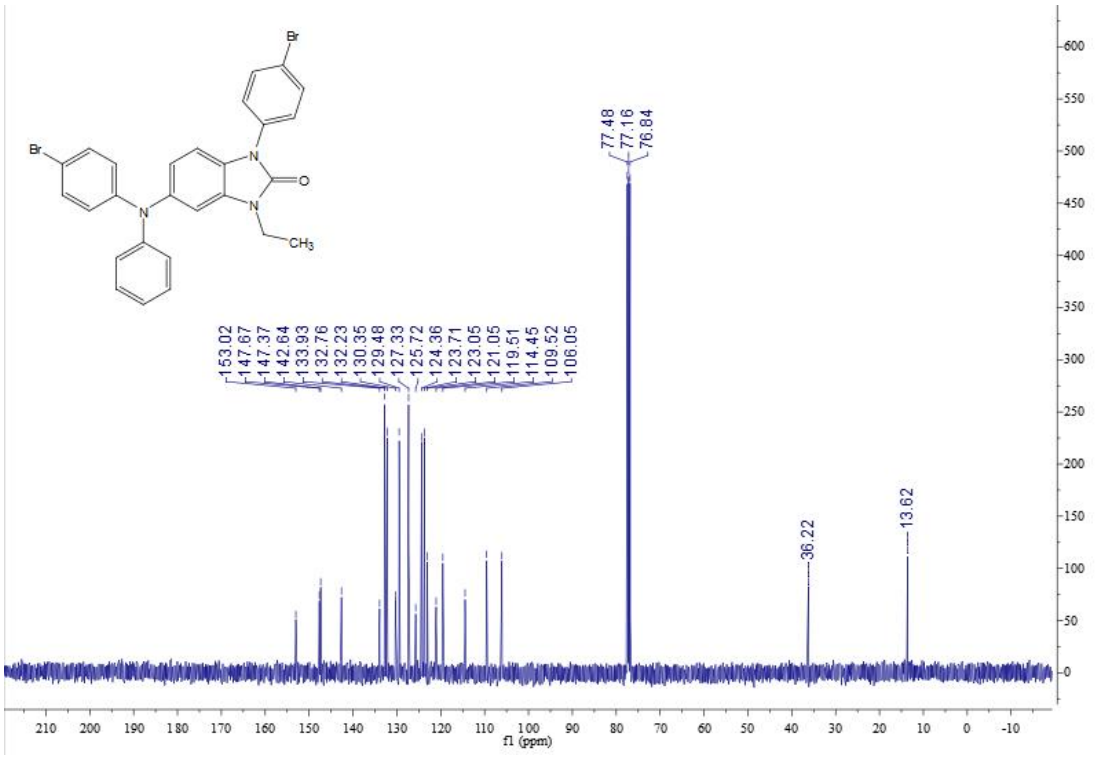

Figure S62. ^{1}H-NMR (400 MHz, $CDCl_3$) spectrum of **5if**, related to **Scheme 5**.

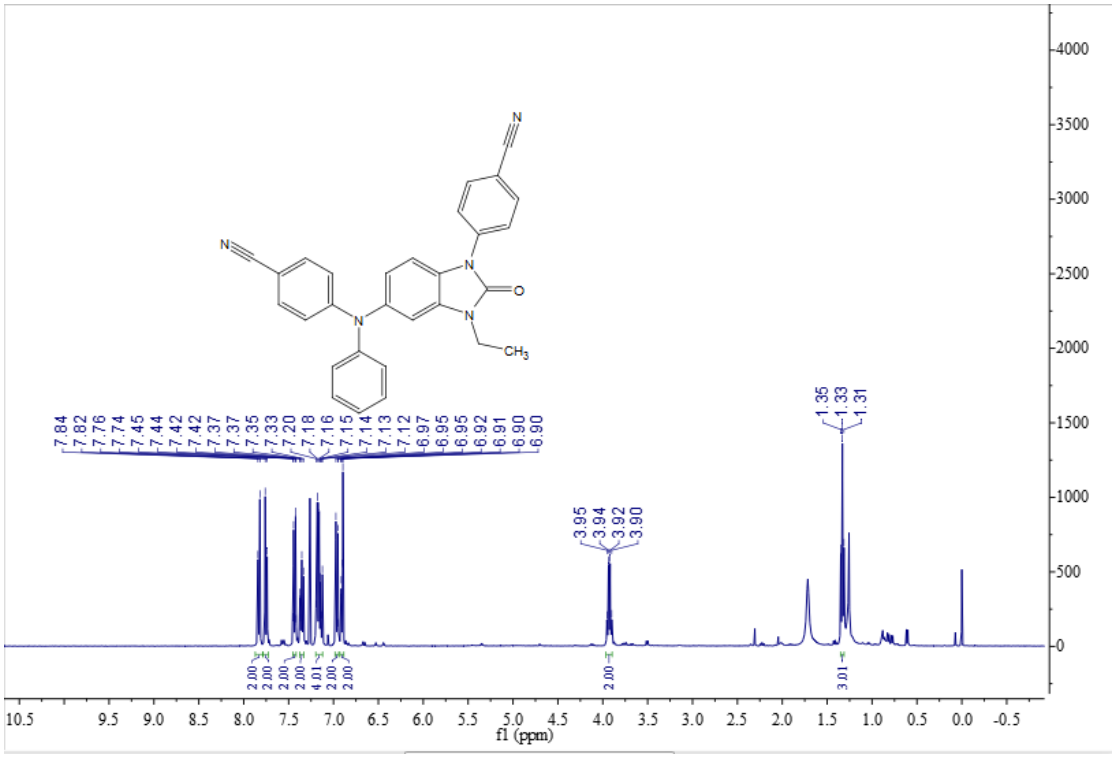

Figure S63. ^{13}C-NMR (100 MHz, $CDCl_3$) spectrum of **5if**, related to **Scheme 5**.

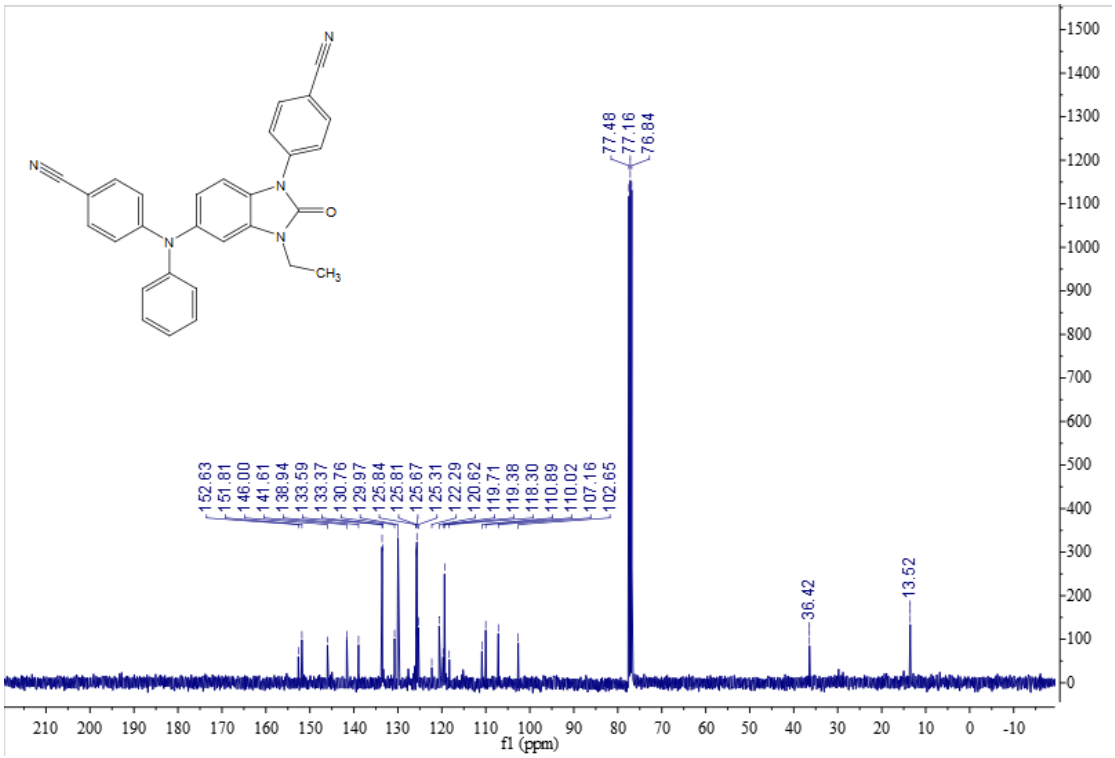

Figure S64. ^{1}H-NMR (400 MHz, $CDCl_3$) spectrum of **5bg**, related to **Scheme 5**.

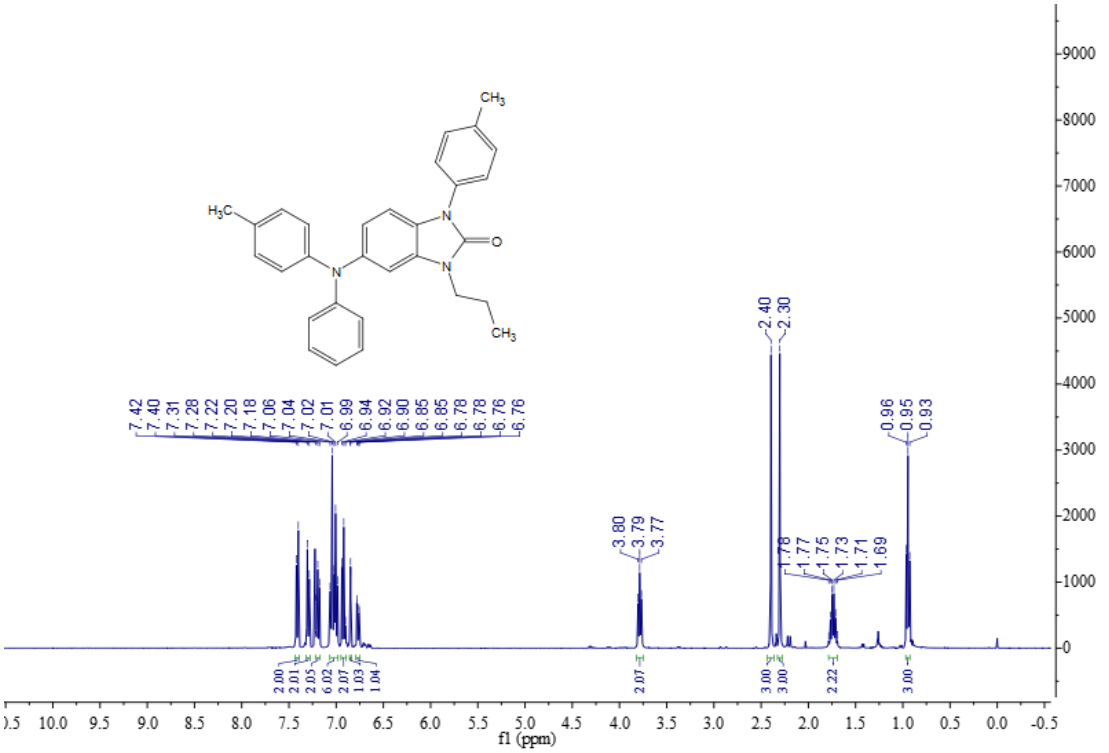

Figure S65. ^{13}C-NMR (100 MHz, $CDCl_3$) spectrum of **5bg**, related to **Scheme 5**.

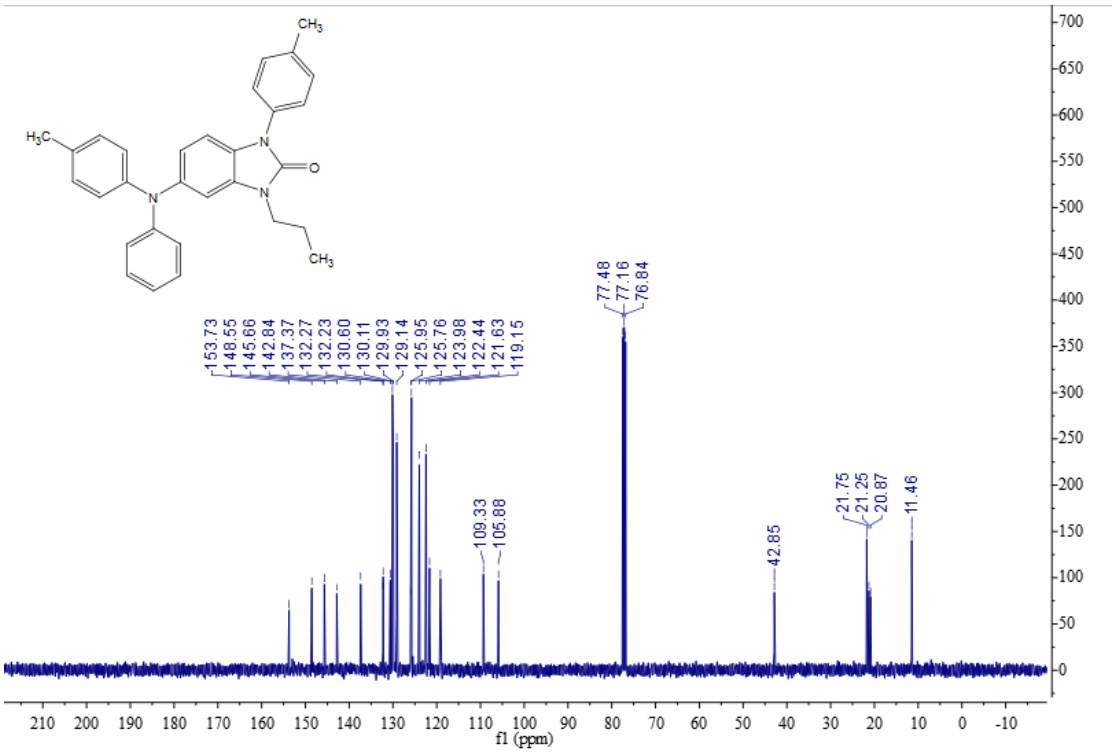

Figure S66. ^{1}H-NMR (400 MHz, $CDCl_3$) spectrum of **5jg**, related to **Scheme 5**.

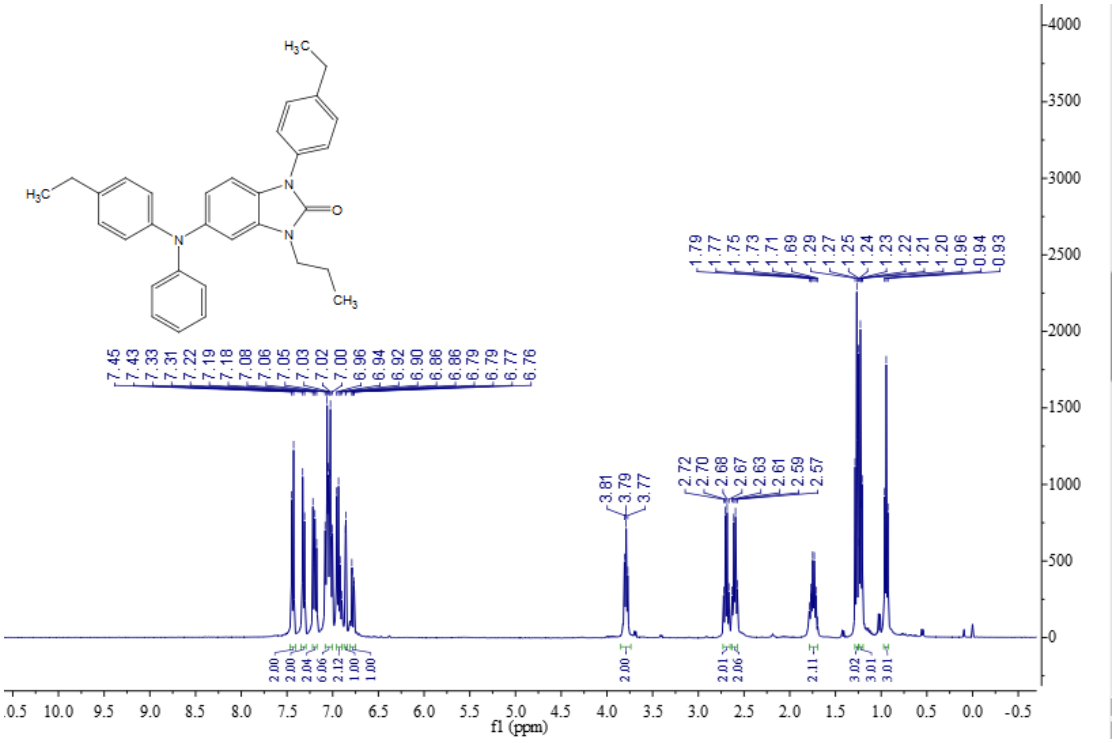

Figure S67. ^{13}C-NMR (100 MHz, $CDCl_3$) spectrum of **5jg**, related to **Scheme 5**.

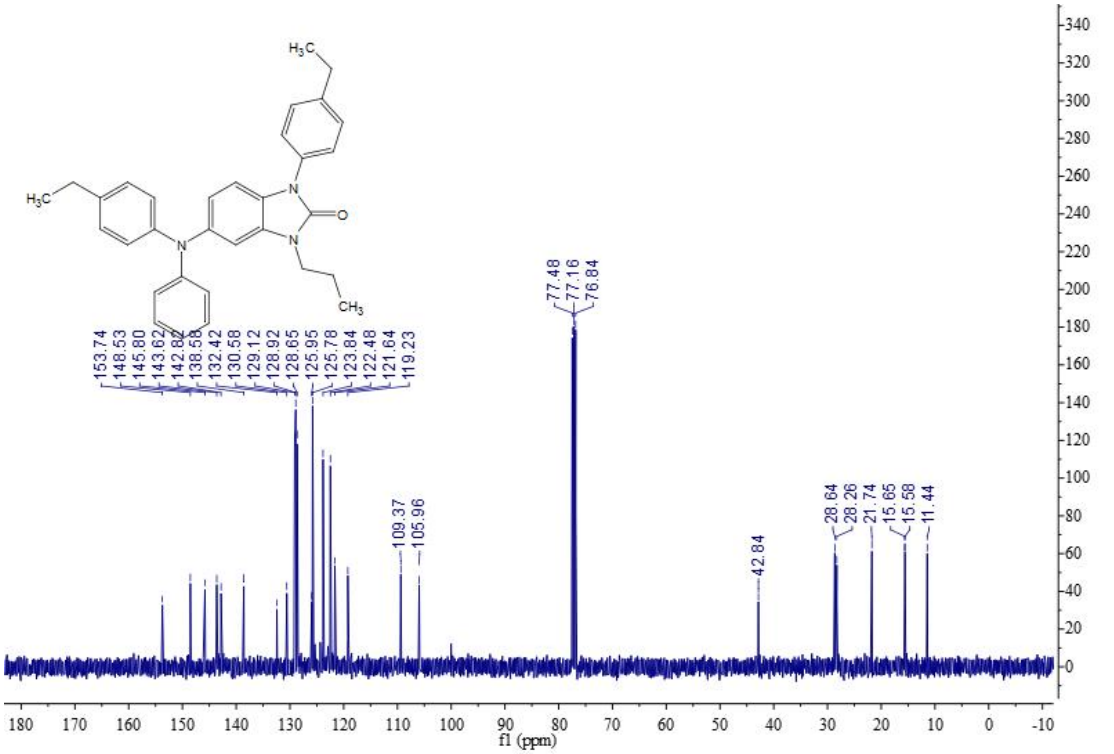

Figure S68. ^{1}H-NMR (400 MHz, $CDCl_3$) spectrum of **5kg**, related to **Scheme 5**.

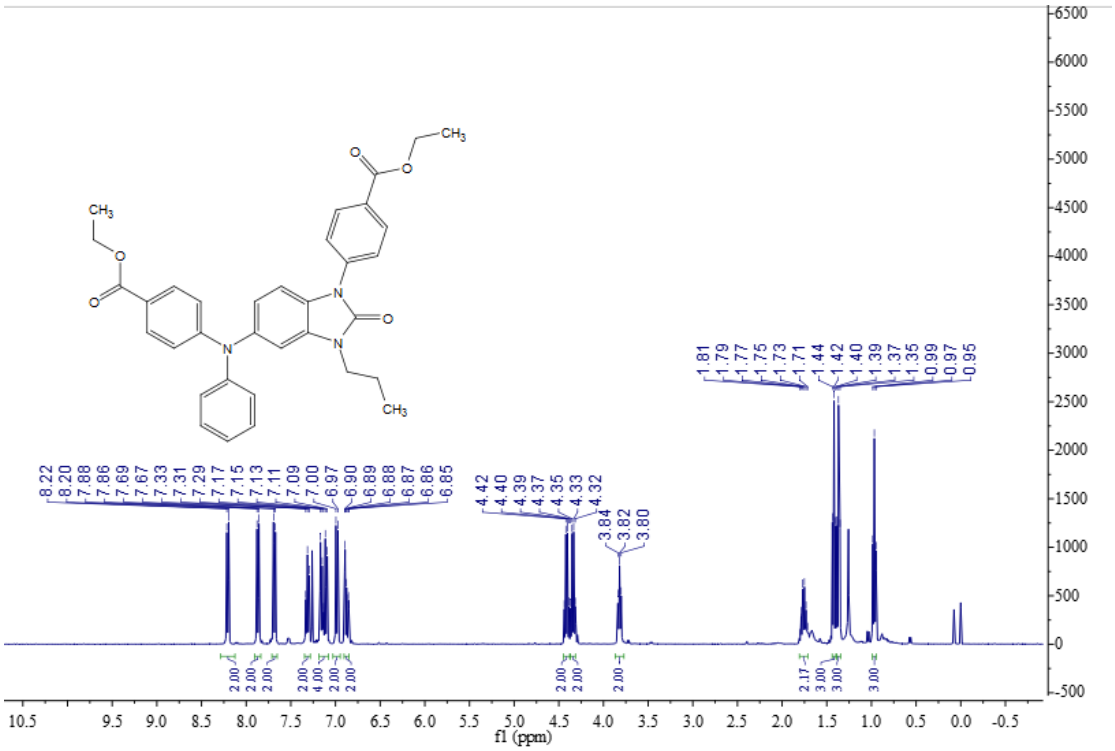

Figure S69. ^{13}C-NMR (100 MHz, $CDCl_3$) spectrum of **5kg**, related to **Scheme 5**.

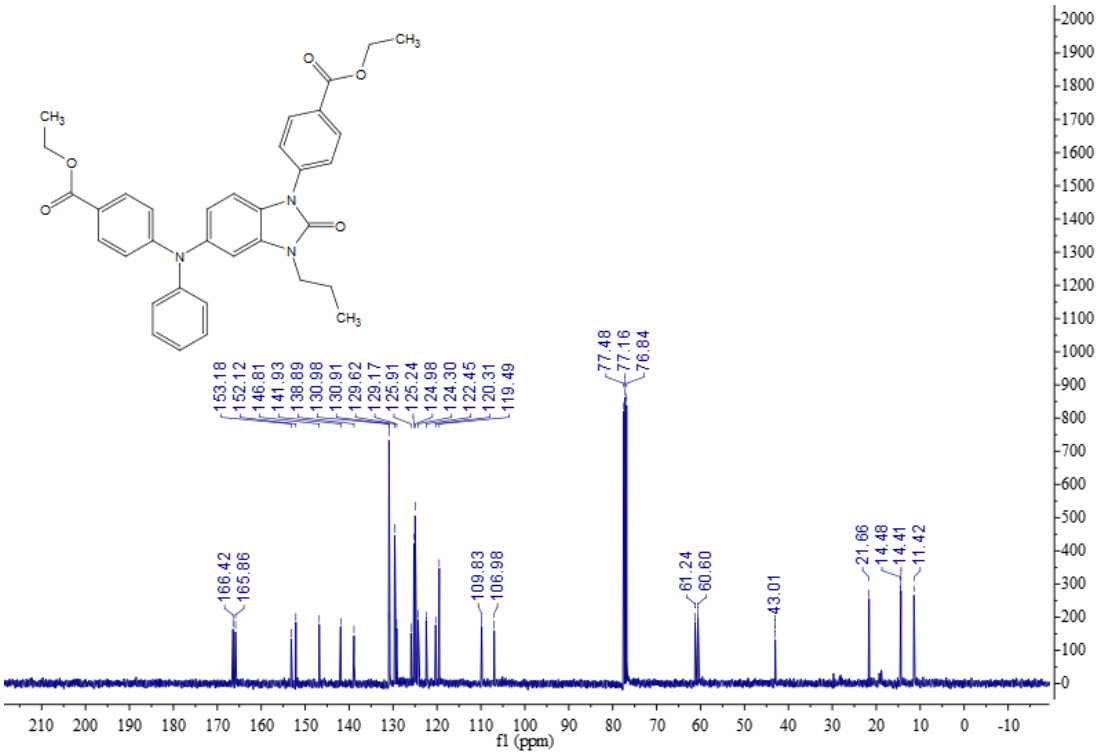

Figure S70. ^{1}H-NMR (400 MHz, $CDCl_3$) spectrum of **5lg**, related to **Scheme 5**.

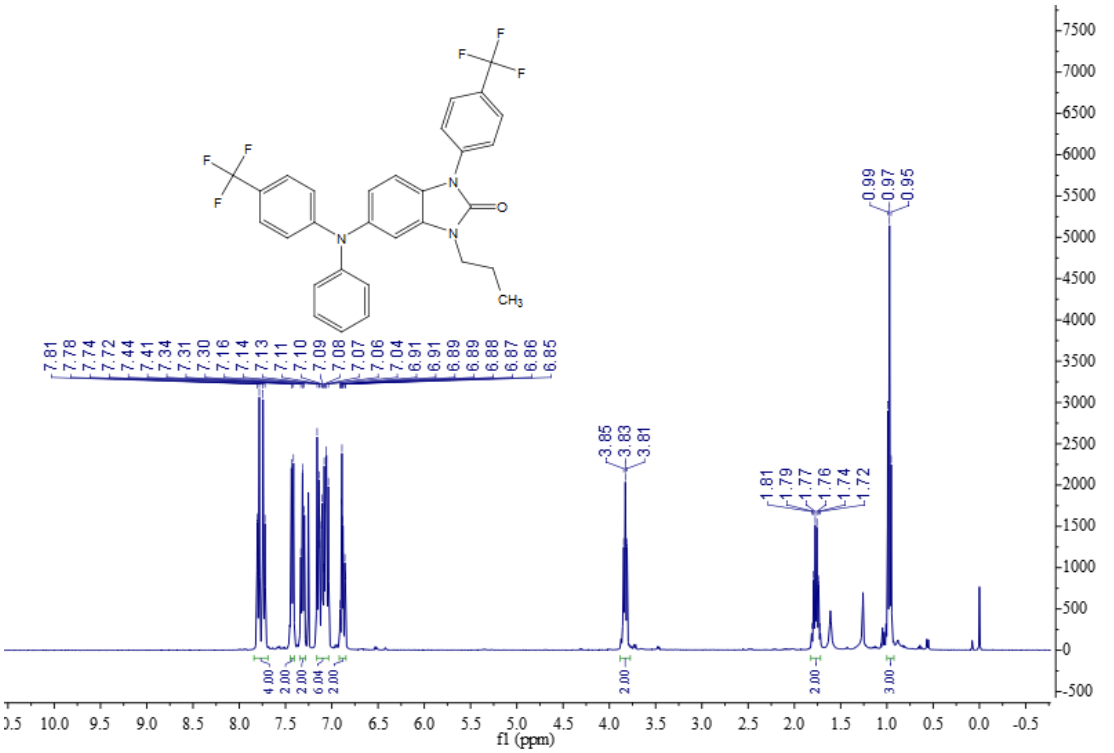

Figure S71. ^{13}C-NMR (100 MHz, $CDCl_3$) spectrum of **5lg**, related to **Scheme 5**.

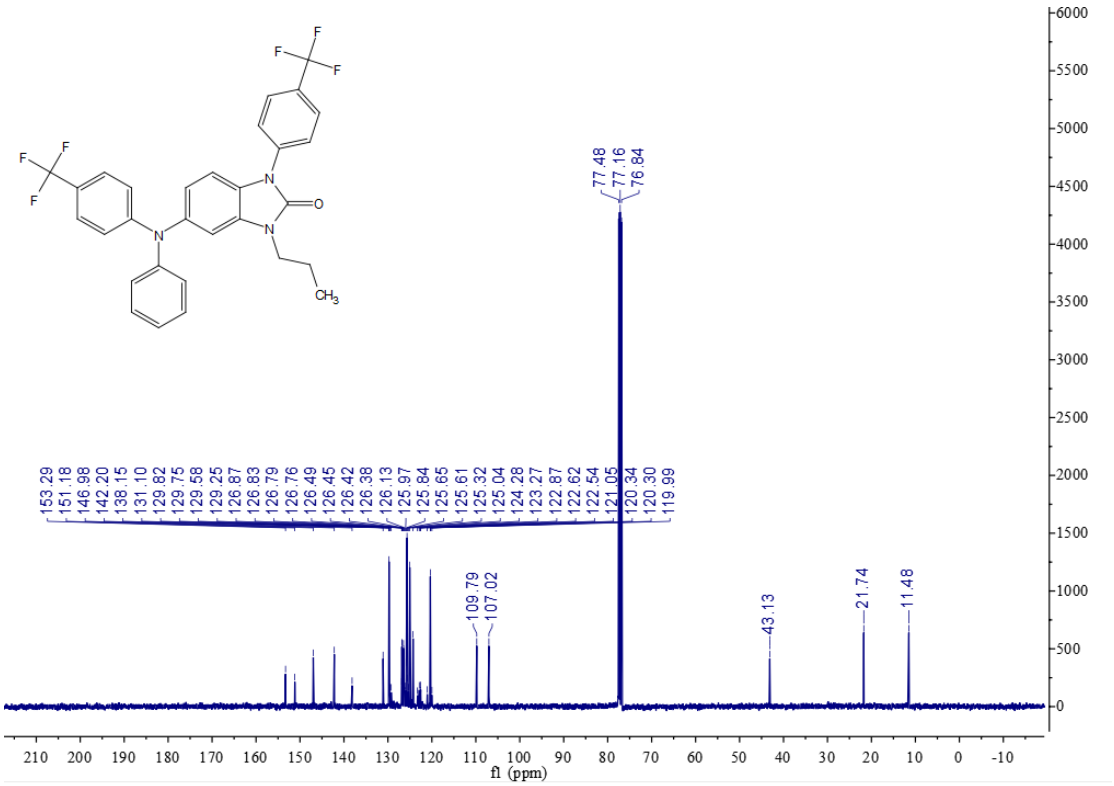

Figure S72. ^{1}H-NMR (400 MHz, $CDCl_3$) spectrum of **5mf**, related to **Scheme 5**.

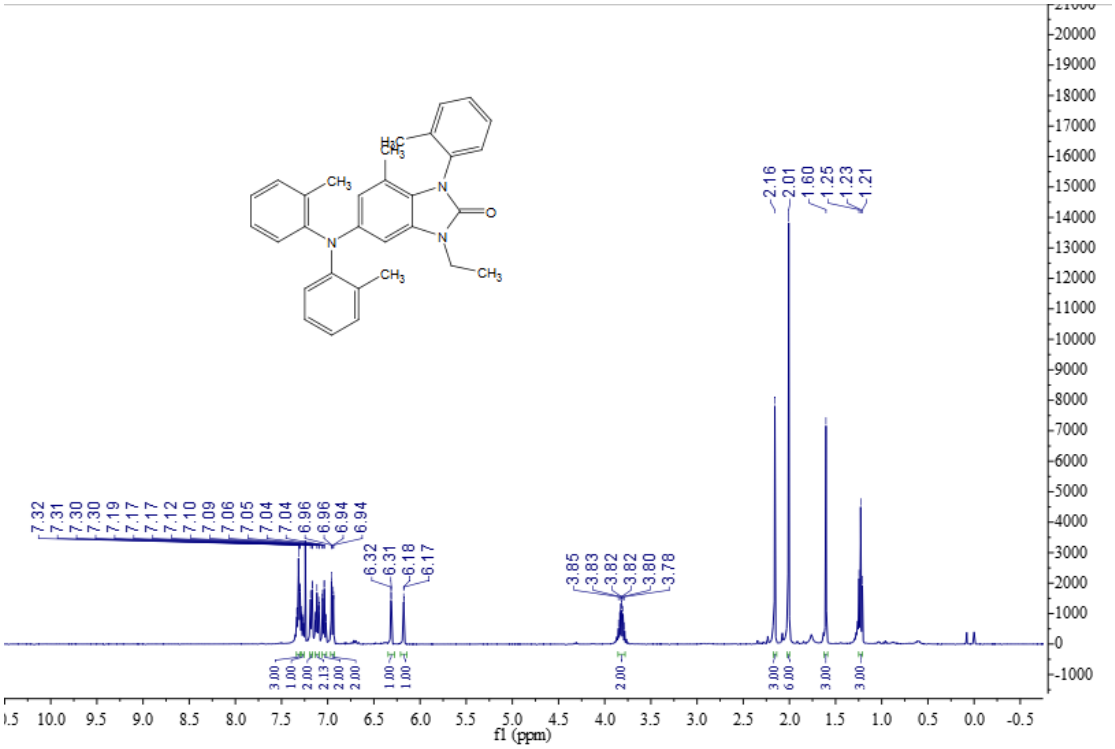

Figure S73. ^{13}C-NMR (100 MHz, $CDCl_3$) spectrum of **5mf**, related to **Scheme 5**.

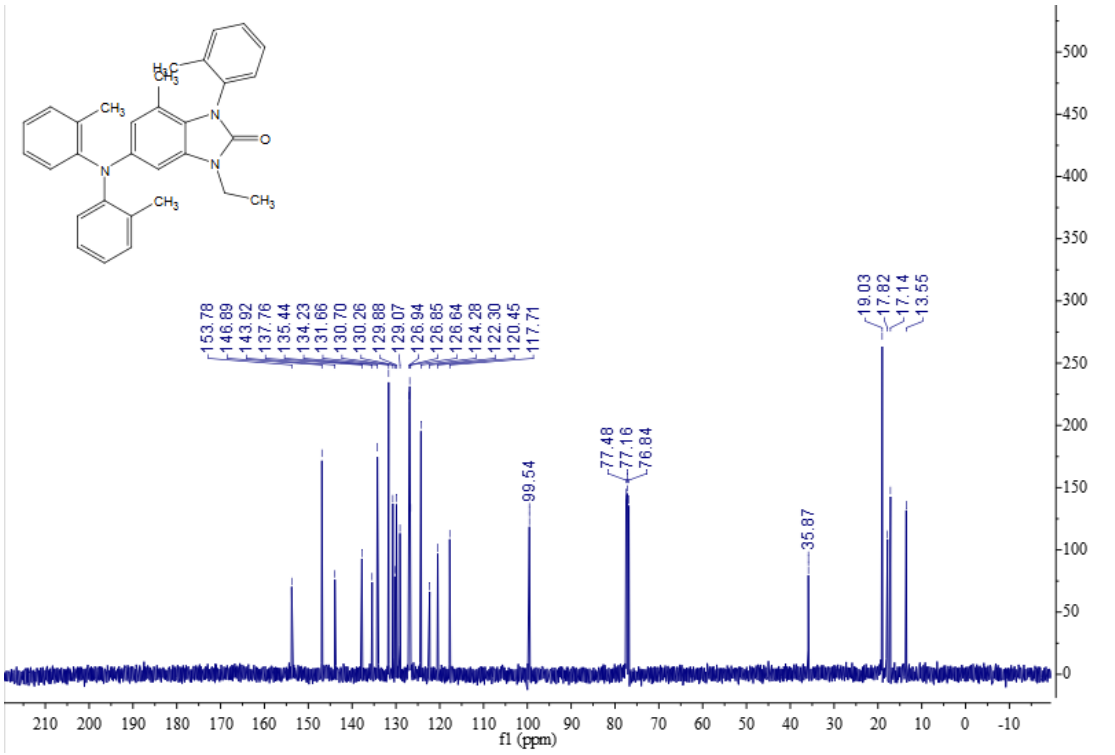

Figure S74. ^{1}H-NMR (400 MHz, $CDCl_3$) spectrum of **5nf**, related to **Scheme 5**.

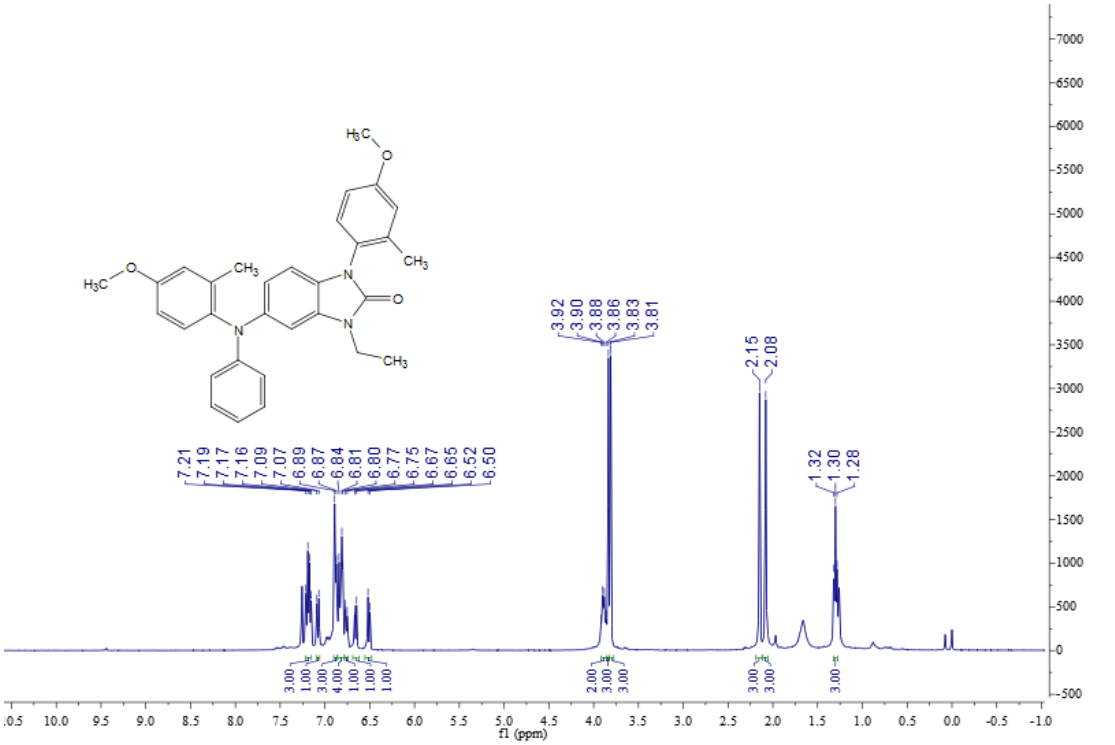

Figure S75. ^{13}C-NMR (100 MHz, $CDCl_3$) spectrum of **5nf**, related to **Scheme 5**.

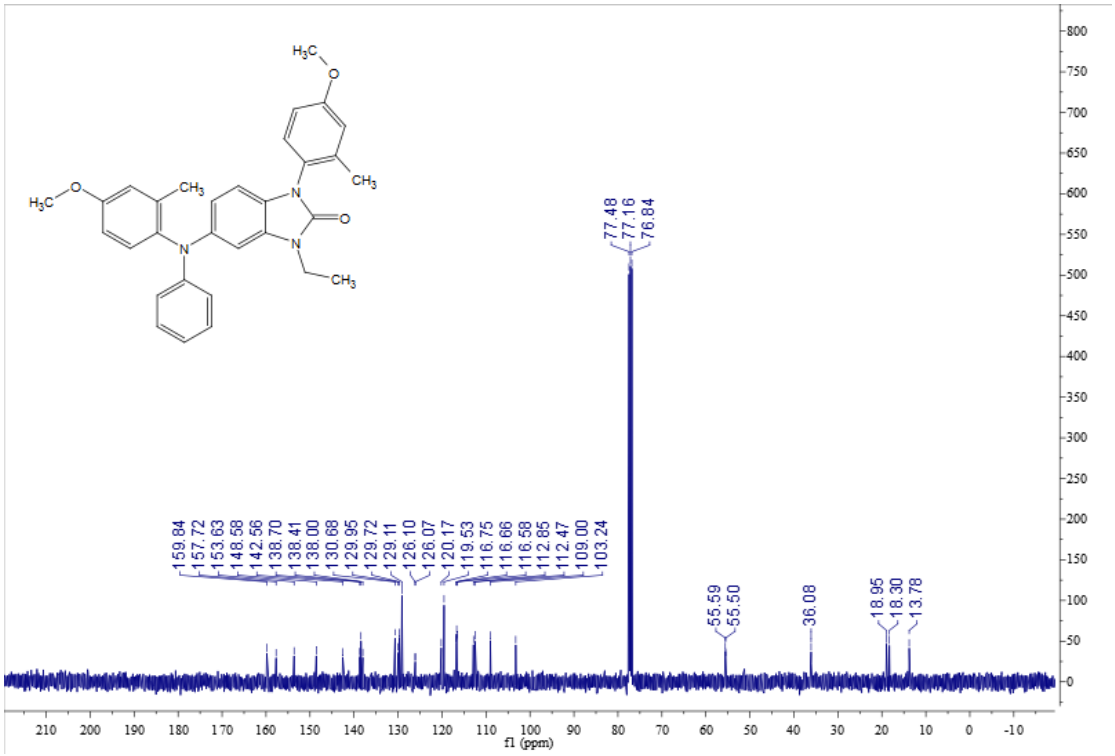

Figure S76. ^{1}H-NMR (400 MHz, $CDCl_3$) spectrum of **5og**, related to **Scheme 5**.

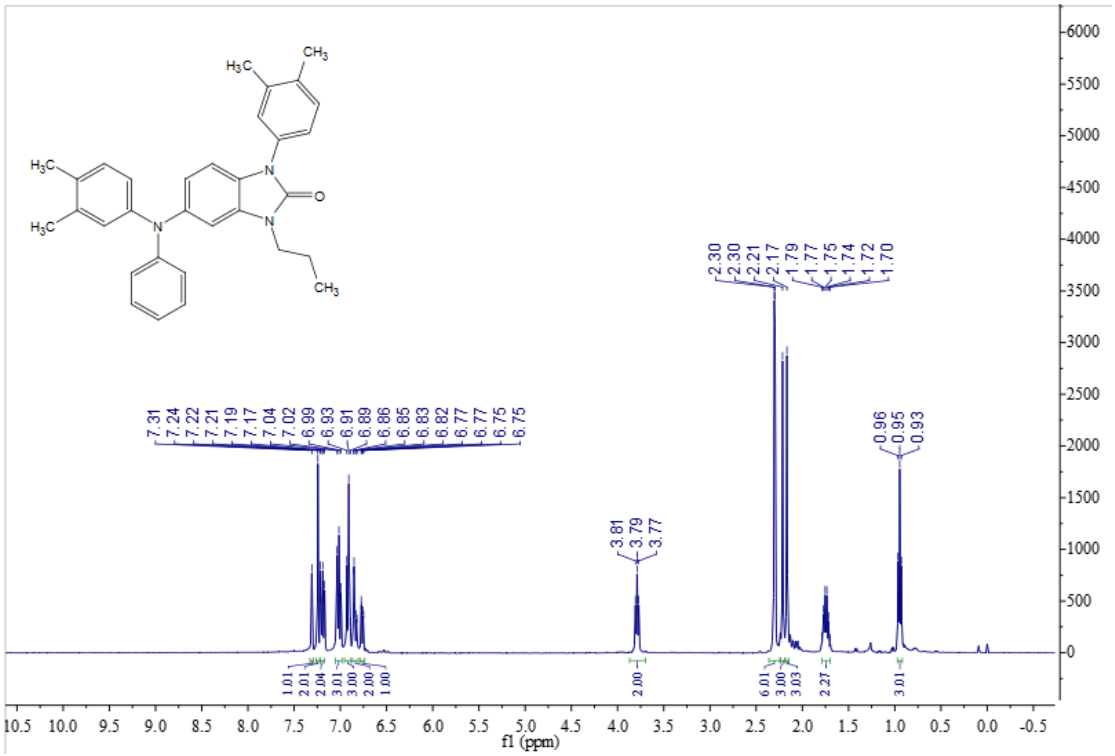

Figure S77. ^{13}C-NMR (100 MHz, $CDCl_3$) spectrum of **5og**, related to **Scheme 5**.

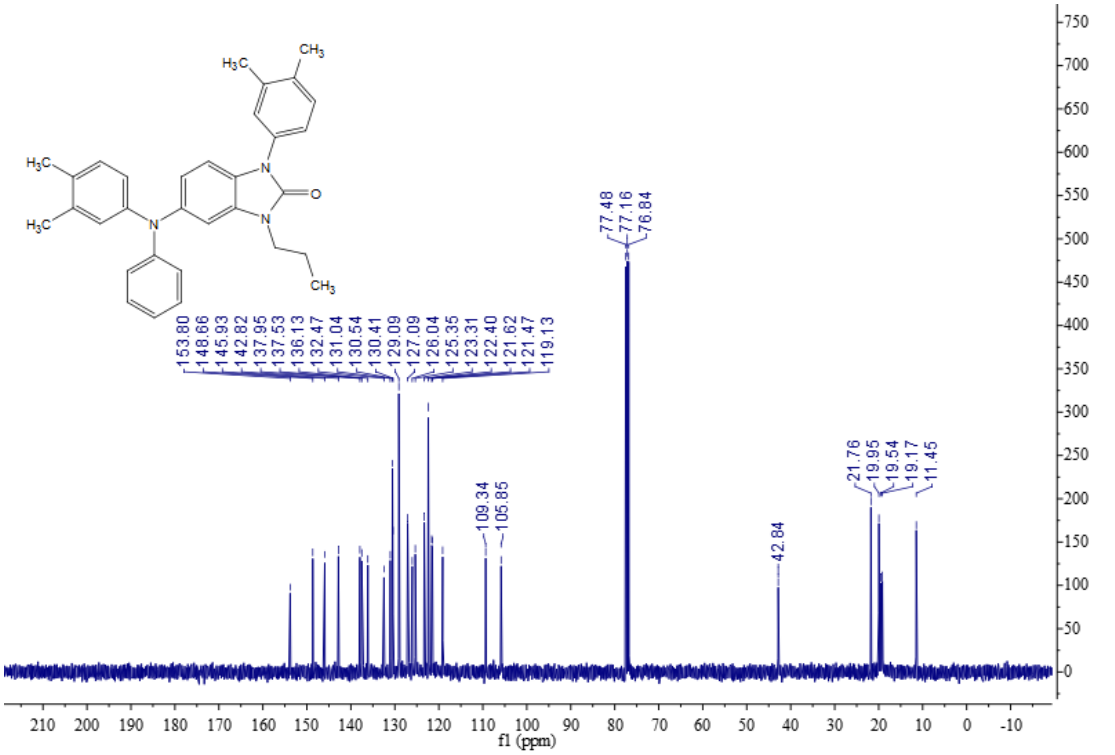

Figure S78. ^{1}H-NMR (400 MHz, $CDCl_3$) spectrum of **5pf**, related to **Scheme 5**.

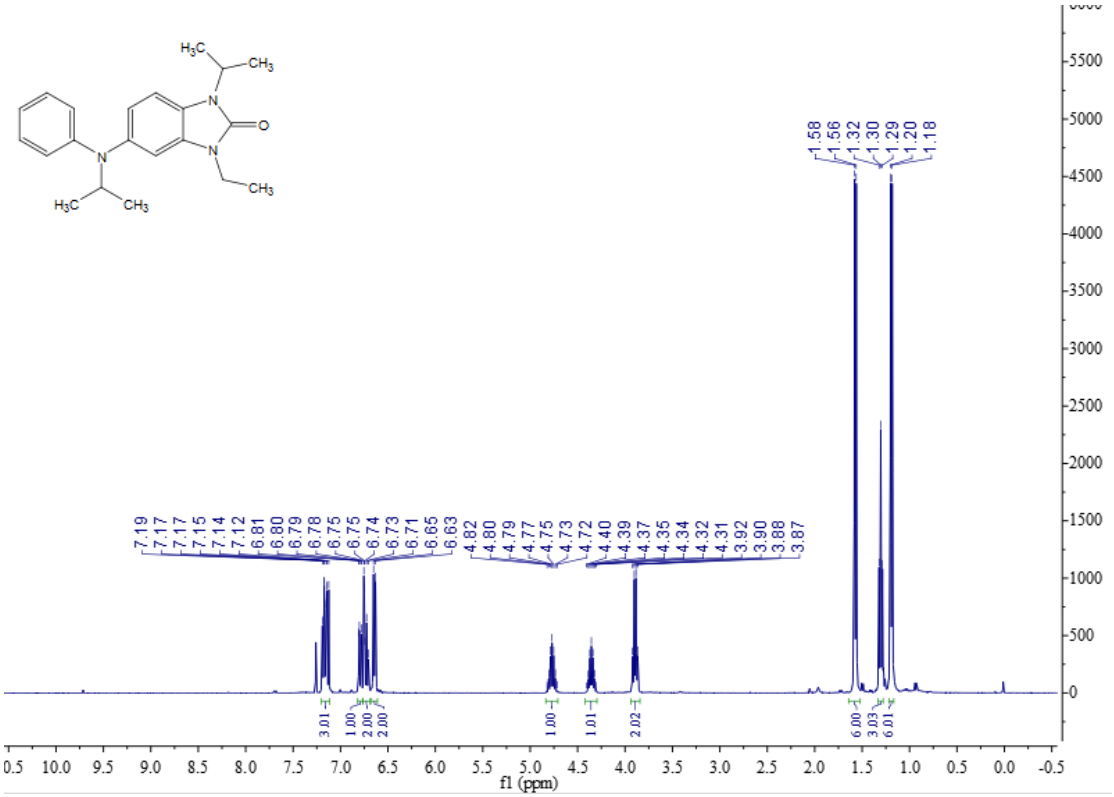

Figure S79. ^{13}C-NMR (100 MHz, $CDCl_3$) spectrum of **5pf**, related to **Scheme 5**.

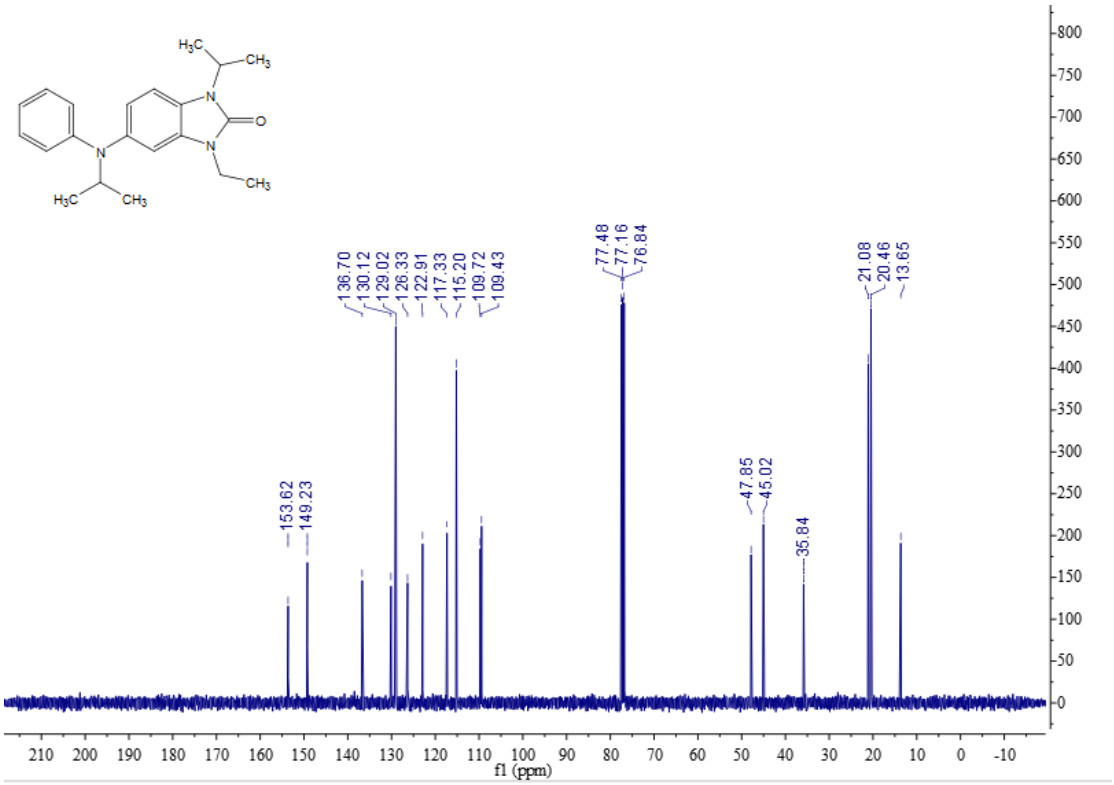

Figure S80. ^{1}H-NMR (400 MHz, $CDCl_3$) spectrum of **1q**, related to **Scheme 6**.

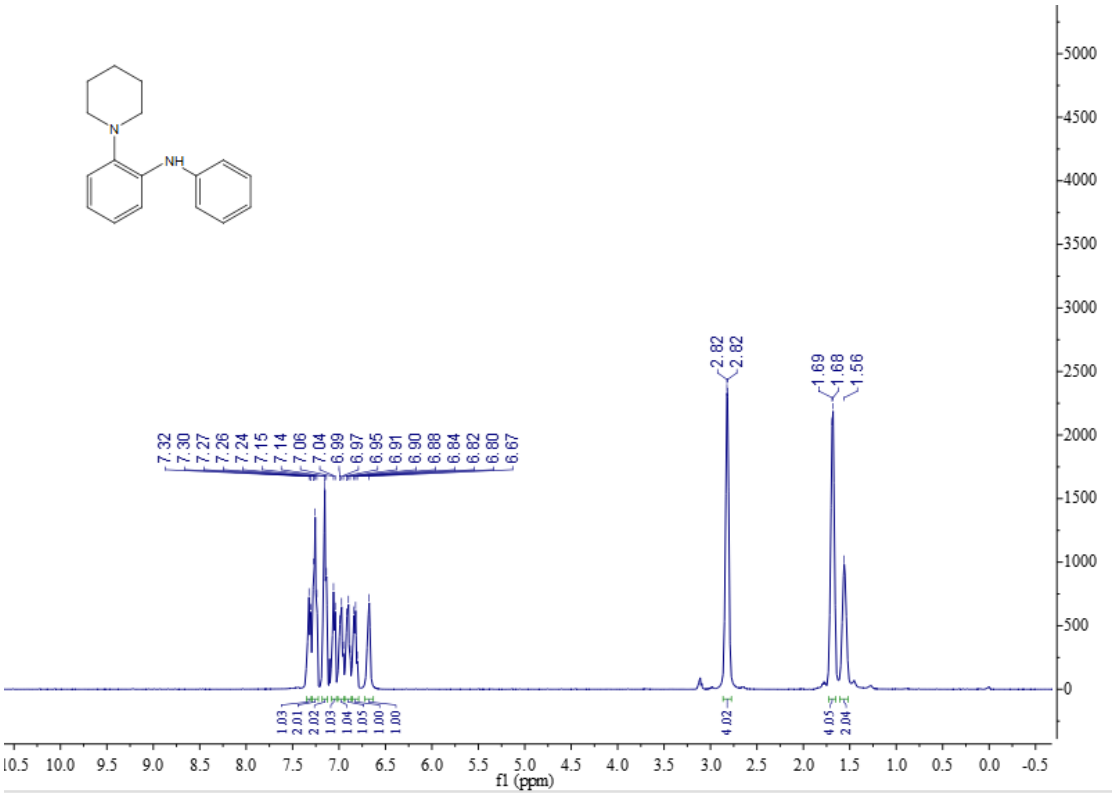

Figure S81. ^{13}C-NMR (100 MHz, $CDCl_3$) spectrum of **1q**, related to **Scheme 6**.

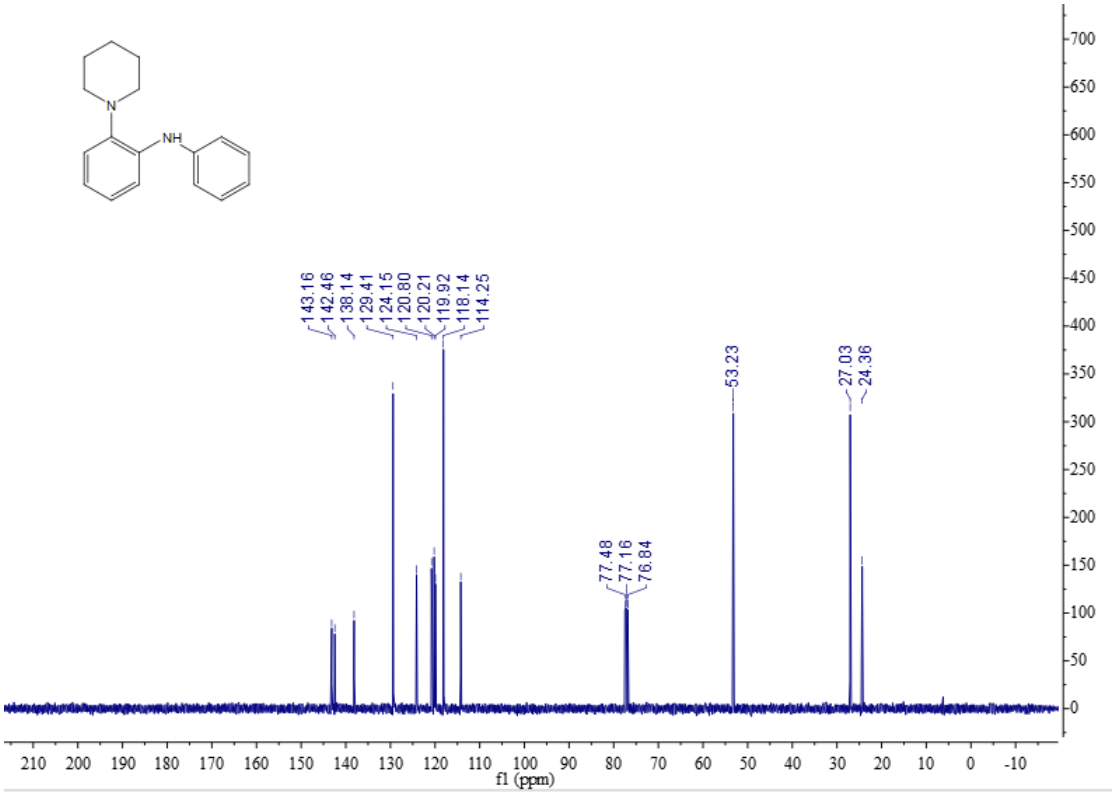

Figure S82. ^{1}H-NMR (400 MHz, $CDCl_3$) spectrum of **6qa**, related to **Scheme 6**.

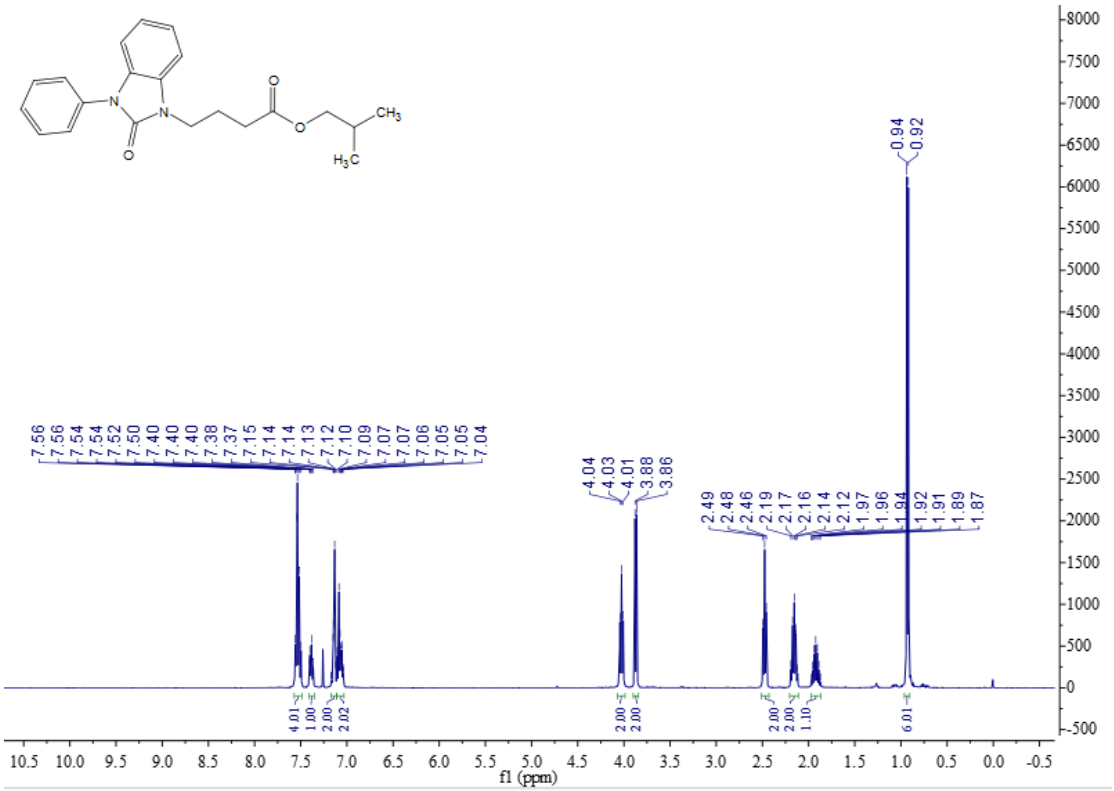

Figure S83. ^{13}C-NMR (100 MHz, $CDCl_3$) spectrum of **6qa**, related to **Scheme 6**.

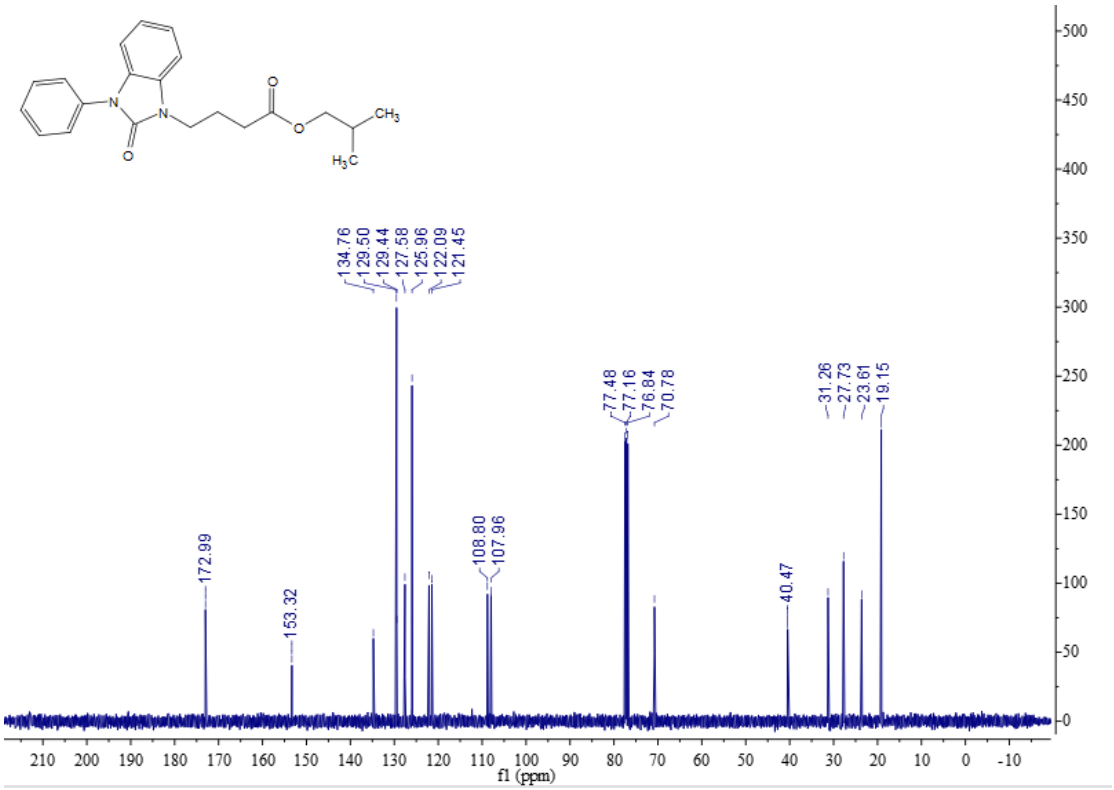

Transparent Methods.

All the obtained products were characterized by melting points (m.p), ^{1}H-NMR, ^{13}C-NMR and infrared spectra (IR). Melting points were measured on an Electrothemal SGW-X4 microscopy digital melting point apparatus and are uncorrected; IR spectra were recorded on a FTLA2000 spectrometer; ^{1}H-NMR and ^{13}C-NMR spectra were obtained on Bruker-400 and referenced to 7.26 ppm for chloroform solvent with TMS as internal standard (0 ppm). Chemical shifts were reported in parts per million (ppm, δ) downfield from tetramethylsilane. Proton coupling patterns are described as singlet (s), doublet (d), triplet (t), multiplet (m); TLC was performed using commercially prepared 100-400 mesh silica gel plates (GF254), and visualization was effected at 254 nm; Unless otherwise stated, all the reagents were purchased from commercial sources (J&K Chemic, TCI, Fluka, Acros, SCRC), used without further purification.

Optimization of reaction conditions.

General procedure for optimization studies. The mixture of diphenylamine **1a** (85 mg, 0.5 mmol), hexamethyleneimine hydrochloride **2a** (34 mg, 0.25 mmol), and catalyst (20 mol %) in *i*-butanol **3a** (1.5 mL) was stirred at 100 °C for 12 h under O_2 atmosphere (using an O_2 balloon). After being cooled to room temperature, the resulting mixture was concentrated by removing the solvent under vacuum, and the residue was purified by preparative TLC on silica (petroleum ether/ethyl acetate = 4/1) to give **4aaa**.

Table S1. Screening of optimal reaction conditions. [a] Related to the first paragraph of "RESULTS AND DISCUSSION" in main text.

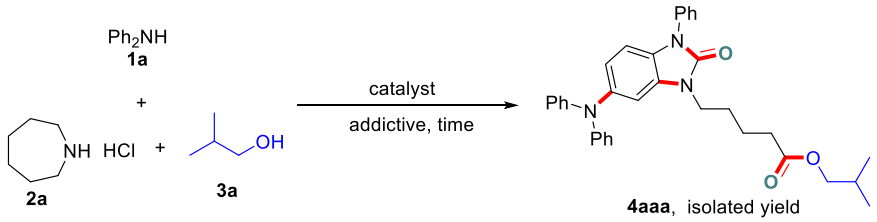

Entry	Catalyst	Additive	Yield% of **4aaa**[b]
1.	CuCl	-	29
2.	$CuCl_2$	-	32
3.	$CuBr_2$	-	trace
4.	$Cu(OAc)_2$	-	nd
5.	$Cu(OTf)_2$	-	19
6.	CuF_2	-	15
7.	$Cu(CH_3CN)_4PF_6$	-	23
8.	CuI	-	nd
9.	$CuCl_2$	pyridine(1.0 eq)	(50, <5, nd)[c]
10.	$CuCl_2$	pyridine(2.0 eq)	(45, 57, 58, 52)[d]
11.	$CuCl_2$	2-phenylpyridine (1.0 eq)	27
12.	$CuCl_2$	4-cyanopyridine (1.0 eq)	25
13.	$CuCl_2$	1,10-phen(1.0 eq)	nd
14.	$CuCl_2$	Ph_3P(1.0 eq)	<5
15.	$CuCl_2$	$Cu(OAc)_2$ (1.0 eq)	25

16.	$CuCl_2$	AgOAc (1.0 eq)	<5
17.	$CuCl_2$	pyridine(2.0 eq) + H_2O_2(2.0 eq)	38
18.	$CuCl_2$	pyridine(2.0 eq) + DCP (2.0 eq)	55
19.	$CuCl_2$	pyridine(2.0 eq) + TBHP(2.0 eq)	42
20.	$CuCl_2$	pyridine(2.0 eq) + DTBP(2.0 eq)	59
21.	$CuCl_2$	pyridine(2.0 eq) + DTBP(1.0 eq)	37
22.	$CuCl_2$	pyridine(2.0 eq) + DTBP(5.0 eq)	45
23.	$CuCl_2$	pyridine(2.0 eq) + NaOH (1.0 eq)	nd
24.	$CuCl_2$	pyridine(2.0 eq) + Na_2CO_3 (1.0 eq)	60
25.	$CuCl_2$	Pyridine(2.0 eq) + Na_2CO_3 (0.2 eq)	43
26.	**$CuCl_2$**	**pyridine(2.0 eq) + Na_2CO_3 (2.0 eq)**	**71**
27.	$CuCl_2$	pyridine(2.0 eq) + Na_2CO_3 (5.0 eq)	41
28.	$CuCl_2$	Na_2CO_3 (1.0 eq)	49
29.	$CuCl_2$	pyridine(2.0 eq) + $NaHCO_3$ (1.0 eq)	56
30.	$CuCl_2$	pyridine(2.0 eq) + K_2CO_3 (1.0 eq)	50
31.	$CuCl_2$	pyridine(2.0 eq) + NaH (1.0 eq)	39
32.	$CuCl_2$	pyridine(2.0 eq) + *t*-BuONa (1.0 eq)	trace
33.	$CuCl_2$	pyridine(2.0 eq) + *t*-BuOK (1.0 eq)	trace
34.	$CuCl_2$	pyridine(2.0 eq) + $CsCO_3$ (1.0 eq)	trace
35.	$CuCl_2$	pyridine(2.0 eq) + CH_3ONa (1.0 eq)	trace
36.	$CuCl_2$	pyridine(2.0 eq) + K_3PO_4 (1.0 eq)	32
37.	$CuCl_2$	pyridine(2.0 eq) + $NaH_2PO_2 \cdot H_2O$ (1.0 eq)	32
38.	$CuCl_2$	pyridine(2.0 eq) + KPF_6 (1.0 eq)	47
39.	$CuCl_2$	pyridine(2.0 eq) + alanine (1.0 eq)	20
40.	$CuCl_2$	pyridine(2.0 eq) + citric Acid (1.0 eq)	trace
41.	$CuCl_2$	pyridine(2.0 eq) + HBF_4 (1.0 eq)	20

[a] Reation conditions: Unless otherwise stated, all the reactions were performed with **1a** (0.50 mmol), **2a** (0.25 mmol), **3a** (1.5 mL) Catalyst (20 mol %) at 100 ^oC for 12 h under O_2 atmosphere (by using an O_2 ballroom). [b] Isolated yield. [c] Yields are with respect to under O_2 atmosphere, under air atmosphere and under N_2 atmosphere, respectively. [d] Yields are with respect to 8h, 12h, 16h and 24h, respectively.

Typical procedure for the synthesis of 4aaa.

The mixture of diphenylamine **1a** (85mg, 0.5 mmol), hexamethyleneimine hydrochloride **2a** (34 mg, 0.25 mmol), $CuCl_2$ (7 mg, 0.05 mmol), Na_2CO_3 (53 mg, 0.5 mmol) and pyridine (40 mg, 0.5 mmol) in *i*-butanol **3a** (1.5 mL) was stirred at 100 °C for 12 h under O_2 atmosphere (using an O_2 balloon). After being cooled to room temperature, the resulting mixture was concentrated by removing the solvent under vacuum, and the residue was purified by preparative TLC on silica (petroleum ether/ethyl acetate = 4/1) to give isobutyl-5-(6-(diphenylamino)-2-oxo-3-phenyl-2,3-dihydro-1*H*-benzo[*d*]imidazol-1-yl)pentanoat e **4aaa**.

Scheme S1. Substrates employed for synthesizing **4** and **5**. Related to **Scheme 3, 4** & **5**.

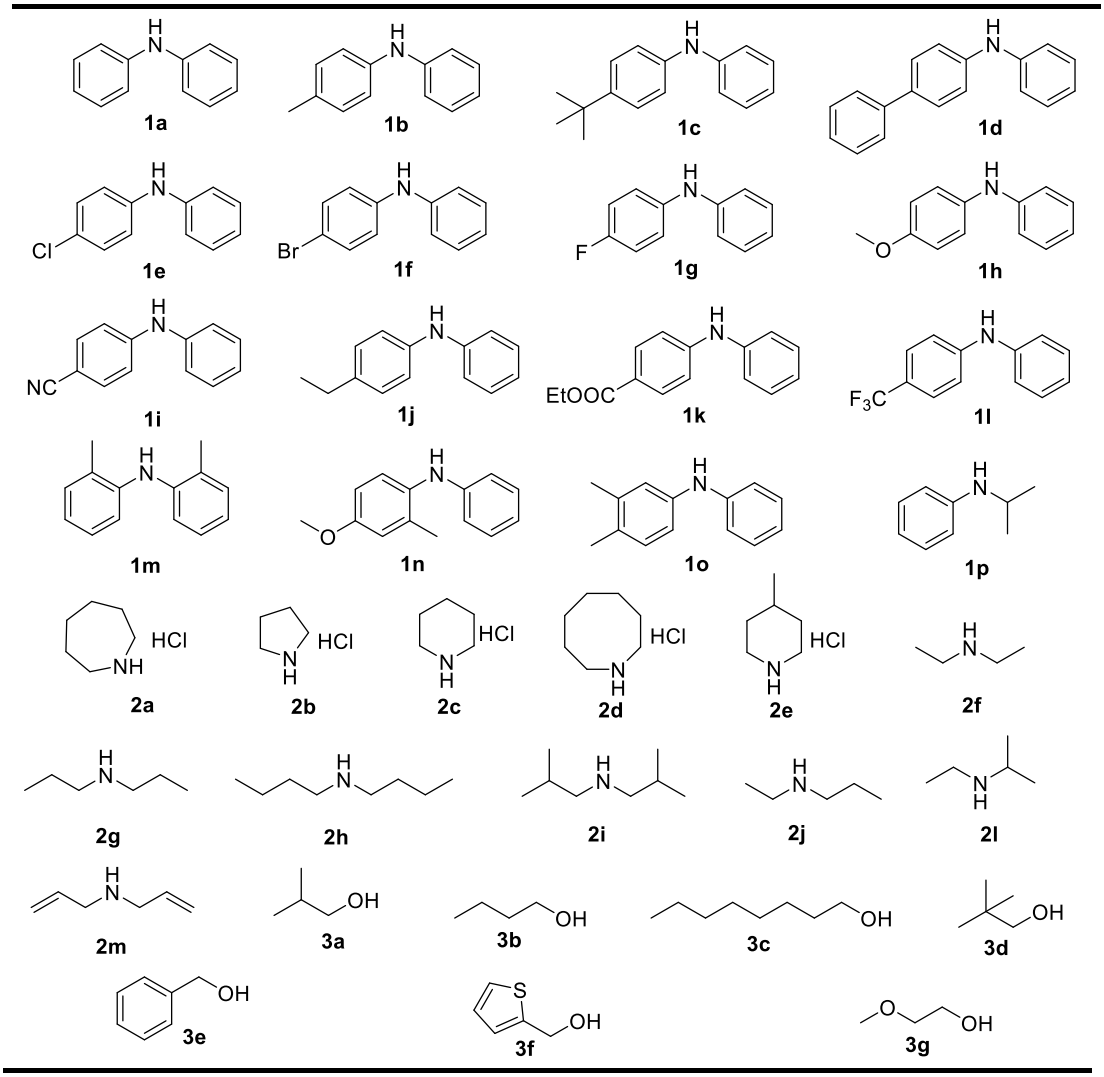

The control Experiments.

(1) The preparation of **1aa** was similar to the literature procedures. (Yang et al., 2012) A mixture of N^1,N^4-diphenylphenylenediamine (3905 mg, 15 mmol), bromobenzene (785 mg, 5 mmol), $Pd_2(dba)_3$ (27 mg, 0.03 mmol), DPPF (34 mg, 0.06 mmol), and *t*-BuONa (1440 mg, 15 mmol) in toluene (10 mL) was refluxed under N_2 atmosphere for 21 h. The reaction mixture was then filtered. The filtrate was evaporated under vacuum to remove the solvent and the crude product was then purified by column chromatography on silica gel eluting with dichloromethane/hexane (1:2), which afforded compounds **1aa** as a white solid (605 mg, 36%).

The analytic data of compound **1aa**: ^{1}H NMR (400 MHz, DMSO) δ 8.14 (s, 1H), 7.26 – 7.18 (m, 6H), 7.03 – 7.11 (m, 4H), 6.92 – 6.99 (m, 8H), 6.79 (t, *J* = 7.2 Hz, 1H).

Under the optimized reaction conditions, the reaction of **1aa** (84 mg, 0.25 mmol) and **2a** (34 mg, 0.25 mmol) was carried out for 12 h. Then, the reaction mixture was purified by preparative TLC on silica eluting with petroleum ether/ethyl acetate (4:1) to give product **4aaa** as a brownish oid (109 mg, 82% yield).

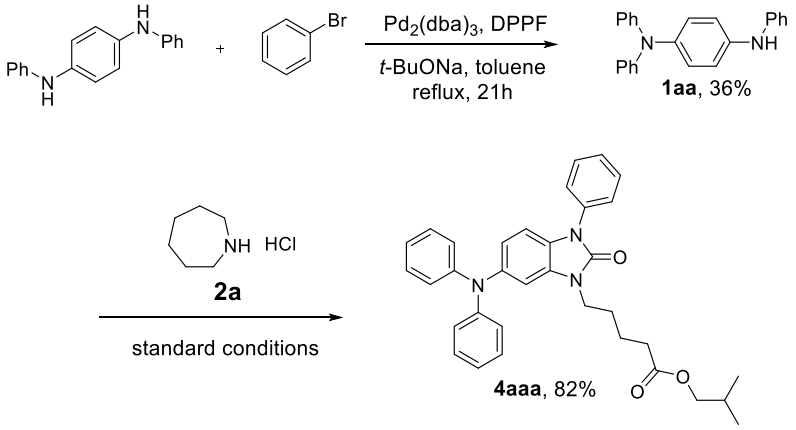

Figure S84. Related to **Scheme 6**.

(2) Under the optimized reaction conditions, the model reaction was carried out for 12 hours by introducing 3.0 equivalent of TEMPO (2,2,6,6-tetramethyl-1-piperidinyloxy), and the crude reaction mixture was analyzed by TLC and GC-MS, which indicated that no **4aaa** was formed during the reaction.

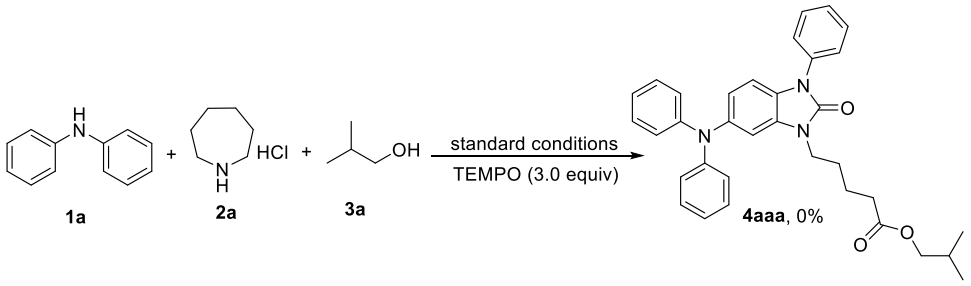

Figure S85. Related to **Scheme 6**.

(3) The preparation of N-phenyl-2-(piperidin-1-yl)aniline **1q** was similar to literature procedures. (Shi et al., 2013) General procedure: a mixture of fresh aniline **1q'** (921 mg, 5.0 mmol), 1,5-diiodopentane (1620 mg, 5.0 mmol), and K_2CO_3 (1382 mg, 10 mmol) in EtOH (10 mL) was refluxed at 75 ^{o}C for 18 h. The suspension was filtered, and the resulting solid was washed

with CH_2Cl_2. The filtered solution was extracted with water, and the organic layer was dried over anhydrous $MgSO_4$ and concentrated in vacuo. Purification by column chromatography on silica gel (eluent: $CHCl_3$) produced an oil.

The analytic data of compound (**1q**): Brownish liquid, (1046 mg, 83% yield); ^{1}H NMR (400 MHz, $CDCl_3$) δ 7.31 (d, *J* = 7.6 Hz, 1H), 7.26 (t, *J* = 6.8 Hz, 2H), 7.14 (d, *J* = 7.2 Hz, 2H), 7.05 (d, *J* = 7.4 Hz, 1H), 6.97 (t, *J* = 7.4 Hz, 1H), 6.90 (t, *J* = 7.0 Hz, 1H), 6.82 (t, *J* = 7.2 Hz, 1H), 6.67 (s, 1H), 2.82 (d, *J* = 2.8 Hz, 4H), 1.69 (d, *J* = 4.0 Hz, 4H), 1.56 (s, 2H). ^{13}C NMR (100 MHz, $CDCl_3$) δ 143.16, 142.46, 138.14, 129.41, 124.15, 120.80, 120.21, 119.92, 118.14, 114.25, 53.23, 27.03, 24.36. IR (KBr): 3042, 2934, 2850, 2807, 1714, 1591, 1512, 1462, 1418, 1314, 1225, 788, 744 cm^{-1}. MS (EI, m/z): 252 $[M]^+$. HRMS (ESI): Calcd. for $C_{17}H_{21}N_2$ $[M+H]^+$: 253.1699; found: 253.1701.

Then, under the standard conditions, the reaction of **1q** (63 mg, 0.25 mmol) add an equivalent of **1a** was carried out, and the reaction mixture was analyzed by TLC, after the reaction finished completely. Then being cooled to room temperature, the resulting mixture was concentrated by removing the solvent under vacuum, and the reaction mixture was purified by preparative TLC on silica gel eluting with petroleum ether / ethyl acetate (20:1) to give product **6qa** as a brownish solid.

The analytic data of compound (**6qa**): Brownish oil liquid, (69 mg, 78% yield); ^{1}H NMR (400 MHz, $CDCl_3$): δ 7.57 – 7.49 (m, 4H), 7.41 – 7.35 (m, 1H), 7.17 – 7.11 (m, 2H), 7.11 – 7.03 (m, 2H), 4.03 (t, *J* = 7.0 Hz, 2H), 3.87 (d, *J* = 6.8 Hz, 2H), 2.48 (t, *J* = 7.2 Hz, 2H), 2.16 (p, *J* = 7.2 Hz, 2H), 1.98 – 1.87 (m, 1H), 0.93 (d, *J* = 6.8 Hz, 6H). ^{13}C NMR (100 MHz, $CDCl_3$): δ 172.99, 153.32, 134.76, 129.50, 129.44, 127.58, 125.96, 122.09, 121.45, 108.80, 107.96, 70.78, 40.47, 31.26, 27.73, 23.61, 19.15. IR (KBr): 3063, 2961, 2875, 2831, 1715, 1598, 1502, 1173, 753, 734, 697 cm^{-1}. MS (EI, m/z): 352 $[M]^+$. HRMS (ESI): Calcd. for $C_{21}H_{25}N_2O_3$ $[M+H]^+$: 353.1860; found: 353.1864.

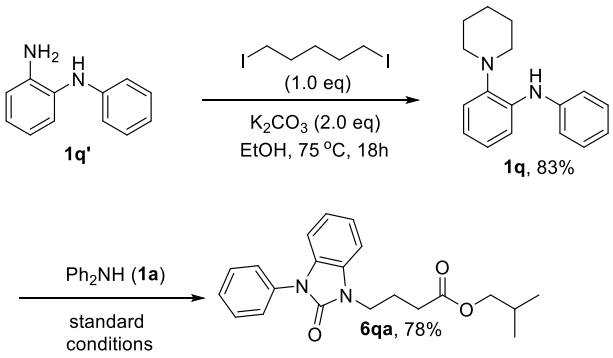

Figure S86. Related to **Scheme 6**.

(4) Under the optimized reaction conditions, the reaction of diarylamine **1r** and dialkylamine **2f** was carried out at 100 °C for 12 hours, and the crude reaction mixture was analyzed by TLC and GC-MS, which indicated that no **5rf** was formed during the reaction.

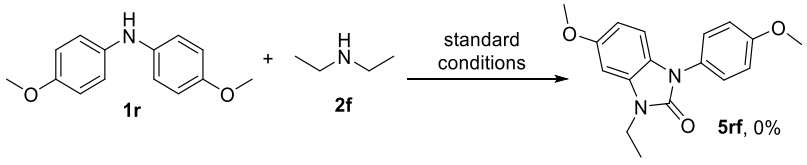

Figure S87. Related to **Scheme 6**.

Single crystal X-ray diffraction of 5al.

Yellow block-like single crystals of **5al** were grown by layering a dichlormethane solution with *n*-hexane at ambient temperature. X-Ray diffraction data of one these crystals were collected on a R-AXIS SPIDER diffractometer. The measurements were performed with Mo-Kα radiation (λ = 0.71073 Å). Data were collected at 296(2) K, using the *ω*- and *φ*- scans to a maximum θ value of 25.03°. The data were refined by full-matrix least-squares techniques on F^2 with SHELXTL-2014. And the structures were solved by direct methods SHELXS-2014. All the non-hydrogen atoms were refined anisotropically. The hydrogen atoms were included at geometrically idealized positions. An ORTEP representation of the structure is shown below.

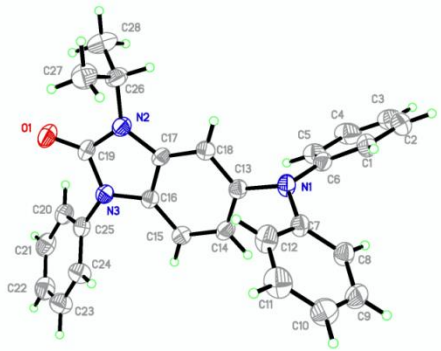

Figure S88. ORTEP drawing of **5al** with the numbering scheme. Related to **Scheme 4**.

Table S2. Crystal data and structure refinement for **5al**. Related to **Scheme 4**.

Identification code	5al	
Empirical formula	$C_{28}H_{25}N_3O$	
Formula weight	419.51	
Temperature	296(2) K	
Wavelength	0.71073 Å	
Crystal system	Monoclinic	
space group	$P2_1/n$	
Unit cell dimensions	a = 7.9689(6) Å	alpha = 90°
	b = 11.6429(9) Å	beta = 97.043(2) °
	c = 24.549(2) Å	gamma = 90°
Volume	2260.5(3) $Å^3$	
Z	4	
Calculated density	1.233 Mg/m^3	
Absorption coefficient	0.076 mm^{-1}	
F(000)	888	
Crystal size	0.23 x 0.20 x 0.18 mm^3	
Theta range for data collection	2.61 to 25.03°.	
Limiting indices	-9<=h<=6, -13<=k<=13, -29<=l<=27	
Reflections collected / unique	14344 / 4002 [R(int) = 0.0486]	

Completeness to theta = 25.03	99.9 %
Absorption correction	None
Max. and min. transmission	0.9865 and 0.9828
Refinement method	Full-matrix least-squares on F^2
Data / restraints / parameters	4002 / 0 / 290
Goodness-of-fit on F^2	1.018
Final R indices [I>2sigma(I)]	R1 = 0.0494, wR2 = 0.1162
R indices (all data)	R1 = 0.0910, wR2 = 0.1392
Extinction coefficient	0.0068(12)
Largest diff. peak and hole	0.192 and -0.147 e. $Å^{-3}$

Table S3. Atomic coordinates (x 10^4) and equivalent isotropic displacement parameters ($Å^2$ x 10^3) for **5al**. U(eq) is defined as one third of the trace of the orthogonalized U^{ij} tensor. Related to **Scheme 4**.

	x	y	z	U(eq)
O(1)	9782(2)	2008(2)	2364(1)	68(1)
N(1)	5689(2)	3364(2)	-310(1)	52(1)
N(2)	7809(2)	2646(2)	1645(1)	52(1)
N(3)	10022(2)	1639(2)	1444(1)	47(1)
C(1)	3955(3)	1630(2)	-345(1)	62(1)
C(2)	2493(4)	1057(3)	-530(1)	82(1)
C(3)	1222(4)	1595(3)	-858(1)	89(1)
C(4)	1392(3)	2736(3)	-989(1)	84(1)
C(5)	2861(3)	3323(3)	-801(1)	67(1)
C(6)	4176(3)	2770(2)	-487(1)	50(1)
C(7)	6488(3)	4043(2)	-687(1)	48(1)
C(8)	6240(3)	3855(2)	-1248(1)	59(1)
C(9)	7084(3)	4515(2)	-1594(1)	74(1)
C(10)	8177(4)	5354(3)	-1391(1)	85(1)
C(11)	8433(4)	5542(2)	-834(1)	84(1)
C(12)	7596(3)	4899(2)	-482(1)	67(1)
C(13)	6826(3)	2872(2)	129(1)	46(1)
C(14)	8174(3)	2214(2)	7(1)	52(1)
C(15)	9330(3)	1742(2)	413(1)	49(1)
C(16)	9084(3)	1954(2)	948(1)	43(1)
C(17)	7712(3)	2597(2)	1076(1)	44(1)
C(18)	6558(3)	3070(2)	669(1)	47(1)
C(19)	9245(3)	2090(2)	1877(1)	51(1)
C(20)	11657(3)	18(2)	1844(1)	57(1)
C(21)	13073(4)	-673(2)	1875(1)	71(1)
C(22)	14328(3)	-439(2)	1556(1)	74(1)
C(23)	14205(3)	504(2)	1220(1)	73(1)
C(24)	12813(3)	1212(2)	1191(1)	63(1)
C(25)	11521(3)	956(2)	1502(1)	48(1)

C(26)	6652(3)	3298(2)	1954(1)	62(1)
C(27)	7417(3)	4429(2)	2142(1)	80(1)
C(28)	6001(4)	2587(3)	2389(1)	94(1)

Table S4. Bond lengths [Å] and angles [°] for **5al**. Related to **Scheme 4**.

O(1)-C(19)	1.223(3)
N(1)-C(6)	1.412(3)
N(1)-C(13)	1.440(3)
N(1)-C(7)	1.426(3)
N(2)-C(19)	1.376(3)
N(2)-C(17)	1.389(3)
N(2)-C(26)	1.474(3)
N(3)-C(19)	1.398(3)
N(3)-C(16)	1.396(3)
N(3)-C(25)	1.428(3)
C(1)-C(2)	1.370(3)
C(1)-C(6)	1.390(3)
C(2)-C(3)	1.366(4)
C(3)-C(4)	1.377(4)
C(4)-C(5)	1.385(4)
C(5)-C(6)	1.381(3)
C(7)-C(12)	1.385(3)
C(7)-C(8)	1.385(3)
C(8)-C(9)	1.379(3)
C(9)-C(10)	1.362(4)
C(10)-C(11)	1.374(4)
C(11)-C(12)	1.376(3)
C(13)-C(14)	1.382(3)
C(13)-C(18)	1.387(3)
C(14)-C(15)	1.386(3)
C(15)-C(16)	1.374(3)
C(16)-C(17)	1.393(3)
C(17)-C(18)	1.387(3)
C(20)-C(25)	1.375(3)
C(20)-C(21)	1.380(3)
C(21)-C(22)	1.371(3)
C(22)-C(23)	1.370(4)
C(23)-C(24)	1.377(3)
C(24)-C(25)	1.387(3)
C(26)-C(27)	1.499(3)
C(26)-C(28)	1.495(3)
C(6)-N(1)-C(13)	118.11(17)
C(6)-N(1)-C(7)	120.30(18)

C(13)-N(1)-C(7)	114.68(17)
C(19)-N(2)-C(17)	109.80(17)
C(19)-N(2)-C(26)	124.7(2)
C(17)-N(2)-C(26)	125.19(19)
C(19)-N(3)-C(16)	108.99(18)
C(19)-N(3)-C(25)	125.23(19)
C(16)-N(3)-C(25)	125.77(17)
C(2)-C(1)-C(6)	120.7(3)
C(3)-C(2)-C(1)	120.7(3)
C(2)-C(3)-C(4)	119.5(3)
C(5)-C(4)-C(3)	120.1(3)
C(6)-C(5)-C(4)	120.5(3)
C(5)-C(6)-C(1)	118.4(2)
C(5)-C(6)-N(1)	120.3(2)
C(1)-C(6)-N(1)	121.3(2)
C(12)-C(7)-C(8)	118.9(2)
C(12)-C(7)-N(1)	118.6(2)
C(8)-C(7)-N(1)	122.5(2)
C(9)-C(8)-C(7)	120.1(2)
C(8)-C(9)-C(10)	120.9(3)
C(9)-C(10)-C(11)	119.2(2)
C(12)-C(11)-C(10)	120.9(3)
C(7)-C(12)-C(11)	119.9(3)
C(14)-C(13)-C(18)	121.0(2)
C(14)-C(13)-N(1)	119.4(2)
C(18)-C(13)-N(1)	119.56(19)
C(13)-C(14)-C(15)	122.0(2)
C(16)-C(15)-C(14)	117.2(2)
C(15)-C(16)-C(17)	121.4(2)
C(15)-C(16)-N(3)	131.5(2)
C(17)-C(16)-N(3)	107.14(18)
C(16)-C(17)-C(18)	121.3(2)
C(16)-C(17)-N(2)	107.48(19)
C(18)-C(17)-N(2)	131.20(19)
C(17)-C(18)-C(13)	117.2(2)
O(1)-C(19)-N(2)	128.0(2)
O(1)-C(19)-N(3)	125.4(2)
N(2)-C(19)-N(3)	106.51(19)
C(25)-C(20)-C(21)	120.0(2)
C(22)-C(21)-C(20)	120.1(2)
C(21)-C(22)-C(23)	120.0(3)
C(24)-C(23)-C(22)	120.5(2)
C(25)-C(24)-C(23)	119.4(2)
C(20)-C(25)-C(24)	119.9(2)

C(20)-C(25)-N(3)	120.38(19)
C(24)-C(25)-N(3)	119.62(19)
N(2)-C(26)-C(27)	110.78(19)
N(2)-C(26)-C(28)	112.1(2)
C(27)-C(26)-C(28)	115.5(2)

Symmetry transformations used to generate equivalent atoms:

Table S5. Anisotropic displacement parameters ($Å^2$ x 10^3) for **5al**. The anisotropic displacement factor exponent takes the form: $-2\ pi^2\ [\ h^2\ a^{*2}\ U^{11} + ... + 2\ h\ k\ a^*\ b^*\ U^{12}\ ]$. Related to **Scheme 4**.

	U^{11}	U^{22}	U^{33}	U^{23}	U^{13}	U^{12}
O(1)	85(1)	77(1)	40(1)	-3(1)	-1(1)	9(1)
N(1)	52(1)	56(1)	45(1)	9(1)	-3(1)	-14(1)
N(2)	57(1)	56(1)	42(1)	0(1)	7(1)	6(1)
N(3)	52(1)	47(1)	42(1)	3(1)	5(1)	1(1)
C(1)	64(2)	54(2)	71(2)	-7(1)	16(1)	-10(1)
C(2)	72(2)	76(2)	102(3)	-24(2)	28(2)	-27(2)
C(3)	61(2)	121(3)	86(2)	-44(2)	20(2)	-35(2)
C(4)	51(2)	130(3)	68(2)	-9(2)	-1(1)	-8(2)
C(5)	55(2)	84(2)	59(2)	6(1)	-2(1)	-5(1)
C(6)	49(1)	57(2)	43(1)	-4(1)	6(1)	-8(1)
C(7)	52(1)	44(1)	46(2)	7(1)	-1(1)	-7(1)
C(8)	62(2)	61(2)	52(2)	6(1)	1(1)	-12(1)
C(9)	75(2)	89(2)	56(2)	21(2)	6(1)	-11(2)
C(10)	84(2)	86(2)	84(3)	38(2)	12(2)	-18(2)
C(11)	90(2)	60(2)	100(3)	16(2)	1(2)	-35(2)
C(12)	81(2)	54(2)	64(2)	2(1)	-3(1)	-19(1)
C(13)	49(1)	48(1)	41(1)	6(1)	4(1)	-8(1)
C(14)	61(2)	57(1)	38(1)	3(1)	9(1)	-7(1)
C(15)	53(1)	50(1)	47(2)	1(1)	9(1)	0(1)
C(16)	49(1)	39(1)	41(1)	6(1)	6(1)	-6(1)
C(17)	53(1)	44(1)	35(1)	0(1)	9(1)	-7(1)
C(18)	48(1)	45(1)	48(2)	2(1)	7(1)	-3(1)
C(19)	64(2)	52(1)	36(2)	-1(1)	2(1)	-5(1)
C(20)	70(2)	53(1)	48(2)	4(1)	3(1)	1(1)
C(21)	91(2)	62(2)	56(2)	8(1)	-3(2)	17(2)
C(22)	76(2)	74(2)	70(2)	-9(2)	-4(2)	23(2)
C(23)	63(2)	78(2)	80(2)	1(2)	14(1)	5(2)
C(24)	62(2)	54(2)	74(2)	8(1)	13(1)	1(1)
C(25)	55(1)	43(1)	45(1)	-1(1)	0(1)	-1(1)
C(26)	70(2)	68(2)	50(2)	-7(1)	16(1)	10(1)
C(27)	89(2)	66(2)	86(2)	-18(2)	10(2)	11(2)
C(28)	116(2)	93(2)	82(2)	-1(2)	51(2)	7(2)

Table S6. Hydrogen coordinates (x 10^4) and isotropic displacement parameters (Å ^{2} x 10^3) for **5al**. Related to **Scheme 4**.

	x	y	z	U(eq)
H(1A)	4808	1251	-122	75
H(2A)	2364	295	-430	98
H(3A)	250	1194	-992	106
H(4A)	519	3112	-1204	101
H(5A)	2962	4097	-887	80
H(8A)	5502	3282	-1393	70
H(9A)	6906	4386	-1970	88
H(10A)	8743	5796	-1626	102
H(11A)	9182	6111	-693	101
H(12A)	7775	5039	-106	81
H(14A)	8309	2085	-359	62
H(15A)	10234	1301	327	59
H(18A)	5642	3501	754	56
H(20A)	10795	-151	2055	69
H(21A)	13176	-1298	2113	85
H(22A)	15263	-920	1568	89
H(23A)	15069	667	1009	88
H(24A)	12739	1856	965	76
H(26A)	5666	3483	1689	74
H(27A)	7767	4832	1834	120
H(27B)	8379	4299	2410	120
H(27C)	6594	4879	2302	120
H(28A)	5518	1890	2229	141
H(28B)	5151	3010	2549	141
H(28C)	6915	2403	2668	141

Analytic data of the obtained compounds.

(1)isobutyl-5-(6-(diphenylamino)-2-oxo-3-phenyl-2,3-dihydro-1*H*-benzo[*d*]imidazol-1-yl)pentanoate (4aaa)

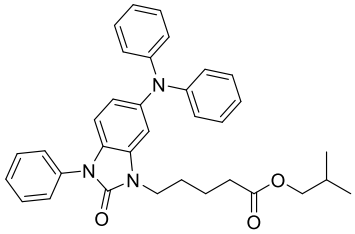

Brownish oil liquid, (95 mg, 71% yield); ^{1}H NMR (400 MHz, $CDCl_3$): δ 7.56 – 7.46 (m, 4H), 7.35 (t, *J* = 7.2 Hz, 1H), 7.25 – 7.19 (m, 4H), 7.08 (d, *J* = 7.6 Hz, 4H), 7.00 – 6.94 (m, 3H), 6.86 (d, *J* =2.0 Hz, 1H), 6.80 (dd, *J* = 8.4, 1.6 Hz, 1H), 3.89 – 3.79 (m, 4H), 2.35 (t, *J* = 7.0 Hz, 2H), 1.94 – 1.84 (m, 1H), 1.81 – 1.73 (m, 2H), 1.73 – 1.65 (m, 2H), 0.90 (d, *J* = 6.8 Hz, 6H). ^{13}C NMR (100 MHz, $CDCl_3$): δ 173.19, 153.48, 148.12, 142.80, 134.79, 130.40, 129.46, 129.19, 127.43, 125.79, 125.75, 123.19, 122.25, 119.43, 109.45, 105.96, 70.48, 40.75, 33.79, 27.76, 27.70, 22.23, 19.12. IR (KBr): 3062, 2959, 2872, 1715, 1594, 1491, 1399, 1274, 1173, 754, 695, 657 cm^{-1}. MS (EI, m/z): 533 $[M]^+$. HRMS (ESI): Calcd. for $C_{34}H_{35}N_3NaO_3$ $[M+H]^+$: 556.2571; found: 556.2579.

(2)isobutyl-5-(2-oxo-6-(phenyl(p-tolyl)amino)-3-(*p*-tolyl)-2,3-dihydro-1*H*-benzo[*d*]imidazol-1-yl)pentanoate (4baa)

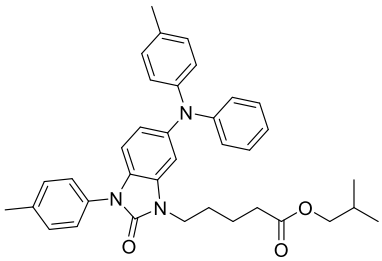

Brownish oil liquid, (107 mg, 76% yield); ^{1}H NMR (400 MHz, $CDCl_3$): δ 7.42 (d, *J* = 8.4 Hz, 2H), 7.32 (d, *J* = 8.4 Hz, 2H), 7.22 (t, *J* = 7.8 Hz, 2H), 7.04 (s, 3H), 7.01 (d, *J* = 8.4 Hz, 2H), 6.97 – 6.93 (m, 2H), 6.85 (d, *J* = 1.6 Hz, 1H), 6.79 (dd, *J* = 8.4, 1.6 Hz, 1H), 3.95 – 3.74 (m, 4H), 2.42 (s, 3H), 2.36 (t, *J* = 7.2 Hz, 2H), 2.33 (s, 3H), 1.96 – 1.86 (m, 1H), 1.83 – 1.66 (m, 4H), 0.92 (d, *J* = 6.8 Hz, 6H). ^{13}C NMR (100 MHz, $CDCl_3$): δ 173.32, 153.70, 148.53, 145.65, 142.98, 137.45, 132.31, 132.21, 130.37, 130.14, 129.96, 129.16, 125.91, 125.77, 124.07, 122.53, 121.72, 119.16, 109.42, 105.68, 70.57, 40.82, 33.89, 27.87, 27.79, 22.32, 21.25, 20.88, 19.18. IR (KBr): 3031, 2925, 1715, 1593, 1492, 1400, 1268, 1108, 811, 747, 652 cm^{-1}. MS (EI, m/z): 561 $[M]^+$. HRMS (ESI): Calcd. for $C_{36}H_{39}N_3NaO_3$ $[M+H]^+$: 584.2884; found: 584.2892.

(3)isobutyl-5-(3-(4-(tert-butyl)phenyl)-6-((4-(tert-butyl)phenyl)(phenyl)amino)-2-oxo-2,3-dihydro-1*H*-benzo[*d*]imidazol-1-yl)pentanoate (4caa)

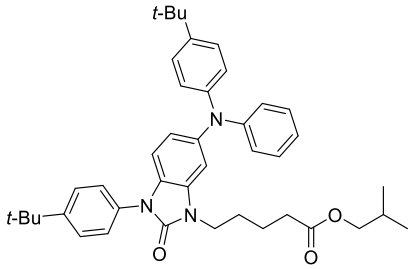

Brownish oil liquid, (100 mg, 62% yield); ^{1}H NMR (400 MHz, $CDCl_3$) δ 7.48 (dd, *J* = 25.4, 8.6 Hz, 2H), 7.26 – 7.18 (m, 4H), 7.06 (d, *J* = 8.0 Hz, 2H), 7.03 – 6.97 (m, 3H), 6.94 (t, *J* = 7.2 Hz, 1H), 6.85 (d, *J* = 1.6 Hz, 1H), 6.80 (dd, *J* = 8.4, 2.0 Hz, 1H), 3.92 – 3.75(m, 4H), 2.35 (t, *J* = 7.0 Hz, 2H), 1.94 – 1.84 (m, 1H), 1.81 – 1.65 (m, 4H), 1.36 (s, 9H), 1.31 (s, 9H), 0.90 (d, *J* = 6.8 Hz, 6H). ^{13}C NMR (100 MHz, $CDCl_3$) δ 173.32, 153.72, 150.50, 148.44, 145.42, 145.37, 142.82, 132.13, 130.38, 129.16, 126.48, 126.09, 125.98, 125.98, 125.35, 123.09, 122.67, 121.78, 119.49, 109.57, 106.01, 70.58, 40.82, 34.80, 34.35, 33.90, 31.55, 31.46, 27.88, 27.79, 22.31, 19.20. IR (KBr): 2961, 2871, 1717, 1597, 1515, 1492, 1399, 1365, 1271, 1115, 834, 788, 752, 698 cm^{-1}. MS (EI, m/z): 645 $[M]^+$. HRMS (ESI): Calcd. for $C_{42}H_{52}N_3O_3$ $[M+H]^+$: 646.4003; found: 646.4010.

(4)isobutyl-5-(3-([1,1'-biphenyl]-4-yl)-6-([1,1'-biphenyl]-4-yl(phenyl)amino)-2-oxo-2,3-dihydro-1*H*-benzo[*d*]imidazol-1-yl)pentanoate (4daa)

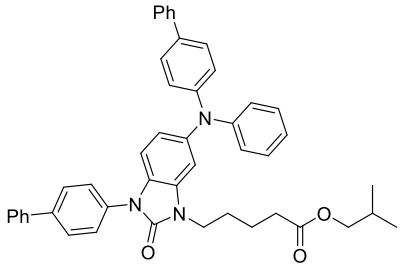

Brownish oil liquid, (113 mg, 66% yield); ^{1}H NMR (400 MHz, $CDCl_3$): δ 7.77 (d, *J* = 8.4 Hz, 2H), 7.69 – 7.64 (m, 4H), 7.61 (d, *J* = 7.2 Hz, 2H), 7.55 – 7.49 (m, 4H), 7.47 (d, *J* = 3.2 Hz, 1H), 7.44 (s, 1H), 7.43 – 7.41 (m, 1H), 7.39 (d, *J* = 7.2 Hz, 1H), 7.32 (dd, *J* = 15.0, 7.4Hz, 3H), 7.19 (d, *J* = 8.4 Hz, 3H), 7.11 (d, *J* = 8.4 Hz, 1H), 7.05 (t, *J* = 7.2 Hz, 1H), 6.96 (d, *J* = 1.6 Hz, 1H), 6.91 (dd, *J* = 8.4, 2.0 Hz, 1H), 3.92 (t, *J* = 6.6 Hz, 2H), 3.86 (d, *J* = 6.8 Hz, 2H), 2.40 (t, *J* = 7.2 Hz, 2H), 1.97 – 1.89 (m, 1H), 1.88 – 1.80 (m, 2H), 1.79 – 1.71 (m, 2H), 0.93 (d, *J* = 6.7 Hz, 6H). ^{13}C NMR (100 MHz, $CDCl_3$): δ 173.27, 153.58, 147.98, 147.49, 142.71, 140.66, 140.46, 140.37, 134.78, 133.97, 130.54, 129.35, 128.95, 128.83, 128.24, 127.82, 127.65, 127.22, 126.87, 126.66, 126.00, 125.92, 123.61, 123.03, 122.63, 119.67, 109.67, 106.16, 70.56, 40.89, 33.85, 27.85, 27.76, 22.30, 19.17. IR (KBr): 3059, 3032, 2959, 2872, 2827, 1715, 1599, 1489, 1399, 1277, 1175, 763, 698 cm^{-1}. MS (EI, m/z): 685 $[M]^+$. HRMS (ESI): Calcd. for $C_{46}H_{44}N_3O_3$ $[M+H]^+$: 686.3377; found: 686.3376.

(5)isobutyl-5-(3-(4-chlorophenyl)-6-((4-chlorophenyl)(phenyl)amino)-2-oxo-2,3-dihydro-1*H*-benzo[*d*]imidazol-1-yl)pentanoate (4eaa)

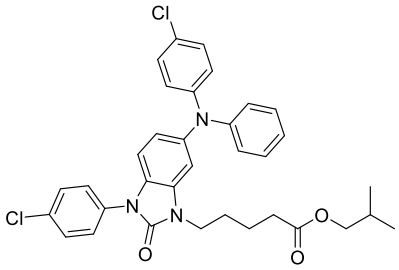

Brownish oil liquid, (96 mg, 64% yield); ^{1}H NMR (400 MHz, $CDCl_3$): δ 7.51 – 7.45 (m, 4H), 7.25 – 7.22 (m, 2H), 7.19 – 7.15 (m, 2H), 7.09 – 7.01 (m, 3H), 7.01 – 6.95 (m, 4H), 6.82 (d, *J* = 2.0 Hz, 1H), 6.79 (dd, *J* = 8.4, 2.0 Hz, 1H), 3.87 – 3.79 (m, 4H), 2.34 (t, *J* = 7.2 Hz, 2H), 1.93 – 1.83 (m, 1H), 1.79 – 1.72 (m, 2H), 1.72 – 1.64 (m, 2H), 0.89 (d, *J* = 6.4 Hz, 6H). ^{13}C NMR (100 MHz, $CDCl_3$): δ 173.27, 153.37, 147.75, 146.81, 142.75, 133.36, 133.37, 130.59, 129.78, 129.45, 129.32, 127.08, 127.02, 125.67, 124.12, 123.57, 122.94, 119.50, 109.51, 106.05, 70.62, 40.96, 33.83, 27.81, 27.79, 22.30, 19.19. IR (KBr): 2961, 2873, 1718, 1589, 1490, 1399, 1173, 1091, 824, 755, 697 cm^{-1}. MS (EI, m/z): 601 $[M]^+$. HRMS (ESI): Calcd. for $C_{34}H_{34}Cl_2N_3O_3$ $[M+H]^+$: 602.1972; found: 602.1971.

(6)isobutyl-5-(3-(4-bromophenyl)-6-((4-bromophenyl)(phenyl)amino)-2-oxo-2,3-dihydro-1*H*-benzo[*d*]imidazol-1-yl)pentanoate (4faa)

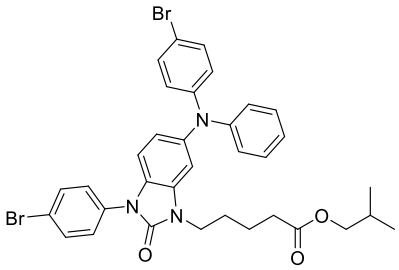

Brownish oil liquid, (105 mg, 61% yield); ^{1}H NMR (400 MHz, $CDCl_3$): δ 7.64 (d, *J* = 8.4 Hz, 2H), 7.44 (d, *J* = 8.4 Hz, 2H), 7.31 (d, *J* = 8.8 Hz, 2H), 7.24 (d, *J* = 8.8 Hz, 2H), 7.06 (d, *J* = 8.0 Hz, 2H), 7.03 (d, *J* = 7.2 Hz, 1H), 7.00 – 6.91 (m, 4H), 6.82 (s, 1H), 6.80 (d, *J* = 8.4 Hz, 1H), 3.89 – 3.79 (m, 4H), 2.35 (t, *J* = 7.0 Hz, 2H), 1.95 – 1.84 (m, 1H), 1.79 – 1.65 (m, 4H), 0.90 (d, *J* = 6.4 Hz, 6H). ^{13}C NMR (100 MHz, $CDCl_3$): δ 173.18, 153.22, 147.55, 147.23, 142.58, 133.80, 132.67, 132.15, 130.53, 129.39, 127.22, 125.55, 124.25, 123.65, 122.99, 120.99, 119.48, 114.38, 109.45, 106.02, 70.54, 40.89, 33.7, 27.72, 27.71, 22.21, 19.11. IR (KBr): 2959, 2872, 2829, 1718, 1596, 1489,1399, 1173, 1072, 1009, 820, 754, 697 cm^{-1}. MS (EI, m/z): 689 $[M]^+$. HRMS (ESI): Calcd. for $C_{34}H_{34}Br_2N_3O_3$ $[M+H]^+$: 690.0961; found: 690.0962.

(7)isobutyl-5-(3-(4-fluorophenyl)-6-((4-fluorophenyl)(phenyl)amino)-2-oxo-2,3-dihydro-1*H*-benzo[*d*]imidazol-1-yl)pentanoate (4gaa)

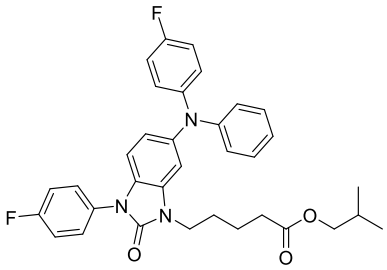

Brownish oil liquid, (95 mg, 67% yield); ^{1}H NMR (400 MHz, $CDCl_3$): δ 7.54 – 7.49 (m, 2H), 7.26 – 7.16 (m, 4H), 7.09 – 7.05 (m, 2H), 7.03 (d, *J* = 7.6 Hz, 2H), 6.99 – 6.91 (m, 4H), 6.83 (d, *J* = 1.6 Hz, 1H), 6.78 (dd, *J* = 8.4, 2.0 Hz, 1H), 3.92 – 3.18 (m, 4H), 2.36 (t, *J* = 7.2 Hz, 2H), 1.95 – 1.85 (m, 1H), 1.82 – 1.74 (m, 2H), 1.74 – 1.63 (m, 2H), 0.91 (d, *J* = 7.2 Hz, 6H). ^{13}C NMR (100 MHz, $CDCl_3$): δ 173.26, 161.61 (d, *J* = 248.5 Hz), 158.73 (d, *J* = 243.7 Hz), 153.57, 148.30, 144.20 (d, *J* = 2.7 Hz), 143.10, 130.73 (d, *J* = 3.1 Hz), 130.44, 129.30, 127.73 (d, *J* = 8.6 Hz), 125.73, 125.66 (d, *J* = 8.1 Hz), 122.48, 122.10, 119.01, 116.52 (d, *J* = 23.0 Hz), 116.12 (d, *J* = 22.5 Hz), 109.30, 105.59, 70.58, 40.89, 33.82, 27.82, 27.77, 22.29, 19.16. ^{19}F NMR (376 MHz, $CDCl_3$) δ -113.62, -119.98. IR (KBr): 3065, 2901, 2874, 1716, 1627, 1596, 1494, 1401, 1222, 833, 750, 696 cm^{-1}. MS (EI, m/z): 569 $[M]^+$. HRMS (ESI): Calcd. for $C_{34}H_{34}F_2N_3O_3$ $[M+H]^+$:570.2563; found: 570.2568.

(8)isobutyl-5-(3-(4-methoxyphenyl)-6-((4-methoxyphenyl)(phenyl)amino)-2-oxo-2,3-dihydro-1*H*-benzo[*d*]imidazol-1-yl)pentanoate (4haa)

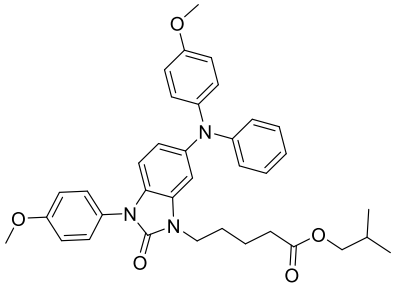

Brownish oil liquid, (93 mg, 63% yield); ^{1}H NMR (400 MHz, $CDCl_3$) δ 7.45 – 7.40 (m, 2H), 7.19 (t, *J* = 8.0 Hz, 2H), 7.10 – 7.06 (m, 2H), 7.03 (s, 1H), 7.02 – 6.97 (m, 3H), 6.92 – 6.86 (m, 2H), 6.85 (s, 1H), 6.84 – 6.80 (m, 2H), 6.77 (dd, *J* = 8.4, 2.0 Hz, 1H), 3.88 – 3.81 (m, 7H), 3.80 (s, 3H), 2.35 (t, *J* = 7.2 Hz, 2H), 1.95 – 1.84 (m, 1H), 1.80 – 1.73 (m, 2H), 1.72 – 1.65 (m, 2H), 0.90 (d, *J* = 6.4 Hz, 6H). ^{13}C NMR (100 MHz, $CDCl_3$) δ 173.37, 158.92, 155.98, 153.88, 148.83, 143.13, 141.22, 130.29, 129.14, 127.53, 127.44, 126.61, 126.01, 121.47, 121.12, 118.68, 114.86, 114.84, 109.25, 105.23, 70.61, 55.67, 55.61, 40.84, 33.92, 27.91, 27.81, 22.35, 19.21. IR (KBr): 2958, 2835, 1712, 1596, 1513, 1492, 1245, 1175, 1033, 830, 790, 748, 696 cm^{-1}. MS (EI, m/z): 593 $[M]^+$. HRMS (ESI): Calcd. for $C_{36}H_{40}N_3O_5$ $[M+H]^+$: 594.2962; found: 594.2964.

(9)isobutyl-3-(6-(diphenylamino)-2-oxo-3-phenyl-2,3-dihydro-1*H*-benzo[*d*]imidazol-1-yl)propanoate (4aba)

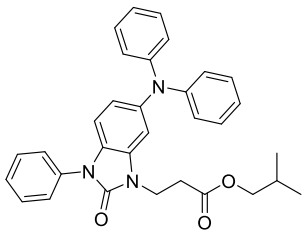

Brownish oil liquid, (57 mg, 45% yield); ^{1}H NMR (400 MHz, $CDCl_3$): δ 7.55 – 7.49 (m, 4H), 7.40 –7.36 (m, 1H), 7.26 – 7.21 (m, 4H), 7.07 (d, *J* = 7.6 Hz, 4H), 7.00 – 6.96 (m, 3H), 6.93 (d, *J* = 1.6 Hz, 1H), 6.82 (dd, *J* = 8.4, 2.0 Hz, 1H), 4.14 (t, *J* = 7.2 Hz, 2H), 3.80 (d, *J* = 6.4 Hz, 2H), 2.79 (t, *J* = 7.2 Hz, 2H), 1.94 – 1.79 (m, 1H), 0.87 (d, *J* = 6.8 Hz, 6H). ^{13}C NMR (100 MHz, $CDCl_3$): δ 171.18, 153.39, 148.23, 142.99, 134.73, 130.21, 129.63, 129.31, 127.69, 126.00,

125.91, 123.28, 122.36, 119.89, 109.64, 106.42, 71.06, 37.41, 33.08, 27.70, 19.15. IR (KBr): 2959, 2927, 2873, 2850, 1714, 1638, 1619, 1597, 1490, 1399, 1105, 754, 695, 616 cm^{-1}. MS (EI, m/z): 505 $[M]^+$. HRMS (ESI): Calcd. for $C_{32}H_{32}N_3O_3$ $[M+H]^+$: 506.2438; found: 506.2443.

(10)isobutyl-4-(6-(diphenylamino)-2-oxo-3-phenyl-2,3-dihydro-1*H*-benzo[*d*]imidazol-1-yl) butanoate (4aca)

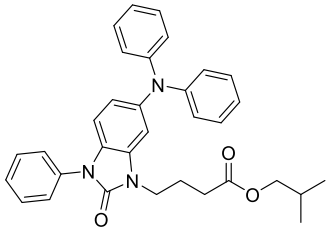

Brownish oil liquid, (87 mg, 66% yield); ^{1}H NMR (400 MHz, $CDCl_3$): δ 7.60 – 7.48 (m, 4H), 7.41 – 7.35 (m, 1H), 7.27 – 7.21 (m, 4H), 7.08 (d, *J* = 7.6 Hz, 4H), 7.02 – 6.95 (m, 3H), 6.90 (d, *J* = 1.6 Hz, 1H), 6.82 (dd, *J* = 8.4, 2.0 Hz, 1H), 3.91 (t, *J* = 6.8 Hz, 2H), 3.81 (d, *J* = 6.4 Hz, 2H), 2.42 (t, *J* = 7.4 Hz, 2H), 2.10 – 2.02 (m, 2H), 1.93 – 1.83 (m, 1H), 0.90 (d, *J* = 6.4 Hz, 6H). ^{13}C NMR (100 MHz, $CDCl_3$): δ 172.74, 153.51, 148.12, 142.90, 134.74, 130.36, 129.49, 129.19, 127.49, 125.78, 125.76, 123.22, 122.26, 119.54, 109.49, 105.95, 70.70, 40.48, 31.46, 27.67, 23.73, 19.11. IR (KBr): 3062, 2960, 2873, 1716, 1595, 1491, 1399, 1273, 1218, 1175, 754, 695, 656 cm^{-1}. MS (EI, m/z): 519 $[M]^+$. HRMS (ESI): Calcd. for $C_{33}H_{34}N_3O_3$ $[M+H]^+$: 520.2595; found: 520.2598.

(11)isobutyl-6-(6-(diphenylamino)-2-oxo-3-phenyl-2,3-dihydro-1*H*-benzo[*d*]imidazol-1-yl) hexanoate (4ada)

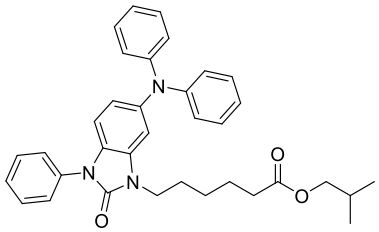

Brownish oil liquid, (85 mg, 62% yield);^{1}H NMR (400 MHz, $CDCl_3$): δ 7.57 – 7.49 (m, 4H), 7.40 – 7.35 (m, 1H), 7.23 (d, *J* = 7.6 Hz, 3H), 7.08 (d, *J* = 8.0 Hz, 4H), 6.98 (t, *J* = 7.6 Hz, 3H), 6.85 (d, *J* = 2.0 Hz, 1H), 6.81 (dd, *J* = 8.4, 2.0 Hz, 1H), 3.89 – 3.79 (m, 4H), 2.29 (t, *J* = 7.6 Hz, 2H), 1.95 – 1.85 (m, 1H), 1.79 – 1.69 (m, 2H), 1.67 – 1.61 (m, 2H), 1.48 – 1.32 (m, 2H), 0.91 (d, *J* = 6.8 Hz, 6H). ^{13}C NMR (100 MHz, $CDCl_3$): δ 173.66, 153.57, 148.22, 142.86, 134.89, 130.52, 129.55, 129.27, 127.52, 125.87, 125.84, 123.26, 122.32, 119.48, 109.51, 106.10, 70.54, 41.15, 34.21, 28.14, 27.80, 26.48, 24.75, 19.20. IR (KBr): 3063, 2963, 2874, 1718, 1628, 1597, 1491, 1401, 1275, 1216, 1174, 754, 695, 657 cm^{-1}. MS (EI, m/z): 547 $[M]^+$. HRMS (ESI): Calcd. for $C_{35}H_{38}N_3O_3$ $[M+H]^+$: 548.2908; found: 548.2909.

(12) isobutyl 2-chloro-4-(6-(diphenylamino)-2-oxo-3-phenyl-2,3-dihydro-1*H*-benzo[*d*]imidazol-1-yl)-2-methylbutanoate (4aea)

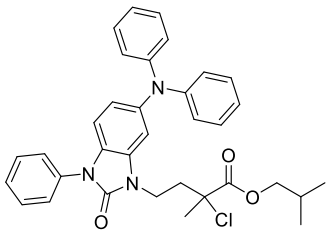

Brownish oil liquid, (80 mg, 56% yield);^{1}H NMR (400 MHz, $CDCl_3$): δ 7.55 – 7.48 (m, 4H), 7.39 – 7.34 (m, 1H), 7.23 (t, *J* = 7.8 Hz, 4H), 7.09 (d, *J* = 7.6 Hz, 4H), 7.00 – 6.95 (m, 3H), 6.92 (d, *J* = 2.0 Hz, 1H), 6.83 (dd, *J* = 8.4, 2.0 Hz, 1H), 4.11 – 3.96 (m, 2H), 3.91 – 3.81 (m, 2H), 2.55 – 2.46 (m, 1H), 2.42 – 2.34 (m, 1H), 1.98 –1.87 (m, 1H), 1.81 (s, 3H), 0.91 (d, *J* = 6.4 Hz, 6H). ^{13}C NMR (100 MHz, $CDCl_3$): δ 170.51, 153.25, 148.13, 143.10, 134.77, 130.02, 129.55, 129.27, 127.56, 125.76, 125.68, 123.46, 122.45, 119.26, 109.53, 105.81, 72.29, 66.86, 39.35, 37.59, 28.09, 27.75, 19.05. IR (KBr): 3063, 2963, 2874, 1718, 1628,1597, 1491, 1401, 1275, 1217, 1174, 754, 695, 619 cm^{-1}. MS (EI, m/z): 567 $[M]^+$. HRMS (ESI): Calcd. for $C_{34}H_{34}ClN_3O_3$ $[M+H]^+$: 568.2361; found: 568.2364.

(13)butyl-5-(6-(diphenylamino)-2-oxo-3-phenyl-2,3-dihydro-1*H*-benzo[*d*]imidazol-1-yl)pentanoate (4aab)

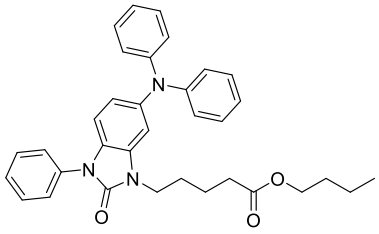

Brownish oil liquid, (96 mg, 72% yield);^{1}H NMR (400 MHz, $CDCl_3$): δ 7.57 –7.48 (m, 4H), 7.37 (t, *J* = 7.2 Hz, 1H), 7.24 (t, *J* = 7.8 Hz, 4H), 7.09 (d, *J* = 8.0 Hz, 4H), 6.98 (t, *J* = 7.6 Hz, 3H), 6.86 (d, *J* = 1.6 Hz, 1H), 6.81 (dd, *J* = 8.4, 2.0 Hz, 1H), 4.04 (t, *J* = 6.6 Hz, 2H), 3.86 (t, *J* = 6.6 Hz, 2H), 2.34 (t, *J* = 7.2 Hz, 2H), 1.79 – 1.66 (m, 4H), 1.62 – 1.55 (m, 2H), 1.40 – 1.31 (m, 2H), 0.92 (t, *J* = 7.4 Hz, 3H). ^{13}C NMR (100 MHz, $CDCl_3$): δ 173.35, 153.59, 148.22, 142.90, 134.88, 130.49, 129.55, 129.2, 127.54, 125.90, 125.86, 123.29, 122.33, 119.52, 109.54, 106.05, 64.36, 40.87, 33.90, 30.76, 27.84, 22.30, 19.23, 13.81. IR (KBr): 3062, 2958, 2932, 2870, 1716, 1626, 1595, 1491, 1399, 1274, 1174, 754, 722, 695 cm^{-1}. MS (EI, m/z): 533 $[M]^+$. HRMS (ESI): Calcd. for $C_{34}H_{36}N_3O_3$ $[M+H]^+$: 534.2751; found: 534.2754.

(46)octyl-5-(6-(diphenylamino)-2-oxo-3-phenyl-2,3-dihydro-1*H*-benzo[*d*]imidazol-1-yl)pentanoate (4aac)

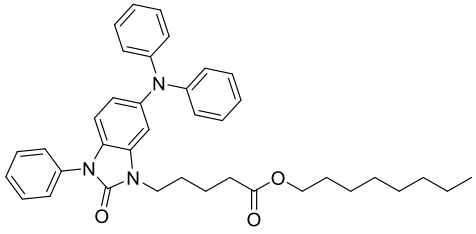

Brownish oil liquid, (105 mg, 71% yield); ^{1}H NMR (400 MHz, $CDCl_3$): δ 7.58 – 7.47 (m, 4H), 7.36 (t, *J* = 7.2 Hz, 1H), 7.23 (t, *J* = 7.8 Hz, 4H), 7.08 (d, *J* = 8.0 Hz, 4H), 7.00 – 6.95 (m, 3H),

6.86 (d, *J* = 1.2 Hz, 1H), 6.80 (dd, *J* = 8.4, 2.0 Hz, 1H), 4.03 (t, *J* = 6.8 Hz, 2H), 3.85 (t, *J* = 6.8 Hz, 2H), 2.33 (t, *J* = 7.0 Hz, 2H), 1.81 – 1.73 (m, 2H), 1.72 – 1.64 (m, 2H), 1.61 – 1.55 (m, 2H), 1.26 (s, 10H), 0.87 (t, *J* = 6.4 Hz, 3H). ^{13}C NMR (100 MHz, $CDCl_3$): δ 173.26, 153.50, 148.14, 142.82, 134.81, 130.41, 129.47, 129.20, 127.46, 125.81, 125.78, 123.21, 122.26, 119.44, 109.47, 105.98, 64.59, 40.79, 33.81, 31.81, 29.23, 29.19, 28.65, 27.76, 25.94, 22.66, 22.21, 14.13. IR (KBr): 3063, 2928, 2856, 1718, 1595, 1491, 1399, 1275, 1173, 753, 695 cm^{-1}. MS (EI, m/z): 589 $[M]^+$. HRMS (ESI): Calcd. for $C_{38}H_{44}N_3O_3$ $[M+H]^+$: 590.3377; found: 590.3375.

(15)neopentyl-5-(6-(diphenylamino)-2-oxo-3-phenyl-2,3-dihydro-1*H*-benzo[*d*]imidazol-1-yl)pentanoate (4aad)

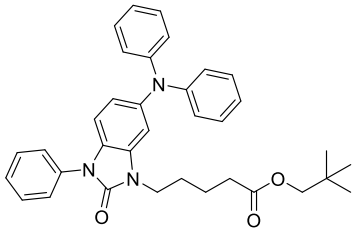

Brownish oil liquid, (98 mg, 72% yield); ^{1}H NMR (400 MHz, $CDCl_3$): δ 7.57 – 7.49 (m, 4H), 7.37 (t, *J* = 7.0 Hz, 1H), 7.26 – 7.21 (m, 4H), 7.09 (d, *J* = 8.0 Hz, 4H), 6.98 (t, *J* = 7.6 Hz, 3H), 6.86 (s, 1H), 6.82 (d, *J* = 8.4 Hz, 1H), 3.87 (t, *J* = 6.6 Hz, 2H), 3.76 (s, 2H), 2.38 (t, *J* = 7.0 Hz, 2H), 1.83 – 1.67 (m, 4H), 0.92 (s, 9H). ^{13}C NMR (100 MHz, $CDCl_3$): δ 173.30, 153.56, 148.19, 142.88, 134.86, 130.46, 129.53, 129.26, 127.51, 125.87, 125.83, 123.32, 122.27, 119.50, 109.52, 106.03, 73.77, 40.83, 33.89, 31.35, 27.87, 26.53, 22.32. IR (KBr): 3062, 2958, 2870, 1717, 1595, 1491, 1400, 1370, 1275, 1173, 754, 696, 658 cm^{-1}. MS (EI, m/z): 547 $[M]^+$. HRMS (ESI): Calcd. for $C_{35}H_{38}N_3O_3$ $[M+H]^+$: 548.2908; found: 548.2911.

(16)benzyl-5-(6-(diphenylamino)-2-oxo-3-phenyl-2,3-dihydro-1*H*-benzo[*d*]imidazol-1-yl)pentanoate (4aae)

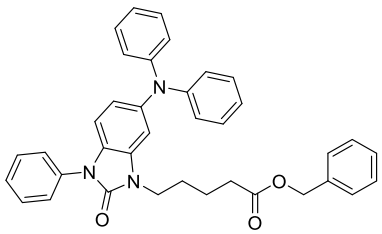

Brownish oil liquid, (88 mg, 62% yield); ^{1}H NMR (400 MHz, $CDCl_3$): δ 7.57 – 7.52 (m, 3H), 7.51 (d, *J* = 8.4 Hz, 1H), 7.41 – 7.29 (m, 7H), 7.23 (d, *J* = 7.6 Hz, 3H), 7.09 (d, *J* = 7.6 Hz, 4H), 6.98 (t, *J* = 8.0 Hz, 3H), 6.86 (d, *J* = 2.0 Hz, 1H), 6.82 (dd, *J* = 8.4, 2.0 Hz, 1H), 5.09 (s, 2H), 3.86 (t, *J* = 6.6 Hz, 2H), 2.40 (t, *J* = 7.0 Hz, 2H), 1.82 – 1.74 (m, 2H), 1.74 – 1.67 (m, 2H). ^{13}C NMR (100 MHz, $CDCl_3$): δ 173.08, 148.22, 142.91, 136.08, 134.86, 130.47, 129.57, 129.30, 128.67, 128.31, 128.29, 127.57, 125.88, 123.30, 122.35, 119.54, 109.57, 106.05, 100.09, 66.32, 40.84, 33.85, 27.81, 22.24. IR (KBr): 3034, 2990, 2936, 2828, 1713, 1630, 1595, 1491, 1399, 753, 695 cm^{-1}. MS (EI, m/z): 567 $[M]^+$. HRMS (ESI): Calcd. for $C_{37}H_{34}N_3O_3$ $[M+H]^+$: 568.2595; found: 568.2592.

(17)thiophen-2-ylmethyl-5-(6-(diphenylamino)-2-oxo-3-phenyl-2,3-dihydro-1*H*-benzo[*d*]i

midazol-1-yl)pentanoate (4aaf)

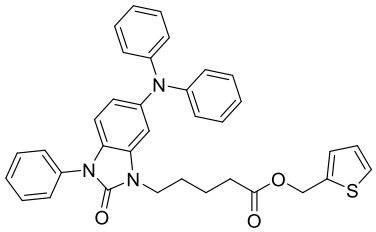

Brownish oil liquid, (102 mg, 71% yield); ^{1}H NMR (400 MHz, $CDCl_3$): δ 7.56 – 7.49 (m, 4H), 7.40 – 7.35 (m, 1H), 7.27 (dd, *J* = 5.2, 0.8 Hz, 1H), 7.25 – 7.21 (m, 4H), 7.09 (d, *J* = 8.0 Hz, 4H), 7.06 (d, *J* = 3.2 Hz, 1H), 7.00 (s, 1H), 6.99 – 6.94 (m, 3H), 6.85 (d, *J* = 2.0 Hz, 1H), 6.82 (dd, *J* = 8.4, 2.0 Hz, 1H), 5.23 (s, 2H), 3.85 (t, *J* = 6.8 Hz, 2H), 2.37 (t, *J* = 7.0 Hz, 2H), 1.79 – 1.73 (m, 2H), 1.73 – 1.64 (m, 2H). ^{13}C NMR (100 MHz, $CDCl_3$): δ 172.86, 153.57, 148.21, 142.89, 138.10, 134.86, 130.46, 129.55, 129.28, 128.17, 127.54, 126.88, 125.88, 125.86, 123.29, 122.34, 119.52, 109.54, 106.05, 60.51, 40.81, 33.74, 27.74, 22.17. IR (KBr): 3063, 2948, 2831, 1713, 1594, 1491, 1370, 754, 696 cm^{-1}. MS (EI, m/z): 573 $[M]^+$. HRMS (ESI): Calcd. for $C_{35}H_{32}N_3O_3S$ $[M+H]^+$: 574.2159; found: 574.2158.

(18)2-methoxyethyl-5-(6-(diphenylamino)-2-oxo-3-phenyl-2,3-dihydro-1*H*-benzo[*d*]imidazol-1-yl)pentanoate (4aag)

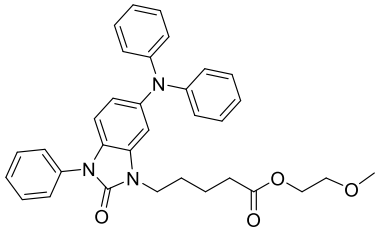

Brownish oil liquid, (84 mg, 63% yield); ^{1}H NMR (400 MHz, $CDCl_3$): δ 7.56 – 7.48 (m, 4H), 7.36 (t, *J* = 7.0 Hz, 1H), 7.23 (t, *J* = 7.8 Hz, 4H), 7.08 (d, *J* = 8.0 Hz, 4H), 6.97 (t, *J* = 7.6 Hz, 3H), 6.85 (d, *J* = 1.6 Hz, 1H), 6.81 (dd, *J* = 8.4, 2.0 Hz, 1H), 4.19 (t, *J* = 4.8 Hz, 2H), 3.85 (t, *J* = 6.8 Hz, 2H), 3.55 (t, J = 4.8 Hz, 2H), 3.35 (s, 3H), 2.38 (t, *J* = 7.2 Hz, 2H), 1.80 – 1.65 (m, 4H). ^{13}C NMR (100 MHz, $CDCl_3$): δ 173.18, 153.54, 148.17, 142.86, 134.82, 130.43, 129.51, 129.24, 127.51, 125.84, 125.83, 123.24, 122.29, 119.49, 109.51, 106.02, 70.50, 63.44, 59.02, 40.83, 33.68, 27.75, 22.18. IR (KBr): 3061, 2944, 1714, 1595, 1491, 1400, 1275, 1174, 754, 696, 658 cm^{-1}. MS (EI, m/z): 535 $[M]^+$. HRMS (ESI): Calcd. for $C_{33}H_{34}N_3O_4$ $[M+H]^+$: 536.2544; found: 536.2550.

(19)5-(diphenylamino)-3-ethyl-1-phenyl-1,3-dihydro-2*H*-benzo[*d*]imidazol-2-one (5af)

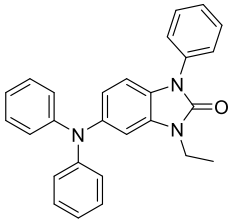

Brownish solid, (78 mg, 78% yield), m.p: 162-163 °C; ^{1}H NMR (400 MHz, $CDCl_3$) δ 7.58 – 7.48 (m, 4H), 7.37 (t, *J* = 7.2 Hz, 1H), 7.20 – 7.26 (m, 4H), 7.08 (d, *J* = 7.6 Hz, 4H), 6.97 (t, *J* = 7.6

Hz, 3H), 6.87 (s, 1H), 6.81 (d, *J* = 8.4 Hz, 1H), 3.90 (q, *J* = 7.2 Hz, 2H), 1.30 (t, *J* = 7.2 Hz, 3H). ^{13}C NMR (100 MHz, $CDCl_3$) δ 153.34, 148.28, 142.88, 134.94, 130.24, 129.57, 129.29, 127.55, 126.01, 125.91, 123.29, 122.32, 119.51, 109.53, 106.03, 36.14, 13.64. IR (KBr): 3058, 3033, 2974, 2929, 2855, 1712, 1592, 1491, 1400, 1276, 1234, 1192, 1082, 1022, 754, 695, 656 cm^{-1}. MS (EI, m/z): 405 $[M]^+$. HRMS (ESI): Calcd. for $C_{27}H_{23}N_3NaO$ $[M+Na]^+$: 428.1733; found: 428.1727.

(20)5-(diphenylamino)-1-phenyl-3-propyl-1,3-dihydro-2*H*-benzo[*d*]imidazol-2-one (3ag)

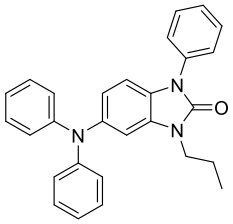

Brownish oil liquid, (90 mg, 86% yield); ^{1}H NMR (400 MHz, $CDCl_3$): δ 7.42 – 7.60 (m, 4H), 7.38 – 7.31 (m, 1H), 7.19 – 7.24 (m, 4H), 7.11 – 7.04 (m, 4H), 7.01 – 6.92 (m, 3H), 6.87 (d, *J* = 2.0 Hz, 1H), 6.80 (dd, *J* = 8.4, 2.0 Hz, 1H), 3.79 (t, *J* = 7.2 Hz, 2H), 1.79 – 1.70 (m, 2H), 0.94 (t, *J* = 7.4 Hz, 3H). ^{13}C NMR (100 MHz, $CDCl_3$): δ 153.59, 148.20, 142.74, 134.91, 130.68, 129.48, 129.22, 127.44, 125.88, 125.81, 123.18, 122.24, 119.46, 109.42, 106.20, 42.86, 21.71, 11.43. IR (KBr): 3030, 2965, 2923, 2875, 1714, 1608, 1593, 1518, 1492, 1400, 1271, 1224, 1075, 753, 695, 658 cm^{-1}. MS (EI, m/z): 419 $[M]^+$. HRMS (ESI): Calcd. for $C_{28}H_{25}N_3NaO$ $[M+Na]^+$: 442.1890; found: 442.1887.

(21)3-butyl-5-(diphenylamino)-1-phenyl-1,3-dihydro-2*H*-benzo[*d*]imidazol-2-one (5ah)

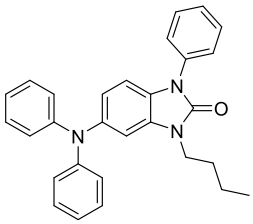

Brownish oil liquid, (80 mg, 74% yield); ^{1}H NMR (400 MHz, $CDCl_3$): δ 7.57 – 7.47 (m, 4H), 7.36 (t, *J* = 7.2 Hz, 1H), 7.23 (t, *J* = 7.4 Hz, 4H), 7.08 (d, *J* = 8.0 Hz, 4H), 6.97 (t, *J* = 7.8 Hz, 3H), 6.86 (s, 1H), 6.80 (d, *J* = 8.8 Hz, 1H), 3.83 (t, *J* = 7.0 Hz, 2H), 1.73 – 1.65 (m, 2H), 1.41 – 1.32 (m, 2H), 0.91 (t, *J* = 7.4 Hz, 3H). ^{13}C NMR (100 MHz, $CDCl_3$): δ 153.61, 148.23, 142.80, 134.94, 130.65, 129.53, 129.25, 127.48, 125.85, 123.25, 122.29, 119.39, 109.45, 106.19, 41.08, 30.50, 20.15, 13.83. IR (KBr): 3060, 3036, 2956, 2930, 2866, 1715, 1593, 1490, 1399, 1373, 1274, 1217, 1181, 1026, 754, 695, 658 cm^{-1}. MS (EI, m/z): 433 $[M]^+$. HRMS (ESI): Calcd. for $C_{29}H_{27}N_3NaO$ $[M+Na]^+$: 456.2046; found: 4562043.

(22)5-(diphenylamino)-3-isobutyl-1-phenyl-1,3-dihydro-2*H*-benzo[*d*]imidazol-2-one (5ai)

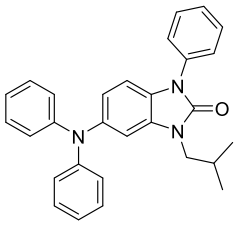

Brownish oil liquid, (67 mg, 62% yield); ^{1}H NMR (400 MHz, $CDCl_3$): δ 7.57 – 7.48 (m, 4H), 7.39 – 7.34 (m, 1H), 7.20 – 7.25 (m, 4H), 7.05 – 7.10 (m, 4H), 7.00 – 6.95 (m, 3H), 6.85 (d, *J* = 2.0 Hz, 1H), 6.80 (dd, *J* = 8.4, 2.0 Hz, 1H), 3.64 (d, *J* = 7.2 Hz, 2H), 2.10 – 2.21 (m, 1H), 0.94 (d, *J* = 6.4 Hz, 6H). ^{13}C NMR (100 MHz, $CDCl_3$): δ 153.92, 148.25, 142.76, 134.99, 131.10, 129.55, 129.27, 127.51, 125.89, 123.24, 122.30, 119.49, 109.44, 106.56, 48.78, 28.09, 20.33. IR (KBr): 3057, 2959, 2924, 2852, 1715, 1631, 1595, 1490, 1398, 1274, 1224, 1188, 1088, 1026, 753, 695, 656 cm^{-1}. MS (EI, m/z): 433 $[M]^+$. HRMS (ESI): Calcd. for $C_{29}H_{27}N_3NaO$ $[M+Na]^+$: 456.2046; found: 456.2045.

(23)5-(diphenylamino)-3-hexyl-1-phenyl-1,3-dihydro-2*H*-benzo[*d*]imidazol-2-one (5aj)

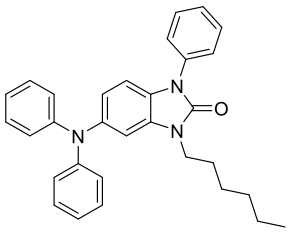

Brownish oil liquid, (86 mg, 75% yield); ^{1}H NMR (400 MHz, $CDCl_3$): δ 7.46 – 7.60 (m, 4H), 7.32 – 7.39 (m, 1H), 7.23 (t, *J* = 7.6 Hz, 4H), 7.08 (d, *J* = 7.6 Hz, 4H), 7.01 – 6.94 (m, 3H), 6.86 (d, *J* = 2.0 Hz, 1H), 6.80 (dd, *J* = 8.4, 2.0 Hz, 1H), 3.82 (t, *J* = 7.2 Hz, 2H), 1.741.66 (m, 2H), 1.36 – 1.24 (m, 6H), 0.85 (t, *J* = 7.0 Hz, 3H). ^{13}C NMR (100 MHz, $CDCl_3$): δ 153.58, 148.24, 142.80, 134.96, 130.67, 129.52, 129.26, 127.47, 125.90, 125.85, 123.25, 122.29, 119.39, 109.45, 106.20, 41.37, 31.51, 28.31, 26.54, 22.55, 14.12. IR (KBr): 3066, 3033, 2953, 2928, 2857, 1715, 1626, 1594, 1490, 1398, 1370, 1274, 1176, 1092, 753, 695, 657 cm^{-1}. MS (EI, m/z): 461 $[M]^+$. HRMS (ESI): Calcd. for $C_{31}H_{31}N_3NaO$ $[M+Na]^+$: 484.2359; found: 484.2363.

(24)5-(diphenylamino)-3-isopropyl-1-phenyl-1,3-dihydro-2*H*-benzo[*d*]imidazol-2-one (5al)

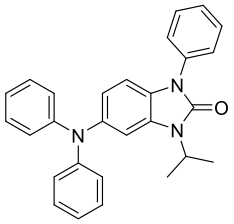

Brownish solid, (37 mg, 35% yield), m.p: 89-90 °C; ^{1}H NMR (400 MHz, $CDCl_3$): δ 7.48 – 7.55 (m, 4H), 7.37 (t, *J* = 6.6 Hz, 1H), 7.23 (d, *J* = 7.6 Hz, 3H), 7.09 (d, *J* = 7.6 Hz, 4H), 6.97 (d, *J* = 7.2 Hz, 4H), 6.79 (d, *J* = 8.0 Hz, 1H), 4.71 – 4.61 (m, 1H), 1.49 (d, *J* = 6.8 Hz, 6H). ^{13}C NMR (100 MHz, $CDCl_3$): δ 153.06, 148.28, 142.54, 134.89, 129.56, 129.43, 129.29, 127.59, 126.11,

123.29, 122.32, 119.12, 109.43, 107.38, 45.42, 20.23. IR (KBr): 3063, 3042, 2968, 2929, 2869, 1712, 1629, 1593, 1491, 1388, 1273, 1236, 1176, 752, 695, 660 cm^{-1}. MS (EI, m/z): 419 $[M]^+$. HRMS (ESI): Calcd. for $C_{28}H_{25}N_3NaO$ $[M+Na]^+$: 442.1890; found: 442.1888.

(25)3-allyl-5-(diphenylamino)-1-phenyl-1,3-dihydro-2*H*-benzo[*d*]imidazol-2-one (5am)

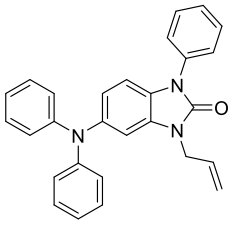

Brownish oil liquid, (65 mg, 62% yield); ^{1}H NMR (400 MHz, $CDCl_3$): δ 7.61 – 7.47 (m, 4H), 7.35 – 7.41 (m, 1H), 7.19 – 7.27 (m, 4H), 7.02 – 7.11(m, 4H), 7.02 – 6.94 (m, 3H), 6.85 – 6.80 (m, 2H), 5.81 – 5.93(m, 1H), 5.12 – 5.22(m, 2H), 4.52 – 4.41 (m, 2H). ^{13}C NMR (100 MHz, $CDCl_3$): δ 153.42, 148.21, 142.92, 134.93, 131.73, 130.39, 129.60, 129.28, 127.62, 125.92, 123.39, 122.39, 119.46, 118.07, 109.51, 106.61, 43.66. IR (KBr): 3066, 3024, 2959, 2929, 2852, 1716, 1635, 1599, 1489, 1395, 1273, 1220, 1177, 752, 696, 655 cm^{-1}. MS (EI, m/z): 417 $[M]^+$. HRMS (ESI): Calcd. for $C_{28}H_{23}N_3NaO$ $[M+Na]^+$: 440.1733; found: 440.1729.

(26)3-ethyl-5-(phenyl(p-tolyl)amino)-1-(p-tolyl)-1,3-dihydro-2*H*-benzo[*d*]imidazol-2-one (5bf)

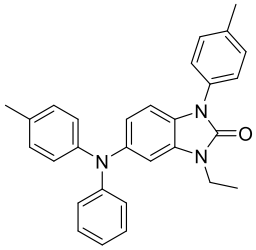

Brownish oil liquid, (89mg, 82% yield); ^{1}H NMR (400 MHz, $CDCl_3$): δ 7.43 – 7.39 (m, 2H), 7.30 (d, *J* = 8.4 Hz, 2H), 7.23 – 7.18 (m, 2H), 7.07 – 6.99 (m, 6H), 6.95 – 6.91 (m, 2H), 6.85 (d, *J* = 2.0 Hz, 1H), 6.78 (dd, *J* = 8.4, 2.0 Hz, 1H), 3.89 (q, *J* = 7.2 Hz, 2H), 2.40 (s, 3H), 2.31 (s, 3H), 1.30 (t, *J* = 7.2 Hz, 3H). ^{13}C NMR (100 MHz, $CDCl_3$): δ 153.45, 148.60, 145.71, 142.96, 137.46, 132.32, 132.28, 130.17, 130.15, 129.97, 129.18, 126.04, 125.83, 124.07, 122.55, 121.70, 119.14, 109.41, 105.68, 36.10, 21.28, 20.90, 13.68. IR (KBr): 3030, 2968, 2926, 2855, 1714, 1627, 1594, 1508, 1492, 1401, 1294, 1234, 811, 750, 696 cm^{-1}. MS (EI, m/z): 433 $[M]^+$. HRMS (ESI): Calcd. for $C_{29}H_{27}N_3NaO$ $[M+Na]^+$:456.2046; found: 456.2047.

(27)1-(4-(tert-butyl)phenyl)-5-((4-(tert-butyl)phenyl)(phenyl)amino)-3-ethyl-1,3-dihydro-2*H*-benzo[*d*]imidazol-2-one (5cf)

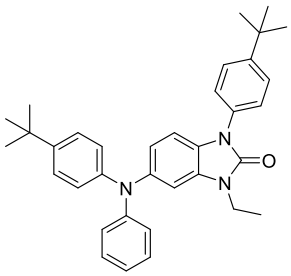

Brownish oil liquid, (65 mg, 50% yield); ^{1}H NMR (400 MHz, $CDCl_3$): δ 7.49 (dd, *J* = 24.0, 8.8 Hz, 4H), 7.25 – 7.18 (m, 4H), 7.06 (d, *J* = 7.8 Hz, 2H), 7.03 (s, 1H), 7.00 (d, *J* = 4.6 Hz, 1H), 6.97 (s, 1H), 6.94 (t, *J* = 7.2 Hz, 1H), 6.88 (d, *J* = 1.8 Hz, 1H), 6.80 (dd, *J* = 8.4, 1.8 Hz, 1H), 3.90 (q, *J* = 7.2 Hz, 2H), 1.36 (s, 9H), 1.31 (s, 9H), 1.31(s, 3H). ^{13}C NMR (100 MHz, $CDCl_3$): δ 153.46, 150.49, 148.51, 145.48, 145.35, 142.81, 132.21, 130.15, 129.17, 126.48, 126.10, 125.40, 123.08, 122.70, 121.77, 119.46, 109.55, 105.97, 36.11, 34.80, 34.36, 31.56, 31.47, 13.66. IR (KBr): 3040, 2959, 2927, 2869, 1714, 1598, 1493, 1402, 1270, 1234, 829, 731, 693 cm^{-1}. MS (EI, m/z): 517 $[M]^+$. HRMS (ESI): Calcd. for $C_{35}H_{39}N_3NaO$ $[M+Na]^+$: 540.2085; found:540.2990.

(28)1-([1,1'-biphenyl]-4-yl)-5-([1,1'-biphenyl]-4-yl(phenyl)amino)-3-ethyl-1,3-dihydro-2*H*-benzo[*d*]imidazol-2-one (5df)

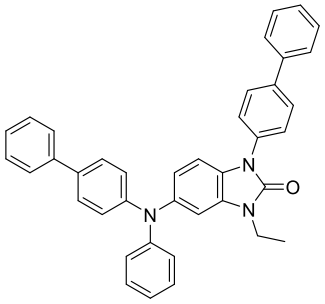

Brownish solid, (75 mg, 54% yield); m.p: 76-77 °C; ^{1}H NMR (400 MHz, $CDCl_3$): δ 7.75 – 7.70 (m, 2H), 7.65 – 7.60 (m, 4H), 7.59 – 7.56 (m, 2H), 7.49 – 7.46 (m, 3H), 7.44 – 7.41 (m, 2H), 7.40 – 7.33 (m, 2H), 7.32 – 7.25 (m, 3H), 7.17 – 7.11 (m, 4H), 7.07 (d, *J* = 8.4 Hz, 1H), 6.99 – 7.04 (m, 1H), 6.92 (d, *J* = 1.6 Hz, 1H), 6.88 (dd, *J* = 8.4, 2.0 Hz, 1H), 3.93 (q, *J* = 7.2 Hz, 2H), 1.33 (t, *J* = 7.2 Hz, 3H). ^{13}C NMR (100 MHz, $CDCl_3$): δ 153.27, 147.98, 147.50, 142.65, 140.63, 140.42, 140.36, 134.74, 133.99, 130.25, 129.29, 128.90, 128.78, 128.20, 127.76, 127.59, 127.19, 126.83, 126.62, 125.98, 123.55, 122.99, 122.55, 119.57, 109.58, 106.07, 36.11, 13.59. IR (KBr): 3060, 3033, 2957, 2928, 2870, 1713, 1590, 1519, 1485, 1398, 1276, 1189, 829, 761, 695 cm^{-1}. MS (EI, m/z): 557 $[M]^+$. HRMS (ESI): Calcd. for $C_{39}H_{31}N_3NaO$ $[M+Na]^+$: 580.2359; found: 580.2354.

(29)1-(4-chlorophenyl)-5-((4-chlorophenyl)(phenyl)amino)-3-ethyl-1,3-dihydro-2*H*-benzo[*d*]imidazol-2-one (5ef)

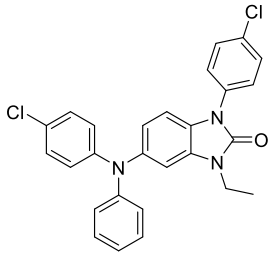

Brownish oil liquid, (65 mg, 55% yield); ^{1}H NMR (400 MHz, $CDCl_3$): δ 7.54 – 7.44 (m, 4H), 7.25 – 7.22 (m, 2H), 7.19 – 7.16 (m, 2H), 7.08 – 7.05 (m, 2H), 7.03 – 6.96 (m, 4H), 6.84 (d, *J* = 2.0 Hz, 1H), 6.80 (dd, *J* = 8.4, 2.0 Hz, 1H), 3.89 (q, *J* = 7.2 Hz, 2H), 1.30 (t, *J* = 7.2 Hz, 3H). ^{13}C NMR (100 MHz, $CDCl_3$): δ 153.10, 147.79, 146.87, 142.73, 133.43, 133.14, 130.34, 129.78, 129.45, 129.32, 127.09, 127.04, 125.77, 124.15, 123.56, 122.92, 119.44, 109.49, 105.99, 36.21, 13.60. IR (KBr): 3060, 2974, 2930, 2873, 1714, 1627, 1590, 1490, 1400, 1308, 1278, 1235, 1192, 1091, 1013, 820, 740, 696 cm^{-1}. MS (EI, m/z): 473 $[M]^+$. HRMS (ESI): Calcd. for $C_{27}H_{21}Cl_2N_3NaO$ $[M+Na]^+$: 496.0954; found: 496.0947.

(30)1-(4-bromophenyl)-5-((4-bromophenyl)(phenyl)amino)-3-ethyl-1,3-dihydro-2*H*-benzo [*d*]imidazol-2-one (5ff)

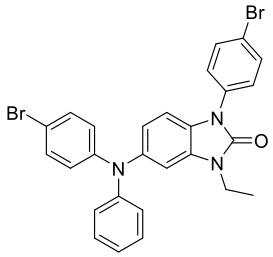

Brownish oil liquid, (105 mg, 75% yield); ^{1}H NMR (400 MHz, $CDCl_3$): δ 7.64 (d, *J* = 7.2 Hz, 2H), 7.44 (d, *J* = 7.6 Hz, 2H), 7.31 (d, *J* = 7.2 Hz, 2H), 7.24 (d, *J* = 7.6 Hz, 2H), 7.07 (d, *J* = 7.6 Hz, 2H), 7.04 – 6.96 (m, 2H), 6.93 (d, *J* = 7.6 Hz, 2H), 6.84 (s, 1H), 6.80 (d, *J* = 8.4 Hz, 1H), 3.89 (q, *J* = 6.8 Hz, 2H), 1.30 (t, *J* = 6.8 Hz, 3H). ^{13}C NMR (100 MHz, $CDCl_3$): δ 153.02, 147.67, 147.37, 142.64, 133.93, 132.76, 132.23, 130.35, 129.48, 127.33, 125.72, 124.36, 123.71, 123.05, 121.05, 119.51, 114.45, 109.52, 106.05, 36.22, 13.62. IR (KBr): 3039, 2959, 2925, 2852, 1708, 1638, 1490, 1403, 1307, 1232, 1072, 810, 748, 700 cm^{-1}. MS (EI, m/z): 561 $[M]^+$. HRMS (ESI): Calcd. for $C_{27}H_{21}Br_2N_3NaO$ $[M+Na]^+$: 583.9944; found:583.9925.

(31)4-(5-((4-cyanophenyl)(phenyl)amino)-3-ethyl-2-oxo-2,3-dihydro-1*H*-benzo[*d*]imidazol -1-yl)benzonitrile (5if)

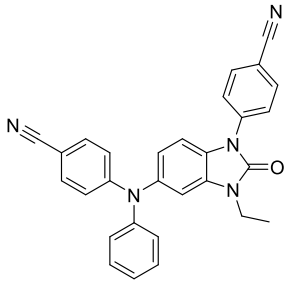

Brownish solid, (35 mg, 31% yield); m.p: 123-124 °C; ^{1}H NMR (400 MHz, $CDCl_3$): δ 7.83 (d, *J*

= 8.6 Hz, 2H), 7.75 (d, *J* = 8.6 Hz, 2H), 7.45 – 7.42 (m, 2H), 7.33 – 7.38 (m, 2H), 7.20 – 7.12 (m, 4H), 6.94 – 6.98 (m, 2H), 6.91 (dd, *J* = 7.2, 1.8 Hz, 2H), 3.93 (q, *J* = 7.2 Hz, 2H), 1.33 (t, *J* = 7.2 Hz, 3H). ^{13}C NMR (100 MHz, $CDCl_3$): δ 152.63, 151.81, 146.00, 141.61, 138.94, 133.59, 133.37, 130.76, 129.97, 125.84, 125.81, 125.67, 125.31, 122.29, 120.62, 119.71, 119.38, 118.30, 110.89, 110.02, 107.16, 102.65, 36.42, 13.52. IR (KBr): 3060, 2962, 2925, 2855, 1714, 1628, 1600, 1492, 1397, 1320, 1235, 1174, 1086, 828, 741, 700 cm^{-1}. MS (EI, m/z): 455 $[M]^+$. HRMS (ESI): Calcd. for $C_{29}H_{21}N_5NaO$ $[M+Na]^+$: 478.1638; found: 478.1636.

(32)5-(phenyl(p-tolyl)amino)-3-propyl-1-(p-tolyl)-1,3-dihydro-2*H*-benzo[*d*]imidazol-2-one (5bg)

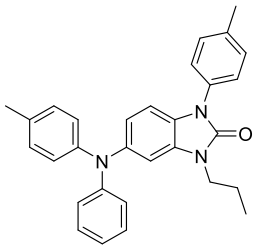

Brownish oil liquid, (80 mg, 72% yield); ^{1}H NMR (400 MHz, $CDCl_3$): δ 7.41 (d, *J* = 8.0 Hz, 2H), 7.29 (d, *J* = 8.4 Hz, 2H), 7.22 – 7.17 (m, 2H), 7.07 – 6.98 (m, 6H), 6.92 (t, *J* = 7.8 Hz, 2H), 6.85 (d, *J* = 1.8 Hz, 1H), 6.77 (dd, *J* = 8.4, 2.0 Hz, 1H), 3.79 (t, *J* = 7.2 Hz, 2H), 2.40 (s, 3H), 2.30 (s, 3H), 1.79 – 1.69 (m, 2H), 0.94 (t, *J* = 7.4 Hz, 3H).^{13}C NMR (100 MHz, $CDCl_3$): δ 153.73, 148.55, 145.66, 142.84, 137.37, 132.27, 132.23, 130.60, 130.11, 129.93, 129.14, 125.95, 125.76, 123.98, 122.44, 121.63, 119.15, 109.33, 105.88, 42.85, 21.75, 21.25, 20.87, 11.46. IR (KBr): 3057, 3034, 2965, 2925, 2874, 1714, 1593, 1512, 1490, 1399, 1314, 1223, 1187, 1019, 811, 746, 696 cm^{-1}. MS (EI, m/z): 447 $[M]^+$. HRMS (ESI): Calcd. for $C_{30}H_{29}N_3NaO$ $[M+Na]^+$: 470.2203; found: 470.2205.

(33)1-(4-ethylphenyl)-5-((4-ethylphenyl)(phenyl)amino)-3-propyl-1,3-dihydro-2*H*-benzo[*d*]imidazol-2-one (5jg)

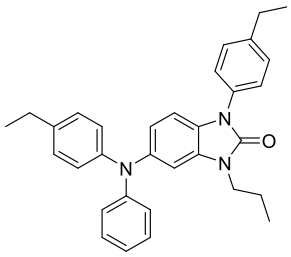

Brownish oil liquid, (97 mg, 82% yield); ^{1}H NMR (400 MHz, $CDCl_3$): δ 7.44 (d, *J* = 8.0 Hz, 2H), 7.32 (d, *J* = 8.4 Hz, 2H), 7.22 – 7.17 (m, 2H), 7.08 – 7.00 (m, 6H), 6.96 – 6.90 (m, 2H), 6.86 (d, *J* = 2.0 Hz, 1H), 6.78 (dd, *J* = 8.4, 2.0 Hz, 1H), 3.79 (t, *J* = 7.2 Hz, 2H), 2.69 (q, *J* = 7.6 Hz, 2H), 2.60 (q, *J* = 7.6 Hz, 2H), 1.79 – 1.69 (m, 2H), 1.27 (t, *J* = 7.8 Hz, 3H), 1.24 – 1.20 (m, 3H), 0.94 (t, *J* = 7.4 Hz, 3H). ^{13}C NMR (100 MHz, $CDCl_3$): δ 153.74, 148.53, 145.80, 143.62, 142.82, 138.58, 132.42, 130.58, 129.12, 128.92, 128.65, 125.95, 125.78, 123.84, 122.48, 121.64, 119.23, 109.37, 105.96, 42.84, 28.64, 28.26 , 21.74 , 15.65, 15.58, 11.44. IR (KBr): 3032, 2962, 2929, 2868, 1716, 1598, 1494, 1398, 1271, 1226, 1182, 829，697，648 cm^{-1}. MS (EI, m/z): 475 $[M]^+$. HRMS (ESI): Calcd. for $C_{32}H_{33}N_3NaO$ $[M+Na]^+$: 498.2516; found:498.2520.

(34)ethyl4-(5-((4-(ethoxycarbonyl)phenyl)(phenyl)amino)-2-oxo-3-propyl-2,3-dihydro-1*H*-benzo[*d*]imidazol-1-yl)benzoate (5kg)

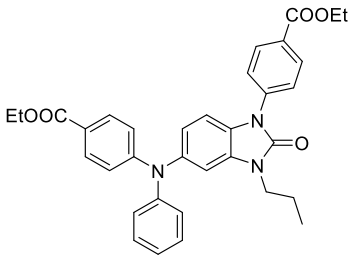

Brownish oil liquid, (77 mg, 55% yield); ^{1}H NMR (400 MHz, $CDCl_3$): δ 8.21 (d, *J* = 8.6 Hz, 2H), 7.87 (d, *J* = 8.8 Hz, 2H), 7.68 (d, *J* = 8.6 Hz, 2H), 7.31 (t, *J* = 7.8 Hz, 2H), 7.18 – 7.08 (m, 4H), 6.98 (d, *J* = 8.8 Hz, 2H), 6.90 – 6.85 (m, 2H), 4.41 (q, *J* = 7.0 Hz, 2H), 4.34 (q, *J* = 7.2 Hz, 2H), 3.82 (t, *J* = 7.2 Hz, 2H), 1.81 – 1.71 (m, 2H), 1.42 (t, *J* = 7.2 Hz, 3H), 1.37 (t, *J* = 7.2 Hz, 3H), 0.97 (t, *J* = 7.4 Hz, 3H).^{13}C NMR (100 MHz, $CDCl_3$): δ 166.42, 165.86, 153.18, 152.12, 146.81, 141.93, 138.89, 130.98, 130.91, 129.62, 129.17, 125.91, 125.24, 124.98, 124.30, 122.45, 120.31, 119.49, 109.83, 106.98, 61.24, 60.60, 43.01, 21.66, 14.48, 14.41, 11.42. IR (KBr): 3001, 2936, 2879, 1725, 1588, 1511, 1462, 1421, 1265, 1223, 1141, 1084, 1029, 854, 807, 748 cm^{-1}. MS (EI, m/z): 563 $[M]^+$. HRMS (ESI): Calcd. for $C_{34}H_{33}N_3NaO_5$ $[M+Na]^+$: 586.2312; found: 586.2313.

(35)5-(phenyl(4-(trifluoromethyl)phenyl)amino)-3-propyl-1-(4-(trifluoromethyl)phenyl)-1, 3-dihydro-2*H*-benzo[*d*]imidazol-2-one (5lg)

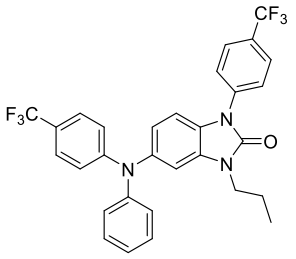

Brownish solid, (58 mg, 42% yield), m.p: 119-126 °C; ^{1}H NMR (400 MHz, $CDCl_3$): δ 7.76 (dd, *J* = 24.6, 8.6 Hz, 4H), 7.42 (d, *J* = 8.6 Hz, 2H), 7.32 (t, *J* = 7.8 Hz, 2H), 7.16 – 7.04 (m, 6H), 6.92 – 6.85 (m, 2H), 3.83 (t, *J* = 7.2 Hz, 2H), 1.82 – 1.72 (m, 2H), 0.97 (t, *J* = 7.4 Hz, 3H). ^{13}C NMR (100 MHz, $CDCl_3$): δ 153.29, 151.18, 146.98, 142.20, 138.15, 131.10, 129.82, 129.75, 129.58, 129.25, 126.81 (q, *J* = 3.7 Hz), 126.49, 126.44 (q, *J* = 3.7 Hz), 126.13, 125.97, 125.84, 125.65, 125.61, 125.32, 125.04, 124.28, 123.27, 122.87, 122.62, 122.54, 121.05, 120.34, 120.30, 119.99, 109.79, 107.02, 43.13, 21.74, 11.48. IR (KBr): 3064, 2973, 2940, 2879, 1714, 1588, 1553, 1490, 1396, 1321, 1223, 1161, 1110, 827, 742, 695 cm^{-1}. MS (EI, m/z): 555 $[M]^+$. HRMS (ESI): Calcd. for $C_{30}H_{23}F_2N_3NaO$ $[M+Na]^+$: 578.1638; found:578.1633.

(36)6-(di-o-tolylamino)-1-ethyl-4-methyl-3-(o-tolyl)-1,3-dihydro-2*H*-benzo[*d*]imidazol-2-one (5mf)

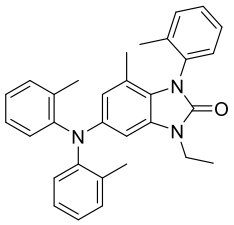

Brownish oil liquid, (71 mg, 62% yield); ^{1}H NMR (400 MHz, $CDCl_3$): δ 7.34 – 7.30 (m, 3H), 7.29 – 7.26 (m, 1H), 7.19 – 7.16 (m, 2H), 7.14 – 7.09 (m, 2H), 7.04 (td, *J* = 7.2, 1.4 Hz, 2H), 6.95 (dd, *J* = 7.8, 1.0 Hz, 2H), 6.31 (d, *J* = 2.0 Hz, 1H), 6.18 (d, *J* = 1.2 Hz, 1H), 3.86 – 3.78 (m, 2H), 2.16 (s, 3H), 2.01 (s, 6H), 1.60 (s, 3H), 1.23 (t, *J* = 7.2 Hz, 3H). ^{13}C NMR (100 MHz, $CDCl_3$): δ 153.78, 146.89, 143.92, 137.76, 135.44, 134.23, 131.66, 130.70, 130.26, 129.88, 129.07, 126.94, 126.85, 126.64, 124.28, 122.30, 120.45, 117.71, 99.54, 35.87, 19.03, 17.82, 17.14, 13.55. IR (KBr): 3060, 3021, 2968, 2926, 2855, 1712, 1620, 1601, 1489, 1402, 1378, 1265, 1234, 1116, 1059, 750, 720, 653, 625 cm^{-1}. MS (EI, m/z): 461 $[M]^+$. HRMS (ESI): Calcd. for $C_{31}H_{31}N_3NaO$ $[M+Na]^+$: 484.2359; found: 484.22359.

(37)3-ethyl-1-(4-methoxy-2-methylphenyl)-5-((4-methoxy-2-methylphenyl)(phenyl)amino)-1,3-dihydro-2*H*-benzo[*d*]imidazol-2-one (5nf)

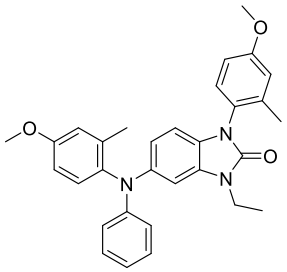

Brownish solid, (74 mg, 60% yield); m.p: 77-78 °C; ^{1}H NMR (400 MHz, $CDCl_3$): δ 7.15 – 7.22(m, 3H), 7.08 (d, *J* = 8.8 Hz, 1H), 6.88 (d, *J* = 7.6 Hz, 3H), 6.86 – 6.78 (m, 4H), 6.76 (d, *J* = 8.8 Hz, 1H), 6.66 (d, *J* = 8.4 Hz, 1H), 6.51 (d, *J* = 8.4 Hz, 1H), 3.89 (q, *J* = 7.2 Hz, 2H), 3.83 (s, 3H), 3.81 (s, 3H), 2.15 (s, 3H), 2.08 (s, 3H), 1.30 (t, *J* = 7.0 Hz, 3H). ^{13}C NMR (100 MHz, $CDCl_3$): δ 159.84, 157.72, 153.63, 148.58, 142.56, 138.70, 138.41, 138.00, 130.68, 129.95, 129.72, 129.11, 126.10, 126.07, 120.17, 119.53, 116.75, 116.66, 116.58, 112.85, 112.47, 109.00, 103.24, 55.59, 55.50, 36.08, 18.95, 18.30, 13.78. IR (KBr): 3060, 2956, 2926, 2852, 1710, 1625, 1600, 1492, 1403, 1300, 1232, 1193, 1160, 1113, 1044, 804, 749, 695 cm^{-1}. MS (EI, m/z): 493 $[M]^+$. HRMS (ESI): Calcd. for $C_{31}H_{32}N_3NO_3$ $[M+H]^+$: 494.2438; found: 494.2432.

(38)1-(3,4-dimethylphenyl)-5-((3,4-dimethylphenyl)(phenyl)amino)-3-propyl-1,3-dihydro-2*H*-benzo[*d*]imidazol-2-one (5og)

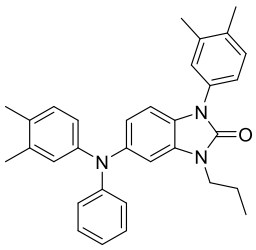

Brownish oil liquid, (74 mg, 62% yield); ^{1}H NMR (400 MHz, $CDCl_3$): δ 7.31 (s, 1H), 7.24 (s, 2H),

7.22 – 7.17 (m, 2H), 7.05 – 6.98 (m, 3H), 6.91 (t, *J* = 7.6 Hz, 3H), 6.87 – 6.81 (m, 2H), 6.76 (dd, *J* = 8.4, 2.0 Hz, 1H), 3.79 (t, *J* = 7.2 Hz, 2H), 2.30 (d, *J* = 2.8 Hz, 6H), 2.21 (s, 3H), 2.17 (s, 3H), 1.79 – 1.70 (m, 2H), 0.95 (t, *J* = 7.4 Hz, 3H). ^{13}C NMR (100 MHz, $CDCl_3$): δ 153.80, 148.66, 145.93, 142.82, 137.95, 137.53, 136.13, 132.47, 131.04, 130.54, 130.42, 129.09, 127.09, 126.04, 125.35, 123.31, 122.40, 121.62, 121.47, 119.13, 109.34, 105.85, 42.84, 21.76, 19.95, 19.54, 19.17, 11.45. IR (KBr): 3026, 2963, 2926, 2868, 1715, 1599, 1495, 1398, 1304, 1272, 809, 741, 702 cm^{-1}. MS (EI, m/z): 475 $[M]^+$. HRMS (ESI): Calcd. for $C_{32}H_{33}N_3NaO$ $[M+Na]^+$: 498.2516; found:498.2517.

(39)3-ethyl-1-isopropyl-5-(isopropyl(phenyl)amino)-1,3-dihydro-2*H*-benzo[*d*]imidazol-2-one (5pf)

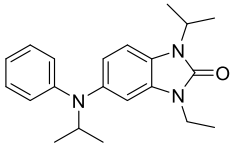

Brownish oil liquid, (71 mg, 84% yield); ^{1}H NMR (400 MHz, $CDCl_3$): δ 7.20 – 7.11 (m, 3H), 6.79 (dd, *J* = 8.2, 1.8 Hz, 1H), 6.76 – 6.69 (m, 2H), 6.64 (d, *J* = 8.2 Hz, 2H), 4.77 (hept, *J* = 7.0 Hz, 1H), 4.35 (hept, *J* = 6.6 Hz, 1H), 3.89 (q, *J* = 7.2 Hz, 2H), 1.57 (d, *J* = 7.0 Hz, 6H), 1.30 (t, *J* = 7.2 Hz, 3H), 1.19 (d, *J* = 6.6 Hz, 6H). ^{13}C NMR (100 MHz, $CDCl_3$): δ 153.62, 149.23, 136.70, 130.12, 129.02, 126.33, 122.91, 117.33, 115.20, 109.72, 109.43, 47.85, 45.02, 35.84, 21.08, 20.46, 13.65. IR (KBr): 3059, 2975, 2875, 1705, 1595, 1494, 1401, 1385, 1359, 1305, 749 cm^{-1}. MS (EI, m/z): 337 $[M]^+$. HRMS (ESI): Calcd. for $C_{21}H_{28}N_3O$ $[M+H]^+$: 338.2227; found:338.2232.

Supplemental Reference.

Yang, T. F., Chiu, K. Y., Cheng, H. C., Lee, Y. W., Kuo, M. Y. and Su, Y. O. (2012). Studies on the structure of N-phenyl-substituted hexaaza[1_6]paracyclophane: synthesis, electrochemical properties, and theoretical calculation. J. Org. Chem. *77*, 8627-8633.

Shi, R., Lu, L., Zhang, H., Chen, B., Sha, Y., Liu, C., and Lei, A. (2013). Palladium/copper catalyzed oxidative C–H alkenylation/N-dealkylative carbonylation of tertiary Anilines. Angew. Chem. Int. Ed. *52*, 10582 –10585.